

1997

# Development of immunoaffinity chromatography for the separation of myosin isozymes

Sara E. Acevedo  
*San Jose State University*

Follow this and additional works at: [https://scholarworks.sjsu.edu/etd\\_theses](https://scholarworks.sjsu.edu/etd_theses)

---

## Recommended Citation

Acevedo, Sara E., "Development of immunoaffinity chromatography for the separation of myosin isozymes" (1997). *Master's Theses*. 1488.

DOI: <https://doi.org/10.31979/etd.f5gh-vxvk>

[https://scholarworks.sjsu.edu/etd\\_theses/1488](https://scholarworks.sjsu.edu/etd_theses/1488)

This Thesis is brought to you for free and open access by the Master's Theses and Graduate Research at SJSU ScholarWorks. It has been accepted for inclusion in Master's Theses by an authorized administrator of SJSU ScholarWorks. For more information, please contact [scholarworks@sjsu.edu](mailto:scholarworks@sjsu.edu).

## INFORMATION TO USERS

This manuscript has been reproduced from the microfilm master. UMI films the text directly from the original or copy submitted. Thus, some thesis and dissertation copies are in typewriter face, while others may be from any type of computer printer.

**The quality of this reproduction is dependent upon the quality of the copy submitted.** Broken or indistinct print, colored or poor quality illustrations and photographs, print bleedthrough, substandard margins, and improper alignment can adversely affect reproduction.

In the unlikely event that the author did not send UMI a complete manuscript and there are missing pages, these will be noted. Also, if unauthorized copyright material had to be removed, a note will indicate the deletion.

Oversize materials (e.g., maps, drawings, charts) are reproduced by sectioning the original, beginning at the upper left-hand corner and continuing from left to right in equal sections with small overlaps. Each original is also photographed in one exposure and is included in reduced form at the back of the book.

Photographs included in the original manuscript have been reproduced xerographically in this copy. Higher quality 6" x 9" black and white photographic prints are available for any photographs or illustrations appearing in this copy for an additional charge. Contact UMI directly to order.

# UMI

A Bell & Howell Information Company  
300 North Zeeb Road, Ann Arbor MI 48106-1346 USA  
313/761-4700 800/521-0600



DEVELOPMENT OF IMMUNOAFFINITY CHROMATOGRAPHY  
FOR THE SEPARATION OF MYOSIN ISOZYMES

A Thesis

Presented to

The Faculty of the Department of Chemistry  
San Jose State University

In Partial Fulfillment  
of the Requirements for the Degree  
Master of Science

by

Sara E. Acevedo

August 1997

**UMI Number: 1386189**

**Copyright 1997 by  
Acevedo, Sara E.**

**All rights reserved.**

---

**UMI Microform 1386189  
Copyright 1997, by UMI Company. All rights reserved.**

**This microform edition is protected against unauthorized  
copying under Title 17, United States Code.**

---

**UMI**  
300 North Zeeb Road  
Ann Arbor, MI 48103

© 1997

Sara E. Acevedo

ALL RIGHTS RESERVED

APPROVED FOR THE DEPARTMENT OF CHEMISTRY

*Laura Silberstein*

Dr. Laura Silberstein

*Pamela C Stacks*

Dr. Pamela Stacks

*Roy Okuda*

Dr. Roy Okuda

APPROVED FOR THE UNIVERSITY

*Serena W. Stanford*

Serena W. Stanford

## ABSTRACT

### DEVELOPMENT OF IMMUNOAFFINITY CHROMATOGRAPHY FOR THE SEPARATION OF MYOSIN ISOZYMES

by Sara E. Acevedo

Multiple isozymes of the skeletal muscle protein, myosin, have been postulated to exist based on immunohistochemical studies. Distinct myosin isozymes could be separated by immunoaffinity chromatography using matrices bearing monoclonal antibodies to myosin heavy chain epitopes.

The goals of this study were: 1) to separate putative distinct isozymes of myosin using anti-myosin immunoaffinity chromatography, and 2) to determine if distinct isozymes bear only a single type of heavy chain epitope, or if any isozymes carry combinations of different epitopes.

Monoclonal antibodies to two heavy chain epitopes of fast-contracting myosin and one of slow-contracting myosin were purified and coupled to inert chromatographic supports. Three different anti-myosin immunoaffinity matrices were produced, each one specific to a distinct myosin heavy chain epitope. Technical difficulties prevented analysis of the column peaks, thus, at the time of this writing, the separation of isozymes has not yet been achieved.



Dedicated to my Mom and Dad, who taught me to value education.

With special thanks to my husband, William, and my sister, Joan, who encouraged me every step of the way, and to my brother, Bill, who was the first to suggest that I give chemistry a try since he thought I might like it (I do).

This work was supported by an Academic Research Enhancement Award (grant #1R15AR4209301A1) from the National Institutes of Health.

# TABLE OF CONTENTS

## LISTS

Symbols and Abbreviations .....	viii
Figures .....	xii
Tables .....	xv

## INTRODUCTION AND THEORY

Myosin .....	17
Monoclonal Antibodies .....	30
Putative Myosin Isozymes .....	40
Immunoaffinity Chromatography .....	46
Study Goals and Approach .....	55

## MATERIALS AND METHODS

Analyses and Assays .....	62
Myosin Preparation .....	67
Monoclonal Antibody Preparation .....	70
Immunoaffinity Columns .....	74

## RESULTS

Myosin Preparation .....	78
Monoclonal Antibody Preparation .....	86
Anti-Myosin Immunoaffinity Columns .....	109
Detection of Myosin Epitopes .....	115

## DISCUSSION AND CONCLUSIONS

Myosin Preparation .....	130
Monoclonal Antibody Preparation .....	136
Anti-Myoain Immunoaffinity Columns .....	140
Detection of Myosin Epitopes .....	142
Future Work .....	143

## APPENDICES

Buffers and Reagents .....	146
Materials .....	150
Equipment .....	151

REFERENCES .....	153
------------------	-----

COPYRIGHT RELEASE LETTERS .....	158
---------------------------------	-----

## LISTS

### Symbols and Abbreviations

Å	angstroms
Ab	antibody
$\epsilon^{1\%_{280\text{nm}}}$	extinction coefficient at 280 nm for a 1% solution (units are mL/mg-cm)
$\Gamma$	ionic strength
ABTS	2,2'-azino-bis-(3-ethylbenz-thiazoline-6-sulfonic acid) (substrate to HRP)
anti-F22 column	an immunoaffinity column that will bind F22+ myosin isozyms (analogous abbreviation is used for other anti-myosin immunoaffinity columns)
ATP	adenosine triphosphate
AU	absorbance units
AUFS	absorbance units (AU) full scale
BSA	bovine serum albumin
cm	centimeters
CGM	Cell Growth Media
CNBr	cyanogen bromide
CSN	cell supernatant
DMEM	Dulbecco's modified Eagle's media
DTNB	5,5'-dithiobis-(2-nitrobenzoic acid)
DTT	dithiothreitol
EDTA	ethylenediaminetetraacetic acid
EGTA	ethylene glycol-bis-( $\beta$ -aminoethyl ether) N,N,N',N'-tetraacetic acid
ELISA	enzyme linked immunosorbent assay
EWB	ELISA wash buffer
F22+	myosin isozyms bearing the F22 epitope (analogous abbreviation is used for other isozyms bearing specific epitopes)

F22-	myosin isozyme lacking the F22 epitope (analogous abbreviation is used for other isozymes bearing specific epitopes)
FCS	fetal calf serum
g	grams
Γam	goat anti-mouse (goat antibodies reactive to mouse immunoglobulins)
ΓamIgG	goat anti-mouse IgG
ΓamIgM	goat anti-mouse IgM
ΓamIgG•HRP	goat anti-mouse IgG conjugated to HRP
ΓamIgM•HRP	goat anti-mouse IgM conjugated to HRP
Gdn•HCl	guanidine hydrochloride
h	hours
HRP	horseradish peroxidase
i.d.	inner diameter
Ig	immunoglobulin
IgA	class A immunoglobulin
IgD	class D immunoglobulin
IgE	class E immunoglobulin
IgG	class G immunoglobulin
IgM	class M immunoglobulin
kDa	kilo Daltons
kg	kilograms
krpm	thousands of rotations per minute
L	liters
M	molar concentration (mol/L)
MAb	monoclonal antibody
mAmps	milliamperes

MHC	myosin heavy chain
min	minutes
mL	milliliters
mm	millimeters
mM	millimolar concentration (mmol/L)
mmol	millimoles
MOPC	mineral oil-induced plasmocytoma originated IgM (IgM standard for homo-isotypic ELISAs)
MQ H <sub>2</sub> O	water dispensed from a Millipore MilliQ <sup>®</sup> Water Purification System
MW	molecular weight
NCS	neonatal calf serum
ng	nanograms
nm	nanometers
PBS	phosphate buffered saline
pK <sub>ε</sub>	pK of lysine's side chain (ε) amino group
PPi	pyrophosphate
RT	room (ambient) temperature
SAS	saturated ammonium sulfate
SCB	Sepharose column buffer
SDS-PAGE	sodium dodecylsulfate polyacrylamide gel electrophoresis
sec	seconds
SEC	size exclusion chromatography
μg	micrograms
μL	microliters
UV-VIS	ultraviolet-visible
V <sub>0</sub>	void volume from an immunoaffinity column

$V_e$	eluted volume from an immunoaffinity column
v/v	volume/volume (in dilutions)
w/v	weight/volume (in dilutions)
X+	symbol to represent generic myosin isozyme possessing a given epitope X
X-	symbol to represent generic myosin isozyme lacking a given epitope X

## Figures

- Figure 1. A diagram of a single elongated muscle cell, or fiber. (Page 18).
- Figure 2. An electron micrograph of a longitudinal section of a striated muscle fiber. (Page 19).
- Figure 3. A diagram of individual myosin molecules aggregated into a thick filament with the M Line at the center. (Page 19).
- Figure 4. Diagram and photomicrograph of a single myosin molecule. (Page 20).
- Figure 5. Ribbon diagram of a single myosin head. (Page 22).
- Figure 6. An electron micrograph of honeybee flight muscle in which crossbridges have formed between the thick and thin filaments. (Page 23).
- Figure 7. Diagram of a single sarcomere before and after contraction. (Page 24).
- Figure 8. Over the course of the myosin preparation, the ionic strength of the buffers are varied to alternately solubilize and precipitate myosin relative to the other proteins present. (Page 25).
- Figure 9. In SEC, molecules of different sizes travel different paths through the column bed and therefore have different retention times. (Page 28).
- Figure 10. The fractionation range and corresponding chromatogram for a hypothetical size exclusion matrix. (Page 29).
- Figure 11. Diagram of an IgG-class immunoglobulin. (Page 32).
- Figure 12. Diagram and clay model of an IgM-class immunoglobulin. (Page 33).
- Figure 13. Homo-isotypic sandwich ELISAs are based on a sequential series of selective binding steps determined by the immunospecificity of the reagents for the analyte of interest. (Page 38).
- Figure 14. Diagram of the interactions of individual molecules in each successive layer in the hetero-isotypic sandwich ELISA. (Page 39).
- Figure 15. In ATPase histochemical studies, individual fibers within the slow-contracting soleus muscle show pH-dependent staining. (Page 42).
- Figure 16. Serial sections of slow-contracting soleus muscle show different staining patterns in immunohistochemical studies with three anti-slow MAbs. (Page 44).
- Figure 17. Diagram of a theoretical ligand/target interaction in affinity chromatography. (Page 47).
- Figure 18. On a coupled immunoaffinity matrix, the MAbs (ligands) are covalently coupled to the inert matrix through CNBr-activated C6 hydroxyl groups on the polysaccharide matrix and  $\epsilon$  amino groups on the MAb molecules. (Page 48).



- Figure 19. One theoretical scenario of a myosin sample applied to parallel immunoaffinity columns. (Page 53).
- Figure 20. An alternate way to demonstrate the presence of multiple-epitope isozymes involves using two anti-myosin immunoaffinity columns in series. (Page 54).
- Figure 21. Outline of the approach taken in this study. (Page 57).
- Figure 22. Diagram of the interactions of the individual molecules in the layers of the hetero-isotypic sandwich ELISA designed to detect the presence of aggregated myosin. (Page 60).
- Figure 23. SDS-PAGE gel of the major stages of the myosin preparation S8. (Page 81).
- Figure 24. Chromatogram of myosin from preparation S8-H chromatographed on 1.5 x 80-cm Sepharose 2B size exclusion column. (Page 83).
- Figure 25. Diagram of the SDS-PAGE performed on the three peaks eluted from S8-H myosin chromatographed on a 1.5 x 80-cm Sepharose 2B column. (Page 85).
- Figure 26. Flow chart for the SAS precipitation protocol for F22 ascites. (Page 92).
- Figure 27. Size exclusion chromatography of the 30% (v/v) SAS precipitation of F22 ascites (F22<sub>30%</sub>SAS PPT) on a 1.5 x 80-cm Sephacryl S300-HR column to remove albumin from IgM. (Page 96).
- Figure 28. Size exclusion chromatography of the 50% (v/v) SAS precipitation of F22 ascites (F22<sub>50%</sub>SAS PPT) on a 1.5 x 80-cm Sephacryl S300-HR column to remove albumin from IgM. (Page 97).
- Figure 29. Size exclusion chromatography of the 45% (v/v) SAS precipitation of F36 ascites (F36<sub>45%</sub>SAS PPT) on a 1.5 x 80-cm Sephacryl S300-HR column to remove albumin from IgM. (Page 98).
- Figure 30. Size exclusion chromatography of the 50% (v/v) SAS precipitation of F36 ascites (F36<sub>50%</sub>SAS PPT) on a 1.5 x 80-cm Sephacryl S300-HR column to remove albumin from IgM. (Page 99).
- Figure 31. Size exclusion chromatography of S84<sub>50%</sub>SAS PPT on a 1.5 x 80-cm Sephacryl S300-HR column to remove albumin from IgM. (Page 100).
- Figure 32. SDS-PAGE analysis to track the SAS precipitation of IgM from F22 ascites. (Page 103).
- Figure 33. SDS-PAGE analysis to track the removal of albumin from IgM by size exclusion chromatography on the SAS precipitates of MAb-F22. (Page 105).
- Figure 34. SDS-PAGE analysis to track the purification of MAb-F36. (Page 106).
- Figure 35. SDS-PAGE analysis to track the purification of MAb-S84. (Page 107).

- Figure 36. Absorbance values for myosin ('signal') and blank ('noise') samples from a hetero-isotypic sandwich ELISA to determine the optimal concentration of  $\Gamma\alpha$ mIgM•HRP. (Page 120).
- Figure 37. Saturation curve for MAb-25. (Page 122).
- Figure 38. Plot of absorbance values (AU without blanks subtracted) of the blanks as a function of MAb-25 concentration on the plate (data from the MAb-25 saturation ELISA; see Figure 37). (Page 123).
- Figure 39. Absorbance (AU without blanks subtracted) of myosin samples diluted in BSA-Blocking Buffer (data from the proteolysis ELISA, see Table 19, page 117). (Page 125).
- Figure 40. Four models of possible forms in which myosin could exist *in vitro* and their approximate Stokes' radii. (Page 135).

## Tables

- Table 1. The five monoclonal hybridoma cell lines each secrete a unique MAb. (Page 34).
- Table 2. Summary of yields from myosin preparations. (Page 79).
- Table 3. Absorbance data (AU) on the parallel S8 preps. (Page 80).
- Table 4. The most likely contaminating proteins and polypeptides and characteristic myosin degradation products (marked by g) found in glycerinated myosin. (Page 84).
- Table 5. The five monoclonal hybridoma cell lines each secrete a unique MAb. (Page 87).
- Table 6. Typical viability results upon freezing and subsequent thawing of hybridoma cell lines. (Page 88).
- Table 7. The concentration of IgM in the ascites is much higher than in the cell supernatants thus the ascites is a preferable source from which to purify the MAbs. (Page 89).
- Table 8. Raw absorbance readings (average AUs for duplicate wells; blanks not subtracted) from a homo-isotypic sandwich ELISA to determine IgM concentrations in cell supernatants from the cell lines that produce IgM-class anti-myosin MAbs (F22, F36, and S84). (Page 91).
- Table 9. Concentrations of total protein and total IgM in the original ascites. (Page 91).
- Table 10. Yields of total protein and total IgM in the SAS precipitation of IgM from MAb-F22 ascites. (Page 93).
- Table 11. Yields of total protein and total IgM in the purification of IgM from ascites; MAb-F36 at 45% (v/v) SAS; MAb-F36 at 50% (v/v) SAS; and MAb-S84 at 50% (v/v) SAS. (Page 95).
- Table 12. Yields of total protein and total IgM in the 'IgM peak' and 'albumin peak' from the size exclusion chromatography of SAS precipitates of MAb-F22 ascites on Sephacryl S300-HR column. (Page 101).
- Table 13. Yields of total protein and total IgM in the 'IgM peak' and 'albumin peak' from the size exclusion chromatography of SAS precipitates of MAb-F36 and MAb-S84 ascites. (Page 102).
- Table 14. Concentrations of protein and Ig in the final purified MAbs. (Page 108).
- Table 15. Absorbance readings at 280 nm were used to track percent coupling of MAbs to activated matrix. (Page 110).
- Table 16. Final concentration of MAbs on the coupled immunoaffinity matrices based on the starting concentration of IgM in the diluted MAb solutions and the percent coupled as determined in Table 14. (Page 111).
- Table 17. Washes of the MAb-F36 'lo' coupled matrix with 'hi [Salt]' (3 M KCl @ pH 7.2) and 'low pH' (0.5 M KCl @ pH 2.0) 'stripping' eluants showed essentially no loss of protein (<1% relative to the amount coupled). (Page 113).

- Table 18. As shown by an increase in aggregation over time, the myosin was not stable in any of the three 'stripping' eluants. (Page 114).
- Table 19. Raw absorbance readings for myosin sample wells from the proteolysis ELISA (AU without blanks subtracted). (Page 117).
- Table 20. Absorbance data (AU, blanks not subtracted), from a homo-isotypic sandwich ELISA to determine the concentration of IgM-class Igs in BSA and purified MAb-25. (Page 126).
- Table 21. The reagents used in all layers of the hetero-isotypic sandwich ELISA were tested for IgM content. (Page 128).
- Table 22. Correlation of absorbance and SDS-PAGE data with theoretical models for possible species present in fractions from the Sepharose 2B column aides in determining which peaks contain aggregated materials and which contain monodisperse myosin molecules. (Page 133).

## INTRODUCTION AND THEORY

### **Myosin**

*Overview.* Myosin is one of the two main contractile proteins found in muscle, where it serves both structural and functional roles. In muscle fibers, individual myosin molecules are aggregated into long filaments which are interdigitated with filamentous aggregates of the protein actin (Huxley, 1980). During muscle contraction the filaments slide along one another by virtue of conformational changes in the individual myosin molecules and interactions between the two types of filaments (Hanson and Huxley, 1953). Myosin functions as an ATPase providing the energy that drives the conformational changes that result in muscle contraction (Englehardt and Ljubimowa, 1939; Rayment et al., 1993).

*Striated Skeletal Muscle.* Muscle is categorized both by its rate of contraction and its tissue structure. This study uses leg muscle from adult rats which is vertebral striated skeletal muscle containing both 'fast' and 'slow' fibers. The 'fast' and 'slow' designations indicate the relative rates of contraction of these two different types of fibers (Barany, 1967; Goldspink, 1980). The term 'striated' was applied to this type of muscle due to its stripped appearance when viewed under a light microscope (Huxley and Hanson, 1954).

The extremely elongated cells of striated muscle are referred to as muscle fibers (Figure 1). Within each muscle fiber are bundles, or myofibrils, of 'thick' and 'thin' filaments. These filaments are linear aggregates of the two main contractile proteins of muscle, myosin and actin. The myofibrils are subdivided lengthwise into functional units called sarcomeres.

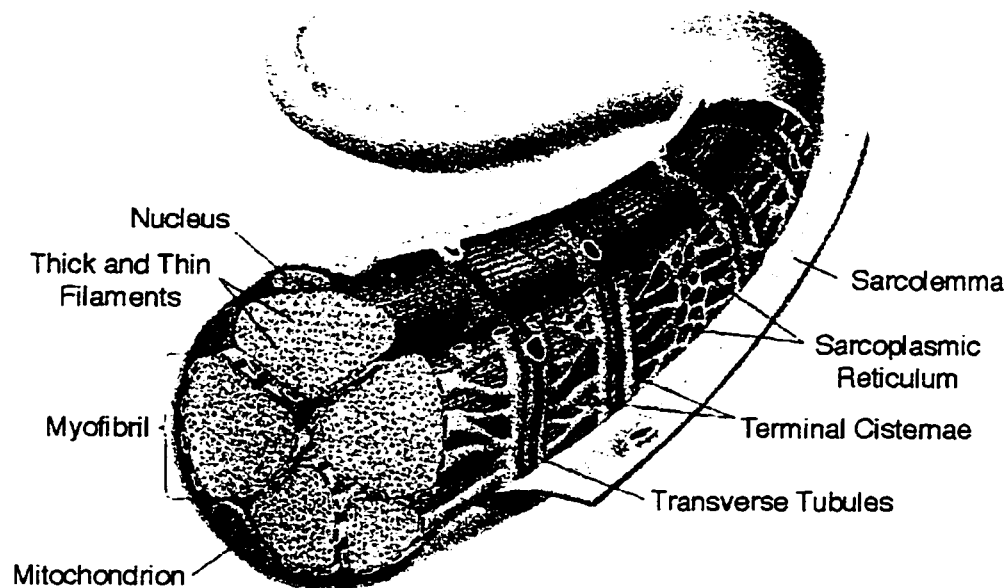


Figure 1. A diagram of a single elongated muscle cell, or fiber. Note the bundles, or myofibrils, within the cell and the lengthwise division into sub-units known as sarcomeres (Reproduced with permission, from Garrett and Grisham, 1995, Figure 36.2.)

An electron micrograph of a longitudinal section of striated muscle fibers clearly shows the striations and sarcomeres (Figure 2). The horizontal striations in Figure 2 are the separate thick and thin filaments; the thick filaments are primarily aggregates of myosin while the thin filaments are aggregates of actin, troponin, and tropomyosin (Goldspink, 1980). Within each sarcomere the thick and thin filaments are interdigitated in hexagonal arrays (Huxley, 1953) and are anchored to the ends of the sarcomere through numerous accessory proteins known as myofibrillar scaffolding proteins. Two types of vertical bands are seen to cut across the myofibrils: 'Z Lines,' which are the ends of the sarcomeres, and 'M Lines,' the length-wise midpoint of each thick filament (Figure 3). On each half of the thick filament, the individually asymmetric myosin molecules are arranged such that they are all oriented in the same direction relative to each other and to the central M Line (Garrett and Grisham, 1995).

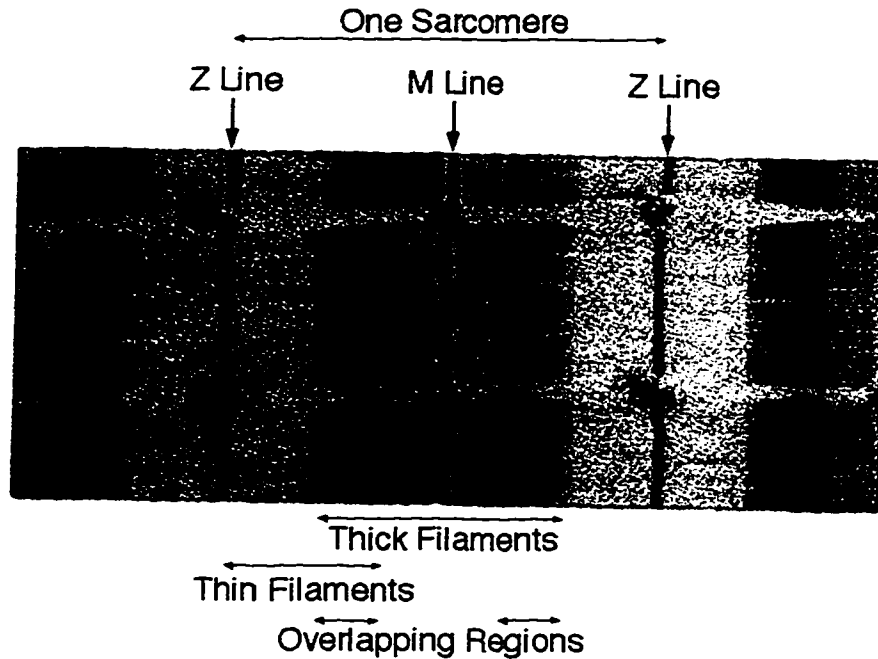


Figure 2. An electron micrograph of a longitudinal section of a striated muscle fiber. The horizontal striations are the thick and thin filaments; the vertical bands are the Z lines and M lines, the ends and midpoints of the sarcomeres, respectively. (Reproduced with permission, from Garrett and Grisham, 1995, Figure 36.4.)

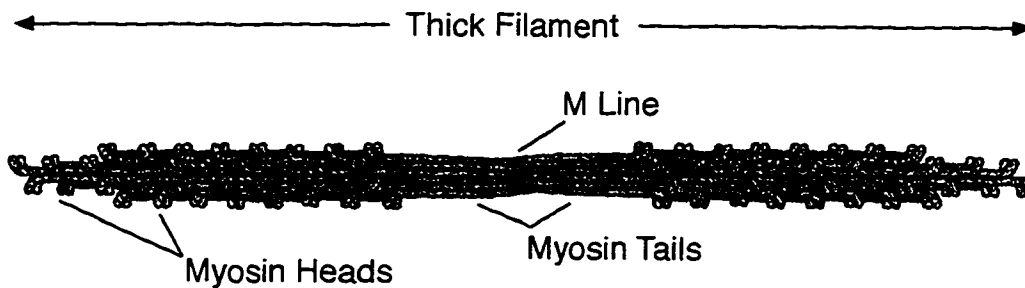


Figure 3. A diagram of individual myosin molecules aggregated into a thick filament with the M Line at the center. Note that the individual myosin molecules are arranged in the thick filaments such that the heads in each half of the filament are directed away from the M Line and toward the ends of the sarcomere. At the M Line, the tails of the center-most individual myosin molecules meet. Several accessory proteins are located in the M Line region to stabilize the thick filament structure (Reproduced with permission, from Garrett and Grisham, 1995, Figure 36.11.)

*Myosin Molecule.* Myosin is a large, asymmetric protein consisting of six polypeptide sub-units: two heavy chains and two pairs of light chains (Lowey, 1986). Each heavy chain has two major domains: a globular head and an alpha-helical tail. The N-terminus of the heavy chain polypeptide is in the globular head while the C-terminus is at the end of the helical tail; the molecular weight of each heavy chain is 220 kDa. Each light chain of myosin is a slightly elongated globular polypeptide. There are two different classes of light chains, 'alkali light chains' and 'DTNB light chains,' distinguished by the chemical treatment required to dissociate the two different types of light chains from the heavy chain. The light chains range in apparent molecular weight from 16 kDa to 25 kDa (Silberstein, 1979; Lowey, 1986).

A complete myosin molecule is shown in Figure 4. The helical tails of two heavy chains are coiled about one another forming a left-handed coiled coil such that both heads are at the same end of the asymmetric molecule. The light chains are non-covalently associated with the heavy chain

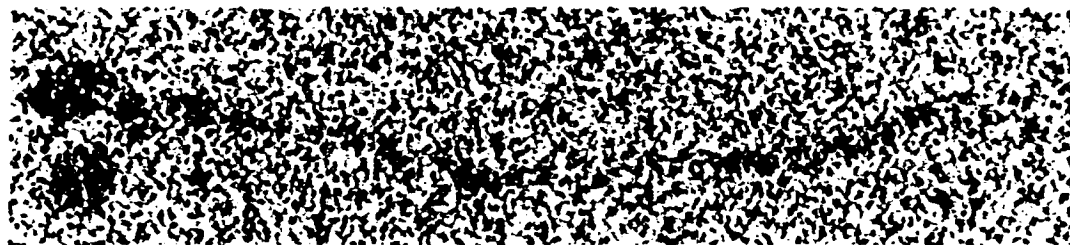
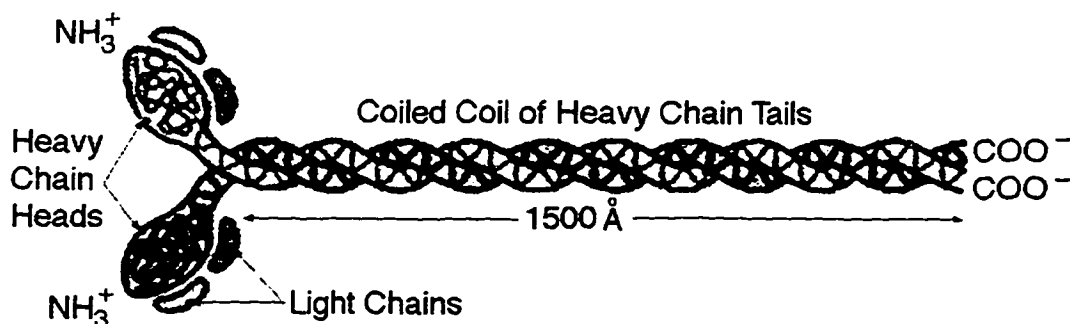


Figure 4. Diagram and photomicrograph of a single myosin molecule. A 'monodisperse' myosin molecule is not aggregated to any other protein molecule. (Reproduced with permission, from Garrett and Grisham, 1995, Figure 36.8.)



heads in heteromeric pairs. Two flexible 'hinge' regions exist along the length of the heavy chain tail. The first is at the junction between the heavy chain head and tail and allows for a large range of motion of the head relative to the tail. The second is approximately one-third of the way along the tail from the head and allows the tail to bend at that point (Lowey, 1986). In the non-aggregated monomeric state, each myosin molecule has a molecular weight of ~520 kDa and is ~1500 Å in length (Lowey, 1986; Rayment et al., 1993; Garrett and Grisham, 1995).

The propensity of individual myosin molecules to aggregate into the thick filaments seen in myofibrils is a function of the tail of the molecule, which is insoluble at physiological ionic strength. At physiological ionic strength, monomeric myosins spontaneously aggregate to form the thick filaments (Goldspink, 1980; Lowey, 1986).

The functional properties of myosin reside in the hydrophilic heads. In muscle contraction, myosin binds adenosine triphosphate (ATP) and actin. It has been shown (Rayment et al., 1993), that the ATP and actin binding sites are on opposite sides of myosin's globular heads (Figure 5). It is also well known that ATP plays a role in the binding of myosin and actin (Szent-Györgyi, 1960; Goldspink, 1980). In addition to binding ATP, myosin acts as an ATPase, hydrolyzing ATP to ADP (Englehardt and Ljubimowa, 1939). The combination of these activities results in muscle contraction.

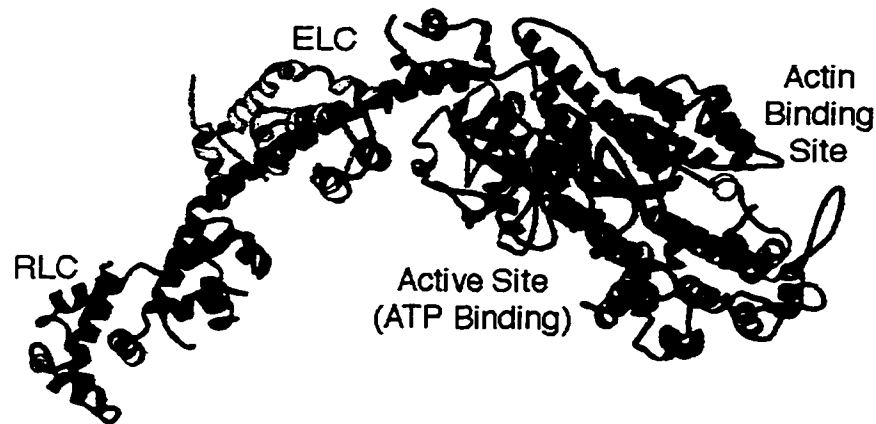


Figure 5. Ribbon diagram of a single myosin head. One pair of light chains (labeled ELC for essential light chain and RLC for regulatory light chain) combine with the head of the heavy chain to form a complete and stable myosin head. Note that the actin and ATP binding sites are on opposite sides of the head. (Adapted from Rayment et al., 1993.)

*Sliding Filament Model.* When a muscle contracts, each sarcomere is literally contracting or getting shorter. The process is described by the Sliding Filament Model (Huxley and Niedergerke, 1954; Huxley and Hanson, 1954), so named because the filaments 'slide' along one another during the process. At a molecular level, conformational changes are occurring in individual myosin molecules, in concert with the ATPase activity, which results in this sliding.

Contraction begins with the heads of the individual myosin molecules in the thick filaments binding ATP molecules; this induces a conformational change that bends the myosin heads away from the thick filament and toward the thin filament. The myosin heads are now positioned so that they can bind to individual actin molecules on the neighboring thin filament, forming what are known as 'crossbridges' between the thick and thin filaments (Figure 6). In what is referred to as the 'oar stroke' of the contraction, as myosin hydrolyzes the ATP its heads continue to bend, pulling against the now bound thin filaments. Since the heads of the myosin molecules on each half of the thick filaments have opposite orientation relative to the M Line at the center of the

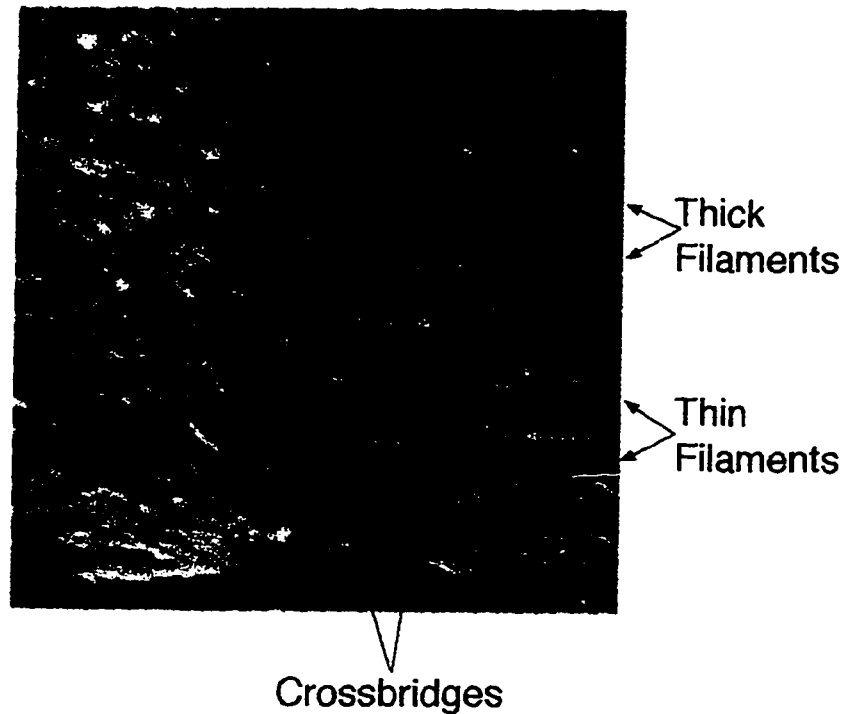


Figure 6. An electron micrograph of honeybee flight muscle showing crossbridges between the thick and thin filaments. Conformational changes in the myosin molecules cause their heads to bend toward and bond to actin molecules in the thin filament thus forming crossbridges between the filaments (Reproduced with permission, from Pollack, 1990, Figure 2.15C.)

sarcomere (Figure 3, page 19), the thin filaments are pulled toward the center of the sarcomere.

Thus, the thick and thin filaments slide past one another and the sarcomere contracts (Figure 7).<sup>1</sup>

The conformational changes occur sequentially as ATP is bound, hydrolyzed, and the hydrolysis products are released. The energy source for the physical changes is the hydrolysis of ATP by myosin. In this way, myosin converts the chemical energy of hydrolysis into the mechanical energy of muscle contraction.

---

<sup>1</sup> Recent re-examinations of data collected by a number of investigators, in support of Sliding Filament Model, suggests that contraction of the filaments also occurs during contraction of the sarcomere (Pollack, 1990, Chapter 2).

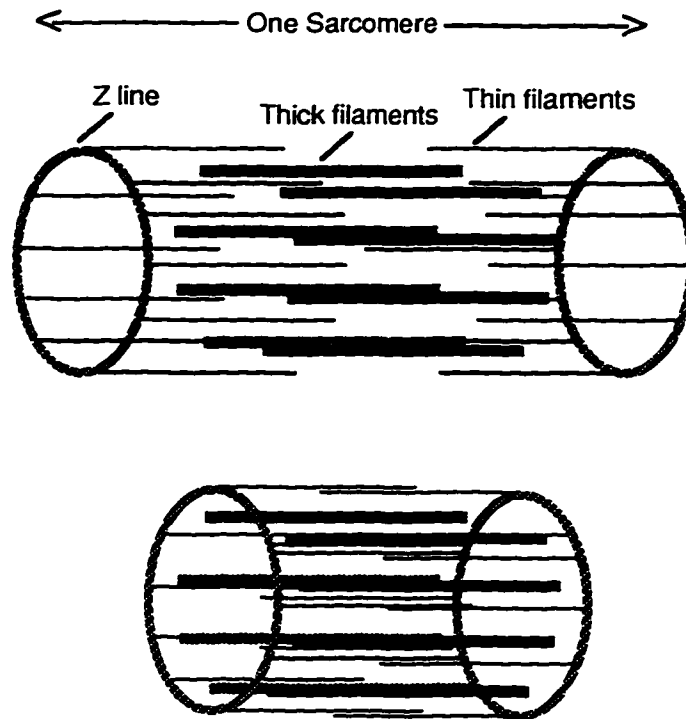


Figure 7. Diagram of a single sarcomere before (top) and after (bottom) contraction. The Sliding Filament Model describes how the sarcomere gets shorter as the filaments slide between one another (interdigitate) during muscle contraction (Re-drawn, from Stryer, 1975, Figure 35.5.)

*Extraction of Myosin from Muscle.* The extraction of myosin from muscle is based on the differential solubility of myosin and other muscle proteins as a function of ionic strength,  $\Gamma$ . Both myosin and actin are insoluble at physiological ionic strength and pH ( $\Gamma = 0.150$  M at pH 7.4) (Goldspink, 1980; Margossian and Lowey, 1982). Aggregation of myosin begins at  $\Gamma = 0.3$  M and it becomes increasingly insoluble as ionic strength decreases (Ebashi and Nonomura, 1973). The major contaminating protein in the purification of myosin from skeletal muscle is actin, which is already quite insoluble at  $\Gamma = 0.3$  M where myosin is still mostly in solution (Ebashi and Nonomura, 1973).

The ionic strength of the extraction buffers is selected to alternately precipitate and solubilize myosin, enabling its physical separation from the other proteins. For example, at  $\Gamma = 0.3$  M when myosin is in solution, centrifugation is used to separate away any insoluble, unwanted proteins which are then easily discarded. Figure 8 charts the ionic strength of the buffers at each step during the purification. Ionic strength values are calculated as

$$\Gamma = \frac{1}{2} \sum cz^2$$

where  $c$  = concentration of each ion in M and  $z$  = charge on each ion; the units of  $\Gamma$  are M (Skoog and West, 1976, 110).

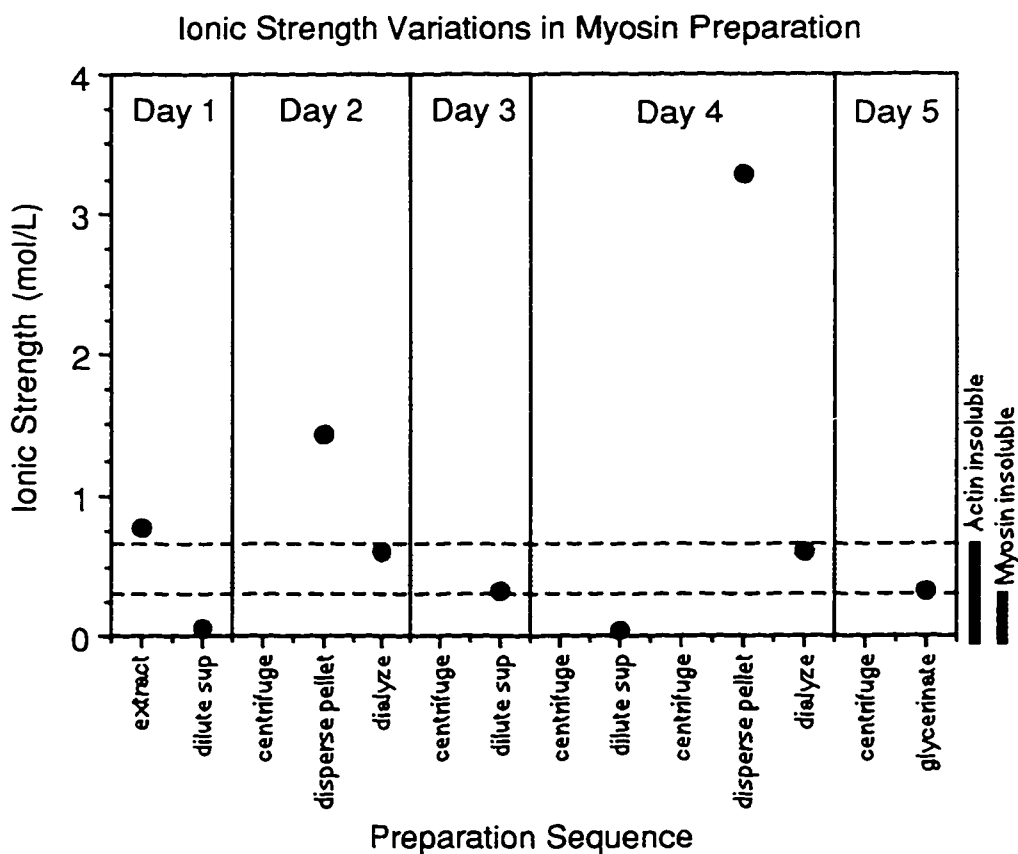


Figure 8. Over the course of the myosin preparation, the ionic strength of the buffers are varied to alternately solubilize and precipitate myosin relative to the other proteins present. In and above the shaded region myosin is soluble but actin is not; below the shaded region myosin and actin are both insoluble.

Once the myosin is purified it is glycerinated for storage. Gently folding the myosin into a homogeneous solution with glycerol allows the myosin to be stored at  $-20\text{ }^{\circ}\text{C}$  without freezing solid. Unfortunately, glycerination and storage of myosin result in some damage and formation of aggregates. Since the myosin must be monodisperse when applied to the anti-myosin immunoaffinity columns, any aggregated material must be removed prior to loading the columns. This is accomplished by size exclusion chromatography.

*Determination of Myosin Yield and Purity.* The protein concentration of myosin samples is determined by absorbance spectroscopy and purity is monitored by Sodium Dodecyl Sulfate Polyacrylamide Gel Electrophoresis (SDS-PAGE) analysis.

Absorbance at 280 nm ( $A_{280}$ ) is due to the aromatic amino acids tyrosine and tryptophan of the protein in a sample.  $A_{280}$  is converted into protein concentration (mg/mL) through Beer's Law ( $\text{mg/mL protein} = A_{280}/\epsilon^{1\%_{280\text{nm}}}$ ) using an extinction coefficient for myosin of  $\epsilon^{1\%_{280\text{nm}}} = 5.0\text{ mL/mg-cm}$  (Margossian and Lowey, 1978; Silberstein, 1979).

Corrections must be made for two possible sources of interference in these samples. If there is aggregated protein present there will be an apparent 'absorbance' at 340 nm, which actually represents light scattering caused by the aggregated material (Slater, 1970; Grant, 1995). The ratio of  $A_{340}$  to  $A_{280}$  expressed as a percent ( $(A_{340}/A_{280}) \times 100$ ), serves as an indicator of the presence of aggregated material, where a low percent indicates primarily non-aggregated (monodisperse) myosin in the sample. A rough correction may be made to the  $A_{280}$  values for the raised baseline the light scattering causes by subtracting  $A_{340}$  from  $A_{280}$  before applying Beers' Law (Grant, 1995). When values of  $(A_{340}/A_{280}) \times 100$  exceed 10% the sample is considered too turbid to obtain a reliable absorbance reading; removal of aggregates by centrifugation is used to reduce the turbidity to an acceptable level (Silberstein, 1979).

Additionally, if nucleic acids are present in the sample, the  $A_{280}$  values are corrected by the method of Warburg and Wharton (as described in Robyt and White, 1987). In this method, the ratio of  $A_{280}/A_{260}$  determines a correction factor by which  $A_{280}$  is multiplied before applying Beers' Law. When  $A_{280}/A_{260} > 1.7$ , the protein is considered free of nucleic acid contamination and no correction is necessary (Robyt and White, 1987).

To track the purification as myosin is extracted, aliquots are taken at various stages of the extraction and analyzed by the Laemmli method of SDS-PAGE to visualize the proteins present. In this method, protein samples are boiled at 100 °C with sodium dodecylsulfate (SDS) and  $\beta$ -mercaptoethanol to completely denature the proteins and to coat them with negatively charged SDS molecules. Once converted to uniform negative charge, the proteins are applied to a porous polyacrylamide gel and are induced to migrate through the gel under the influence of an applied electric field. The rate of migration is directly proportional to the molecular weight of each protein (Robyt and White, 1987). Soaking the electrophoresed gel in a solution of Coomassie Blue stain renders the bands of separated proteins visible since the proteins form colored precipitates with the organic dye (Harris and Angal, 1994). SDS-PAGE analysis of sequential extraction steps shows the gradual removal of key contaminating proteins such as actin (see *Results*).

*Size Exclusion Chromatography of Myosin.* Size Exclusion Chromatography (SEC) is used to separate away any aggregated material from the monodisperse myosin (Silberstein, 1979). The basis of separation in Size Exclusion Chromatography is the hydrodynamic radius of the solute, that is, its effective radius, also known as the Stokes' radius (Snyder and Kirkland, 1979).

The matrices used in SEC are porous inert beaded polymers. Polymers of dextran, agarose, polyacrylamide, and polystyrene have been used to prepare SEC matrices (Fischer, 1969; Robyt and White, 1987). The polymerization is conducted in such a way to create a known, narrow range

of pore sizes in the beads. When passed through a column of this material, a mixed population of proteins is separated according to their Stokes' radius. As shown in Figure 9, as the molecules pass through the column 'bed' they can move through the spaces between the beads as well as in and out of the pores of the beads, depending on their effective radius. Molecules small enough to permeate the pores travel a greater distance to traverse the bed than large molecules, which simply pass between the beads. The net effect is that the smallest molecules are retained on the column the greatest amount of time.

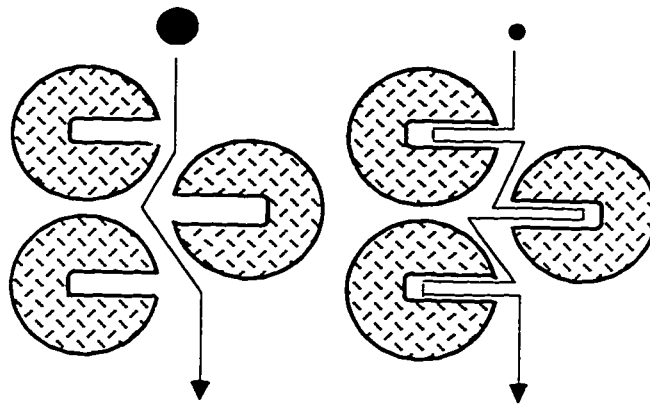


Figure 9. In SEC, molecules of different sizes travel different paths through the column bed and therefore have different retention times. Smaller molecules travel longer paths so are retained longer on the column.

Each matrix has a 'fractionation range' which is defined by the upper and lower size limits of molecules that matrix can separate. Figure 10 shows a diagram of the fractionation range and corresponding chromatogram for a theoretical SEC matrix. Molecules with a Stokes' radius larger than point A on the figure are completely excluded from this matrix and elute in the void volume,  $V_0$ , while molecules with a Stokes' radius smaller than point B are retained the maximum amount of time and elute at  $V_t$ ; molecules in this latter size range are said to 'totally permeate' the gel. In the size range between these two limits, molecules permeate the beads to varying degrees and so are separated according to size and elute as separate peaks between  $V_0$  and  $V_t$ . It is important to



note that the Stokes' radius is mainly a function of molecular weight for globular proteins, however, for asymmetric proteins, such as myosin, the Stokes' radius (i.e., the effective radius) will be much greater than that predicted by molecular weight alone.

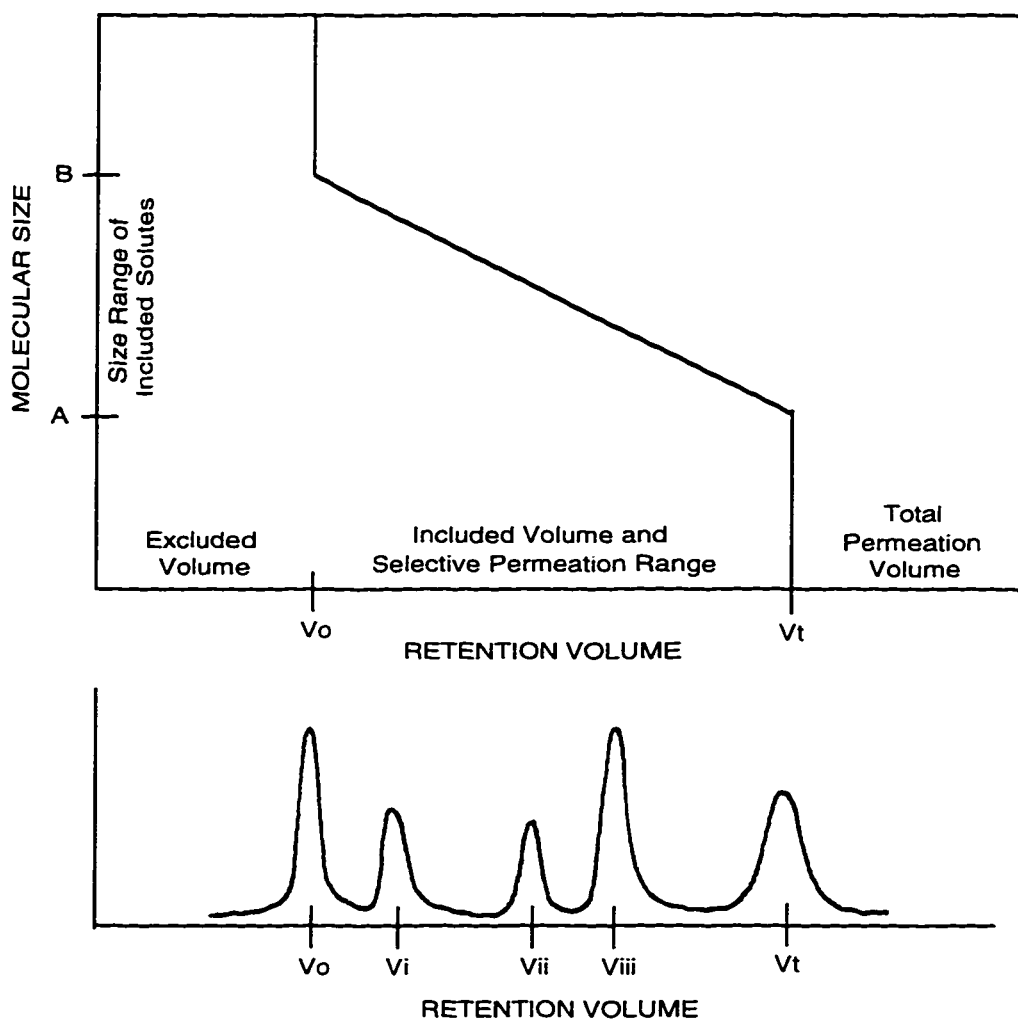


Figure 10. The fractionation range and corresponding chromatogram for a hypothetical size exclusion matrix. For each matrix, solutes can be separated from one another if their effective size falls within a range (A to B) corresponding to the Selective Permeation Range of the matrix. Such solutes elute within the Included Volume of the matrix according to their size. For each different Stokes' Radius a different eluted peak,  $V_i$ , will appear. Solute larger than the fractionation range will be completely excluded from the matrix and elute in the Void Volume,  $V_o$ ; solutes smaller than the fractionation range will be maximally retained and elute as a peak of solutes which totally permeate the matrix,  $V_t$ . (Adapted from Snyder and Kirkland, 1979, Figure 12.2.)

A single myosin molecule has a molecular weight of ~520 kDa (Rayment et al., 1993; Garrett and Grisham, 1995). Aggregates of myosin will at a minimum be dimers, and depending on the exact structure of the aggregate, will have an increased hydrodynamic radius. The SEC matrix selected must have a fractionation range able to resolve the monodisperse myosin from the various aggregates which are likely to be present (see *Discussion and Conclusions*). The expected aggregates would be homo-aggregates of myosin and hetero-aggregates of actin with myosin, actomyosin. The matrix used in this study was Sepharose 2B with a fractionation range of 70 to 40,000 kDa (Smith, 1988, Table 10.9.2). Aggregated material was expected to elute rapidly or even be completely excluded from this matrix, while monodisperse myosin was expected to be well included.

## **Monoclonal Antibodies**

*Overview.* Anti-myosin monoclonal antibodies belonging to immunoglobulin classes IgG and IgM were used in this study. Monoclonal antibodies (MAbs) are the product of hybridoma cells, a genetically identical clone of cells produced by fusing the genetic material from a normal lymphocyte and a myeloma cell (Köhler and Milstein, 1975). Five distinct cell lines were raised, each of which produces a unique anti-myosin monoclonal antibody with binding specificity to a specific myosin epitope (Webster et al., 1988; Silberstein and Blau 1986; Hughes et al., 1993; Cho et al., 1994). The five monoclonal antibodies were collected from cell lines grown both by culturing under sterile conditions and as 'ascites fluids.' Purification of monoclonal antibodies was accomplished by saturated ammonium sulfate precipitation followed by size exclusion chromatography. Enzyme-Linked Immunosorbent Assays (ELISAs) were used to determine the total concentration of MAb in any sample.

*IgG and IgM Class Immunoglobulins.* Immunoglobulins (Igs) comprise the diverse family of hallmark proteins of the immune system (complete review in Eisen, 1980, Chapter 14). Igs have

the ability to bind other molecules with extremely high specificity. The interaction is based on the reaction of the Ig with a chemical marker known as the antigenic determinant, or 'epitope,' on the target molecule, or 'antigen.' For example, when the antigen is a protein the epitope is a specific amino acid sequence of that protein.<sup>2</sup>

Since immunoglobulins are proteins, they can themselves serve as antigens. Igs are categorized into five classes, or 'isotypes,' based on characteristic epitopes they bear. Each Ig molecule bears one of five types of class-defining epitopes, designated  $\gamma$ ,  $\alpha$ ,  $\epsilon$ ,  $\delta$ , or  $\mu$ ; the five corresponding Ig classes are IgG, IgA, IgE, IgD, and IgM. Igs can be either membrane bound or circulating; the latter are called antibodies (Abs). The antibodies used in this study belong to two Ig classes, IgG and IgM.

IgG-class Abs are the smallest and structurally most simple Igs, and can be thought of as having the shape of the letter 'Y.' As can be seen in Figure 11, IgGs are composed of two pairs of non-identical polypeptides covalently bound together by disulfide bridges; the smaller polypeptides are referred to as light chains and the larger as heavy chains. The antigen binding sites are located at the end of each arm of the 'Y' and are formed by the combination of portions of both the heavy and light chains. The binding sites on each arm are identical so each IgG molecule can bind two identical epitopes.<sup>3</sup> A single IgG molecule is ~150 kDa in weight (Eisen, 1990).

---

2 The epitopic amino acid sequence is not necessarily in a linear array on the molecule.

3 The two epitopes can be on the same or two separate molecules of antigen.

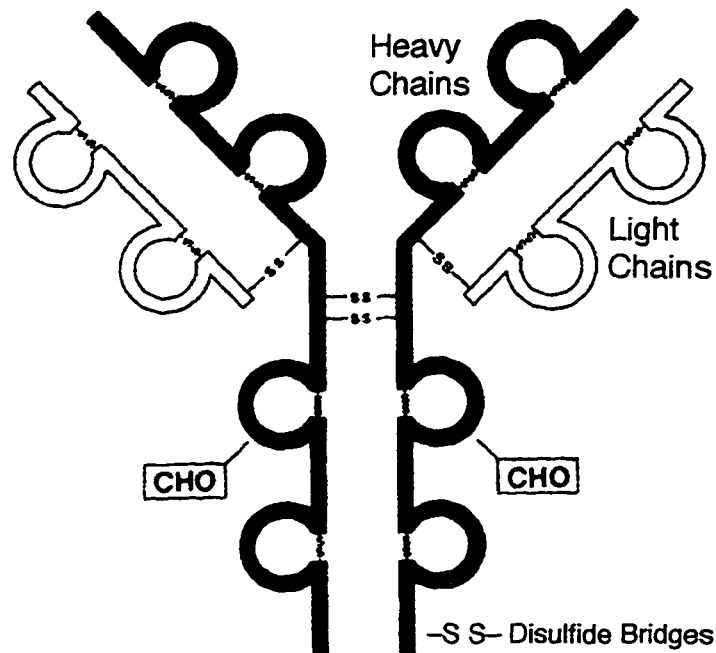


Figure 11. Diagram of an IgG-class immunoglobulin. Two pairs of non-identical polypeptides, known as heavy and light chains, are covalently bound together through disulfide bridges to form a molecule with the shape of the letter 'Y' (Adapted from Eisen, 1990, Figure 14-10.)

At ~900 kDa, IgM-class Abs are the largest and most complex Igs; a diagram and clay model of a single IgM molecule are shown in Figure 12. IgM-class antibodies can be thought of as five individual IgG-class molecules covalently bound together by disulfide bridges and a protein known as the 'J' chain near the bottoms of the Ys. The resultant pentameric IgM macromolecule has a 'spider-like' shape. As with IgG-class antibodies, there is an identical antigen binding site at the end of each arm of each Y, so a single molecule of IgM can potentially bind ten separate but identical epitopes.

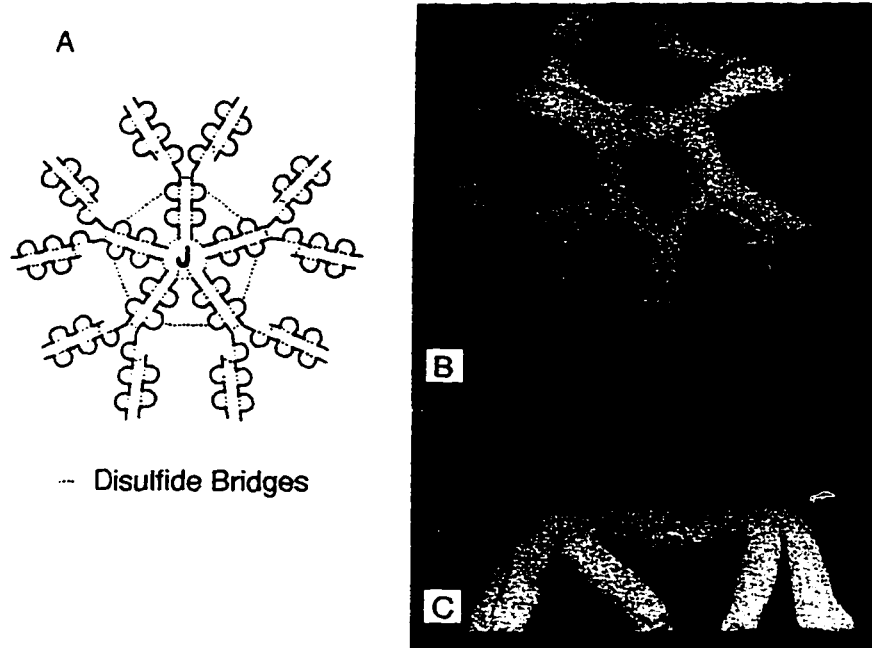


Figure 12. A diagram (A) and clay model (B, top view and C, side view) of an IgM-class immunoglobulin. This complex macromolecule can be thought of as comprising five IgG-like sections joined by disulfide bridges and the J-protein at the bases of the Y's to form an overall 'spider-like' shape (Reproduced with permission, from Eisen, 1990, Figure 14-12.)

*Hybridoma Cells and Monoclonal Antibodies.* Monoclonal antibodies (MAbs) are the product of hybridoma cells, a 'clone' of genetically identical antibody-producing cells. These cells are the result of genetically fusing antibody-producing spleen cells with myeloma cells (Köhler and Milstein, 1975). The resultant cells have the combined characteristics of the spleen cells and the myeloma cells: they secrete antibodies and they are 'immortal,' that is they can be grown continuously in culture. Spleen cells from Balb/c mice, that have been activated to secrete Abs to the epitope of interest, are used in the fusion to produce the hybridoma cell lines. The initial population of resultant hybridoma cells is polyclonal, that is, it comprises many genetically different cell lines producing many unique Abs to distinct epitopes. This polyclonal culture must be subcloned and screened for production of antibodies reactive to specific epitopes of interest until

individual clones with specific reactivities to unique epitopes are isolated. These individual cell lines, or clones, contain genetically identical cells and are designated 'monoclonal.' The antibodies that these individual cell lines secrete are thus called monoclonal antibodies (MAbs), each has binding specificity to a unique epitope.

Five distinct anti-myosin MAbs reactive to five distinct myosin epitopes were used in this study (Table 1). These anti-myosin MAbs were collected from hybridoma cell lines produced by L. Silberstein, and were previously shown to produce MAbs that bind unique myosin heavy chain epitopes (Webster et al., 1988; Silberstein and Blau 1986; Hughes et al., 1993; Cho et al., 1994).

Table 1 shows a summary of the hybridomas cell lines used in this study, the anti-myosin MAbs they secrete (original and current nomenclature), the Ig class of each MAb, the specific epitope to which each MAb reacts, and the contractile type of the muscle fiber on which the epitope has been located.

Hybridoma Cell Line	MAb Secreted		Ig Class of MAb	Myosin Epitope Recognized by MAb	Muscle Fiber Contractile Type
	Silberstein/Blau Nomenclature	Current Nomenclature			
MHC-F22	N2.221	MAb-F22	IgM	F22	Fast
MHC-F36	N3.36	MAb-F36	IgM	F36	Fast
MHC-S84	4A.840	MAb-S84	IgM	S84	Slow
MHC-S95	4A.951	MAb-S95	IgG	S95	Slow
MHC-25	4A.1025	MAb-25	IgG	25	Both

Table 1. The five monoclonal hybridoma cell lines each secrete a unique MAb. Each MAb reacts with a unique myosin heavy chain (MHC) epitope. Each MAb reacts with either fast-contracting (F) muscle fibers or slow-contracting (S) muscle fibers, except for MAb-25 which reacts with all muscle fibers. (These MAbs were originally identified by the designations shown as 'Silberstein/Blau Nomenclature'.)

MAB-F22 and MAB-F36 both react with epitopes on fast-contracting (F) fibers, MAB-S84 and MAB-S95, both react with epitopes on slow-contracting (S) fibers, and MAB-25 reacts with an epitope that occurs on all rat skeletal muscle fibers. All these anti-myosin MABs belong either to Ig-class IgG or IgM, as indicated. While actively growing, these cells secrete MABs into the media in which they are grown. This is an easily collected though dilute source of MABs. In order to acquire more concentrated solutions of MABs, 'ascites' were produced.

*Ascites Production.* Ascites is a MAB-rich fluid that accumulates in the peritoneal cavity of an animal carrying a myeloma tumor (Yokoyama, 1991). The tumor is induced in the animal by intraperitoneal injection of hybridoma cells into the abdominal cavity. As the cells grow within the cavity they secrete MABs into the surrounding fluid. Since the hybridomas are monoclonal (i.e., genetically identical), each ascites contains MABs with identical and unique specificity to myosin. The MABs were purified from the ascites by precipitation with saturated ammonium sulfate followed by size exclusion chromatography.

*Saturated Ammonium Sulfate Precipitation of Immunoglobulin from Ascites.* Immunoglobulins are just one type of protein present in ascites (Andrew and Titus, 1994; Fuller et al., 1988). The Ig can be separated away from the bulk protein in the ascites by precipitation with saturated ammonium sulfate (SAS) (Goding, 1986; Fuller et al., 1988).

This process, known as 'salting out,' is based on the fact that ions and molecules in solution are surrounded by a hydration sphere of water molecules (Harris and Angal, 1994). Adding high amounts of ions to the protein solution sets up a competition between the proteins and the ions for the water molecules (Harris and Angal, 1994; Robyt and White, 1987). The consequence is that the proteins are left relatively non-hydrated so they aggregate and fall out of solution, or precipitate.

The salt concentration range over which a particular protein precipitates may overlap with the precipitating concentration range for other proteins; therefore, the resultant precipitate may not be completely purified, but it is greatly concentrated in the protein of interest. SAS concentrations in the range of 30-50% (v/v) are typically used to precipitate IgM from ascites (Andrew and Titus, 1994). The major contaminant which co-precipitates with immunoglobulin in the SAS precipitation from ascites is serum albumin (Andrew and Titus, 1994; Hockfield et al., 1993). Due to the large size difference between even the smallest immunoglobulins (MW ~150 kDa) and albumin (MW 66 kDa), albumin can be separated from the immunoglobulin by size exclusion chromatography. In this study, the size exclusion matrix selected for the separation of albumin from immunoglobulin is Sephacryl S300-HR. This co-polymer of dextran and bisacrylamide has a fractionation range of 10-1500 kDa (Stellwagen, 1990; Smith, 1988). Once the immunoglobulin is purified, analysis of the total concentrations for immunoglobulins is determined by Enzyme Linked Immunosorbent Assays.

*Enzyme Linked Immunosorbent Assays.* Enzyme Linked Immunosorbent Assays (ELISAs) occur as a series of layers of immunoselective binding which are visualized by a colorimetric enzyme-substrate reaction. This highly specific and sensitive assay is based on the antibody-antigen reaction.

The assays are carried out on microtiter plates made of a PVC- or polystyrene-type plastic (Hockfield et al., 1993); after each step, any unbound material is washed away (see *Materials and Methods*). The wells are 'coated' in the primary (1°) layer with an Ab known to bind the antigen of interest; then any non-coated sites are 'blocked' against non-specific binding with a buffered protein solution. Both the coating and the blocking occur as a simple adsorption of protein onto the plastic (Stevens et al., 1995). When the sample is added to the wells, only the analyte of interest is bound to the plate by virtue of the immunospecificity of the Ab in the 1° layer. The



method of detection of the bound analyte depends upon the specific type of sandwich ELISA. Two versions of sandwich ELISAs were used in this study, 'homo-isotypic' and 'hetero-isotypic.'

A homo-isotypic sandwich ELISA (Figure 13) was used to determine the Ig concentration of purified IgG-class and IgM-class anti-myosin MAbs. In the homo-isotypic sandwich ELISA, the antibody in the 1° layer is a commercially available anti-Ig antibody which reacts with the isotype of the anti-myosin MAb being assayed (i.e., anti- $\mu$  to assay for IgM-class MAbs; anti- $\gamma$  to assay for IgG-class MAbs); the anti-myosin MAb is the antigenic sample in the 2° layer. The 3° layer is an anti-Ig-enzyme conjugate in which the anti-Ig Ab is the same one used in the 1° layer. In this conjugated reagent, the Ab moiety reacts with the sample which is bound to the plate through the 1° layer of Ab, while the enzyme moiety is free to react with its substrate. Note that the MAb of interest is thus 'sandwiched' between the anti-Ig in the 1° layer and the anti-Ig-enzyme in the 3° layer.

The enzyme/substrate reaction results in a color change in which the intensity of the color is a function of the extent of reaction. An Ig standard, applied to the plate in serial dilutions of known concentrations, is used to construct a standard curve of absorbance as a function of Ig concentration. The concentration of Ig in the sample is quantified by comparison to the standard curve.

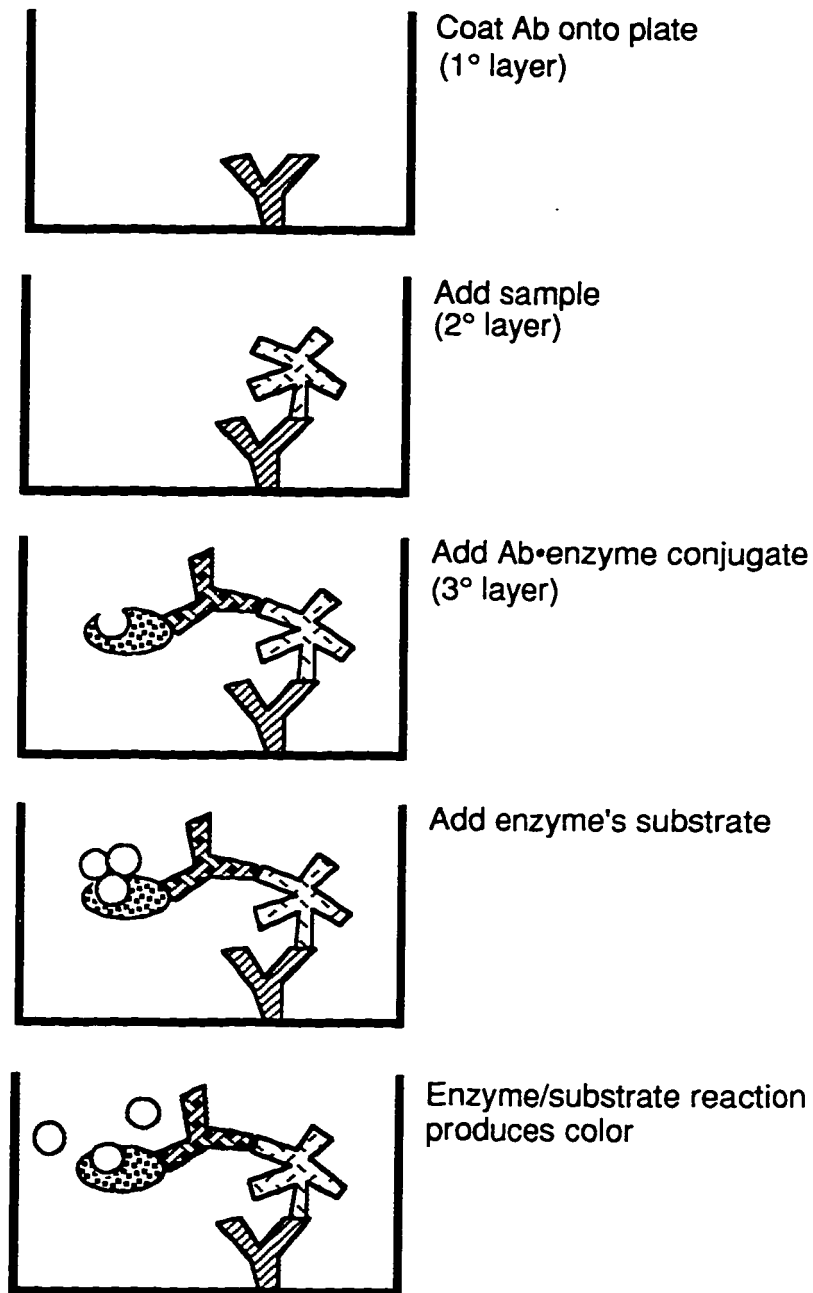


Figure 13. Homo-isotypic sandwich ELISAs are based on a sequential series of selective binding steps determined by the immunospecificity of the reagents for the analyte of interest. The final step is an enzyme/substrate reaction that results in a color change that is quantitatively proportional to the amount of analyte present. In homo-isotypic sandwich ELISAs, the 1° and 3° layers are anti-Ig Abs of the same Ig-class (i.e., isotype); the sample is an anti-myosin MAb (see *Materials and Methods*, for details).

A 'hetero-isotypic' sandwich ELISA was used to detect the presence of specific myosin epitopes in myosin samples or in peaks from the immunoaffinity columns. The hetero-isotypic ELISA has an additional layer compared to the homo-isotypic sandwich ELISA. The final stage of a hetero-isotypic sandwich ELISA is shown in Figure 14. The myosin is sandwiched in the sample layer between two different anti-myosin MAbs in the 1° and 3° layers. In order for this assay to work, the Ig-class of the MAbs in the 1° and 3° layers must be different (i.e., hetero-isotypic). The anti-Ig-enzyme conjugate is added as the 4° layer and is specific for the anti-myosin MAb in the 3° layer. As in the homo-isotypic sandwich ELISA, the enzyme/substrate reaction results in a color change proportional to the concentration of antigen (i.e., the myosin epitope of interest) present; detection occurs spectrophotometrically.

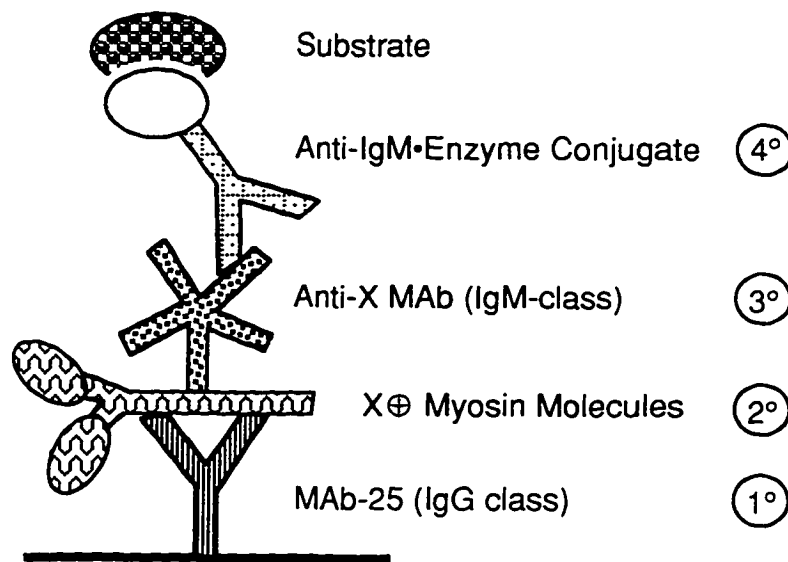


Figure 14. Diagram of the interactions of individual molecules in each successive layer in the hetero-isotypic sandwich ELISA. This ELISA is designed to detect the presence of myosin molecules bearing the epitope X. 1° layer = an IgG-class MAb which binds any myosin molecules; 2° layer = myosin sample (a mix of some molecules with epitope X (X+), and some without (X-)); 3° layer = an IgM-class MAb which binds myosin bearing the epitope X; 4° layer = an anti-IgM-enzyme conjugate. Any molecule of myosin can be bound by the IgG-class anti-myosin MAb in the 1° layer, but the IgM-class anti-myosin MAb in the 3° layer only binds X+ myosin molecules. Finally, the anti-IgM-enzyme conjugate will only bind to IgM-class anti-myosin MAbs bound in the 3° layer.

## **Putative Myosin Isozymes**

*Overview.* Skeletal Muscle has been classified as fast- or slow-contracting by virtue of its relative contractile properties as determined in physiological studies. These contractile properties can change for a given fiber over the course of development (Whalen et al., 1981; Pette, 1980) or in certain disease states (Silberstein and Blau, 1986; Webster et al., 1988). Histochemical studies have shown that chemical differences exist between fast- and slow-contracting muscle fibers (Goldspink, 1980). Furthermore, immunohistochemical studies have shown that the fibers can be divided into many subtypes within the fast and slow classes which suggests that the differences exist at the level of individual myosin molecules (Silberstein and Blau, 1986; Webster et al., 1988; Hughes et al., 1993; Cho et al., 1994). From these sorts of studies it has been postulated that myosin exists in multiple forms, or isozymes (Hughes et al., 1993; Hämläinen and Pette, 1995). It is reasonable to assume that the differences between myosin isozymes is based in differences in their amino acid sequences (i.e., epitopic differences). If this is true, then the sub-populations of isozymes may be separable using immunoaffinity chromatography (Chizzonite et al., 1982; Komuro et al., 1986; Silberstein, 1979; Silberstein and Lowey, 1981).

*Histochemical Studies of Muscle Tissue.* The study of muscle began in the second half of the 19<sup>th</sup> century when microscopy studies identified morphologically distinct types of muscle tissue and observations of 'contractility' began (reviewed in Huxley, 1980). Early in the 20<sup>th</sup> century, it was discovered that muscle contraction is linked to hydrolysis of adenosine triphosphate (ATP) (Englehardt and Ljubimowa, 1939). Two functionally distinct groups of vertebral skeletal muscle, fast- and slow-contracting, were identified and it was later found that the rates of ATP hydrolysis occurring in these muscles correlated with the rates of muscle contraction, as determined by physiologic studies; that is, fast rates of ATP hydrolysis were observed in fast-contracting muscles, slow rates of ATP hydrolysis occur in slow-contracting muscles (Barany et al., 1967).

Modern physiological, biochemical, and histochemical studies have shown that the contractile properties of muscle differ between different muscle groups (e.g. fast- and slow-contracting) (Goldspink, 1980), over the course of development (i.e., in adult, juvenile, and embryonic stages) (Silberstein et al., 1986; Webster et al., 1988), and in certain muscle diseases (Silberstein et al., 1986; Webster et al., 1988).

Histochemical studies have shown that differences exist between individual muscle fibers within a given muscle (Hämäläinen and Pette in 1995). In these studies, muscle tissue sections are treated with a stain that forms a dark precipitate when ATP is hydrolyzed. Pre-treatment of muscle sections with acidic or alkaline buffers results in staining patterns differences between slow- and fast-contracting fibers, indicating a difference between individual fibers in the pH-stability of their ATPase activity.

Figure 15 shows the results of one of the histochemical staining experiments reported by Hämäläinen and Pette in 1995. The ATPase activity of slow-contracting soleus muscle was studied in serial cross sections stained at different pHs. In the top panel, at pH 4.3, fiber 1 is dark while fibers A, B, and D are all pale. At pH 4.55, fiber 1 still stains dark, fibers B and D begin to show some color, fiber A remains pale. Finally, at pH 10.4, fiber 1 is pale while fibers A, B, and D are all dark. Since dark color is indicative of ATPase activity, it can be seen that fiber 1 has the greatest acid-stable ATPase activity while fibers B and D have slightly acid-stable ATPase activity. On the other hand, fibers A, B, and D are all seen to have alkaline-stable ATPase activity while the ATPase activity of fiber 1 is not at all stable at alkaline pH. Similar results were obtained when this type of experiment was repeated with serial sections of the fast-contracting tibialis anterior muscle: some fibers were seen to have acid-stable ATPase activity while some fibers had alkaline-stable ATPase activity.

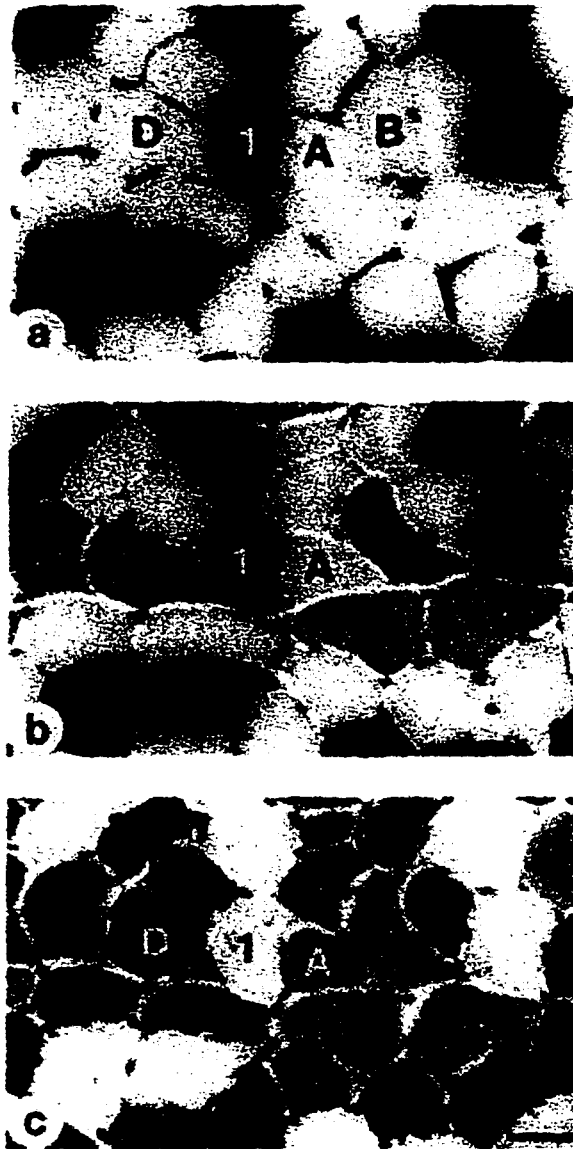


Figure 15. In ATPase histochemical studies, individual fibers within the slow-contracting soleus muscle show pH-dependent staining. Serial cross sections of soleus muscle were stained at (a) pH 4.3, (b) pH 4.55, and (c) pH 10.4. At pH 4.3 and pH 4.55, fiber 1 is dark, indicating that its ATPase activity is acid stable. At pH 10.4 fibers A, B, and D are all dark, indicating that their ATPase activity is alkaline stable; the light color of fiber 1 at this pH indicates that its ATPase activity is not at all alkaline stable. (Reproduced with permission, from Härmäläinen and Pette, 1995.)

These types of staining experiments identified a range of different types of fast- and slow-contracting fibers with respect to the pH sensitivity of their ATPase activity. Since the ATPase activity in muscle tissue is the function of myosin, Hämäläinen and Pette concluded that “the molecular basis of this diversity relates to the expression of various myosin isoforms [within individual fibers] ....” Furthermore, noting that individual myosin molecules are comprised of both heavy and light chains, they point out that “the combinatorial patterns of myosin heavy and light chains create a multiplicity of isomyosins far beyond the number of fiber types that can be histochemically distinguished” (Hämäläinen and Pette, 1995).

If the differences between myosin isozymes exist in their primary amino acid sequences, then the sequence differences that are characteristic of different isozymes can serve as identifying markers of those isozymes. Furthermore, if the differences are sufficient to serve as antigenic determinants, or 'epitopes,' which can be recognized and distinguished by antibodies, then those antibodies can be used to probe for the different isozymes. This is the basis of immunohistochemical studies.

*Immunohistochemical Studies of Muscle Tissue.* The usefulness of histochemical studies in probing for different myosin isozymes has been expanded by making use of the specificity available in immunohistochemical studies. In such studies, the staining patterns are indicative of fiber reactivity to individual anti-myosin MAbs, thus showing which myosin heavy chain epitopes are present in individual fibers.

Immunohistochemical studies such as those reported by Hughes et al. in 1993, led to the postulation of the existence of multiple isozymes of myosin. In their studies, Hughes et al. were able to identify epitopic differences between muscle fibers using the MAbs to myosin heavy chain epitopes that had been developed by Silberstein and Blau.

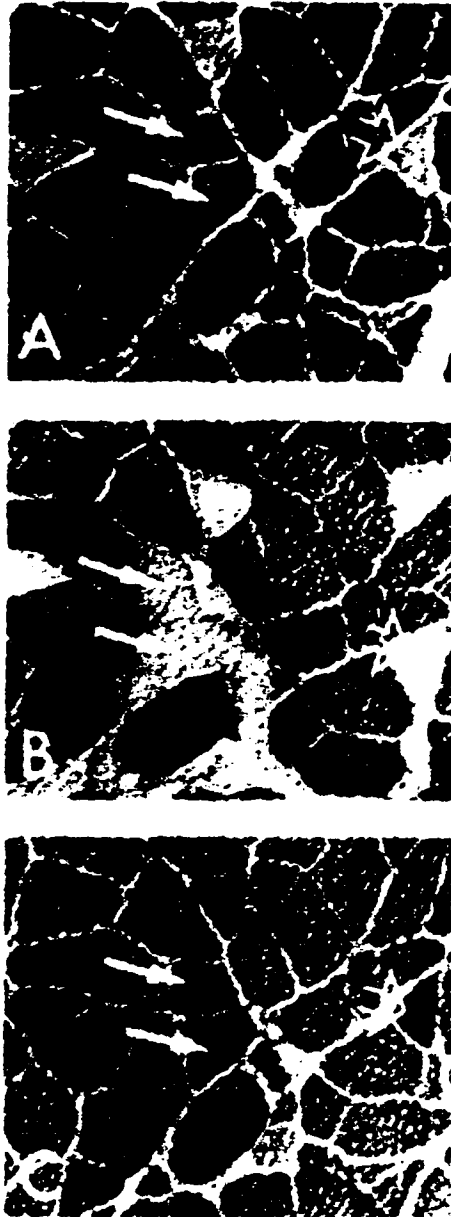


Figure 16. Serial sections of slow-contracting soleus muscle show different staining patterns in immunohistochemical studies with three anti-slow myosin heavy chain MABs. Soleus sections were treated with MAb A4.840 (panel A), MAb A4.951 (panel B), and MAb N2.261 (panel C). A dark color indicates a fiber which has reacted with the MAb, therefore, myosin molecules in that fiber do carry the epitope recognized by that MAb. The solid white arrows on the left indicate fibers which contains myosin heavy chain epitopes A4.840 and N2.261 but not the A4.951 epitope. The open arrow on the right indicates a fiber which contains myosin heavy chain epitope N2.261 but neither A4.840 nor A4.951. (Reproduced with permission, from Hughes et al., 1993).



In their studies, Hughes et al., treated serial sections of muscle tissue were with a panel of MAbs, each previously shown to react with a different myosin heavy chain epitope (Silberstein and Blau, 1986; Webster et al., 1988; Cho, 1992). Figure 16 shows the results of one experiment (Hughes et al., 1993). The panels show three serial sections of slow-contracting soleus muscle which have been treated with three different anti-slow MAbs. In panel A the muscle section has been treated with MAb A4.840, in panel B with MAb A4.951, and in panel C with MAb N2.261. A dark colored fiber indicates reaction with the MAb and so the presence of a given epitope in the muscle fiber. These three MAbs are all known to recognize slow muscle fibers (Silberstein and Blau, 1986). Note however, that individual slow fibers react differently with each of the three MAbs.

The bulk of the fibers in all three panels are dark, indicating that the bulk of these slow fibers react with all three anti-slow MAbs; but there are exceptions. The fibers indicated by the solid white arrows do react (are dark) with MAb A4.840 and MAb N2.261, but do not react (are light) with MAb A4.951; these fibers do contain myosin molecules which carry the A4.840 and N2.261 epitopes, but none with the A4.951 epitope (at least to the level of detection of these experiments). The fiber indicated by the outlined arrow does react with MAb N2.261, but does not react with either MAb A4.840 or MAb A4.951; this fiber only contains myosin molecules that carry the N261.1 epitope. The results of these immunohistochemical studies led Hughes et al. to postulate that multiple isozyms of myosin molecules exist within a single muscle fiber.

Immunohistochemical studies such as this identified epitopic differences between and within individual *muscle fibers*. This in turn, suggests an underlying difference between the *myosin protein molecules* which comprise those different fibers. It is reasonable to assume that the epitopic differences between distinct sub-populations of myosin molecules (i.e., isozyms) are based in differences in their amino acid sequences; that is, that the putative myosin isozyms bear different epitopes.

If distinct sub-populations of myosin exist, separating them from one another would allow analysis and characterization of the distinct isozymes. MAbs reactive to unique myosin heavy chain epitopes can be used in immunoaffinity chromatography to separate epitopically distinct isozymes from one another (Chizzonite et al., 1982; Komuro et al., 1986; Silberstein, 1979; Silberstein and Lowey, 1981). Once separated, the isolated species of isozymes can be analyzed for specific epitopic differences using those same MAbs. MAbs reactive to specific epitopes can be used to identify the presence of those epitopes, including whether each species of isozyme has a singular characteristic epitope, or if any species of isozymes bear combinations of different epitopes.

## **Immunoaffinity Chromatography**

*Overview.* In affinity chromatography the binding specificity of certain 'ligand' molecules for specific 'target' molecules is utilized to isolate the target molecules out of a mixed solution (Cuatrecasas and Afinsen, 1971). The ligand is immobilized on an inert chromatographic support through covalent bonds (Porath, 1968). The target is retained on the column by non-covalent interactions with the ligand. Eluants able to disrupt these interactions are used to recover the target from the column after undesirable materials have been eluted away (Goding, 1986; Pharmacia, 1986). An anti-myosin immunoaffinity column with a specific anti-myosin MAb as its ligand, will only bind those isozymes bearing the epitope recognized by that MAb. If two epitopes can be separated from one another on such a column, then those epitopes represent two distinct sub-populations of myosin molecules (i.e., two different isozymes).

*Affinity Chromatography.* The basis of separation in affinity chromatography is the binding specificity of a ligand for a particular component of a mixed solution (Cuatrecasas and Afinsen, 1971). The interaction between the ligand and its 'target' molecule is of a non-covalent nature and can be based on hydrogen bonding, electrostatic interactions, hydrophobic interactions, Van der

Waals forces, or a combination of these (Pharmacia, 1986). Since the moieties on the target that interact with the ligand are not necessarily adjacent to one another, there are also usually spatial factors involved in binding, such as a correspondence in size, shape, and orientation between the target molecule and the binding site of the ligand (Figure 17).

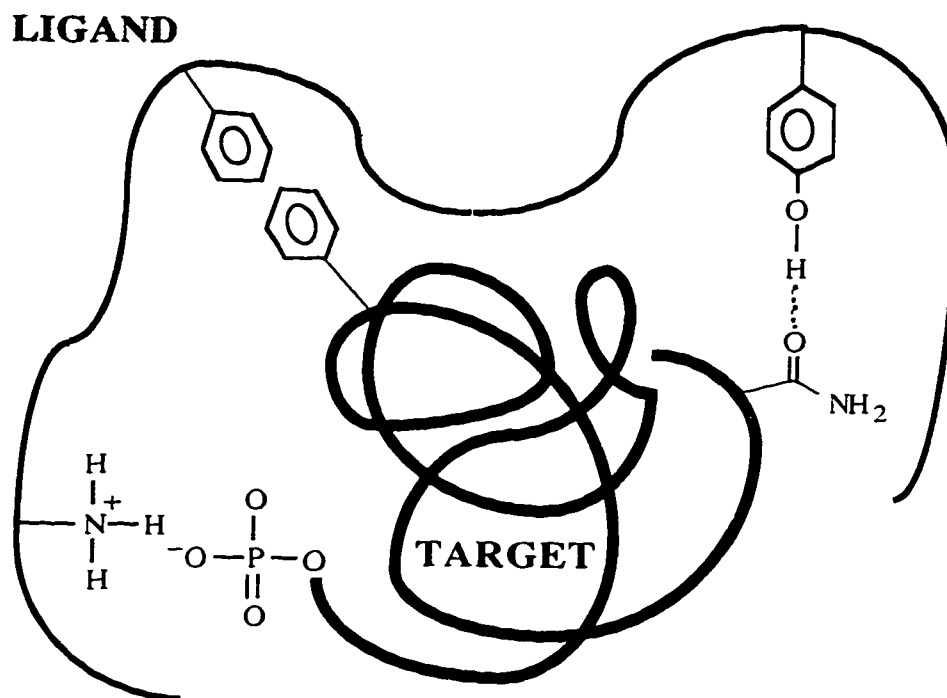


Figure 17. Diagram of a theoretical ligand/target interaction in affinity chromatography. The ligand on the matrix binds to its target molecule through various chemical interactions and through a close 'fit' in size and shape as well as orientation of the interacting moieties on the ligand and target molecules. An affinity matrix bearing these ligand molecules would be able to select and bind molecules of this target and remove them from a mixed solution. In the immunoaffinity chromatography in this study, the ligand is an anti-myosin MAb and the target is a myosin heavy chain epitope.

Affinity matrices are prepared by covalently coupling the ligand to an inert column matrix (Porath, 1968). Materials such as agarose, cellulose, or cross-linked dextrans or polyacrylamides have

been used as the inert matrix (Robyt and White, 1987). Numerous different types of ligands have been employed, such as: enzymes, enzyme substrates, antibodies, antigens, hormones, receptors, nucleotides, and even certain individual amino acids (Pharmacia, 1986; Robyt and White, 1987).

As seen in Figure 18, when the ligand is a protein, the coupling reaction occurs between primary amines on the protein and activated C6 hydroxyl groups on the matrix (Axén et al., 1967; Robyt and White, 1987). The amount of protein that couples onto the activated matrix is a function of the number of reactive amino groups available on the protein, the degree of activation of the matrix, and the pH at which the coupling reaction is performed (Goding, 1986).

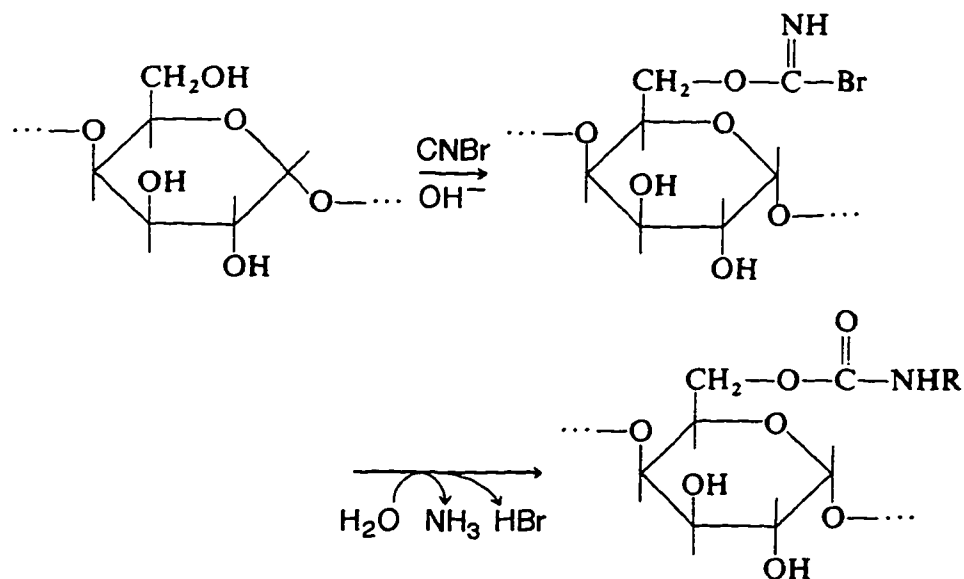


Figure 18. On a coupled immunoaffinity matrix, the MAbs (ligands) are covalently coupled to the inert matrix through CNBr-activated C6 hydroxyl groups on the polysaccharide matrix and  $\epsilon$  amino groups on the MAb molecules. The density of cross-linking is controlled through pH by altering the numbers of available deprotonated  $\epsilon$  amino groups. (Re-drawn from Robyt and White, 1987.)

The most likely primary amines on the protein to be involved in the coupling reaction are the  $\epsilon$  amino groups on lysine (Goding, 1986). The coupling reaction occurs most efficiently at alkaline pH where these  $\epsilon$  amino groups are deprotonated. It is undesirable to couple through either too many or too few amino groups on each protein molecule. Coupling a very high proportion of all available amino groups on each protein molecule raises the chances that coupling will occur in and around its target binding site, which would decrease the ability of the protein to bind to the target. Alternatively, coupling through too few amino groups could result in an unstable matrix. Therefore, the pH of the coupling buffer is used to control the proportion of amino groups present in the deprotonated form during coupling (Axén et al., 1967; Porath, 1968; Pharmacia, 1993).

The coupling reaction occurs most efficiently at slightly alkaline pH where the  $\epsilon$  amino groups are deprotonated (Goding, 1986; Wilcheck, 1984). For the IgM-class MAbs, with a molecular weight of ~900 kDa, there will be ~7,500 amino acids per molecule (assuming an average molecular weight for amino acids of 120 g/mol). The percent of amino acid residues on Igs that are lysines has been determined to be ~7% (Press and Piggot, 1967; Offer et al., 1973), therefore the number of lysine residues per mole of IgM will be ~525. At the  $pK_{\epsilon}$  of lysine's side chain ( $pK_{\epsilon} = 10.54$ ) approximately half of these side chains (~263 per IgM molecule) will be deprotonated at any moment in time. Since it is desirable to couple through only a few lysines per molecule of IgM, then the coupling pH should be well below the  $pK_{\epsilon}$ . As the pH of the coupling buffer is dropped below the  $pK_{\epsilon}$ , the number of lysine side chains in the deprotonated form decreases, thus there are fewer reactive lysines through which to cross-link to the activated matrix. Using the Henderson-Hasselbach equation (Zubay, 1988) it was calculated that at pH 7.4 on average only ~0.5 lysine residues per MAb molecule would be deprotonated at any moment in time. The coupling buffer was adjusted to pH 7.4 and the coupling was allowed to proceed overnight to

maximize the opportunity for lysine residues to equilibrate into the deprotonated form and then be available to couple. From this treatment, it would be expected that a large number of the total available MAb molecules would be coupled to the matrix, but each one would only be coupled through a small number of its lysine residues.

Since the N-substituted isourea covalent bonds that form the cross-links between the lysines and matrix are somewhat subject to nucleophilic attack, protein could be lost from the coupled matrix during use if too few cross-links are made between the matrix and each protein molecule (Goding, 1986; Robyt and White, 1987). In addition, the use of strong 'stripping' buffers (see below) to elute the target from the column subjects the protein to repeated partial denaturation. Multiple cross-links to each protein molecule serve to stabilize the protein preventing excessive, and perhaps irreversible, denaturation (Kamihira et al., 1992).

Once the coupling reactions are complete, any remaining activated sites on the matrices are blocked by incubating the coupled matrices with a non-protein source of primary amine; in this study, ethanolamine was used. Blocking these sites prevents any interactions of these uncoupled, activated sites with the myosin once it is applied to the immunoaffinity columns.

To use an immunoaffinity column, a mixed solution containing the target solute is passed through the column. The specificity of the ligand determines the degree to which the target can be separated out of complex mixtures (Cuatrecasas and Afinsen, 1971). As the targets move through the column they are bound by the ligands, while any undesired molecules (i.e. those not recognized by the ligand) pass freely through the column. Because the binding of the target to the ligand is non-covalent it should be reversible. To elute the target molecules off the column, the specific interaction with the ligand must be disrupted. A 'stripping' eluant is used to remove

the retained target from the column. It disrupts the non-covalent interactions between the target and ligand, allowing collection of the bound target and repeated use of the column.

Typical treatments used to disrupt the ligand/target interactions are: changing the pH, ionic strength, or polarity of the eluant; addition of molecules which compete for the ligand binding; and chaotropic reagents (Harris and Angal, 1994; Pharmacia, 1993). The method used depends upon the basis of the ligand/target binding and the strength of the binding. Additionally, if the binding activity of the ligand on the matrix is to be maintained (i.e., if the matrix is to be reused), or if subsequent analyses or applications of the eluted target molecules are to be performed, the treatment used to elute the target molecules must be compatible with the stability of the ligand and target molecules.

*Anti-Myosin Immunoaffinity Columns.* In this study, the ligand coupled to the inert matrix is an anti-myosin monoclonal antibody (MAb) and the target is a specific myosin heavy chain epitope. The myosin extracted from the striated skeletal adult rat muscle contains a mixed population of possible isozymes, therefore many different epitopes. The binding specificity of the anti-myosin immunoaffinity columns should allow the separation of distinct isozymes from this mixture, based on which myosin heavy chain epitopes, or combinations of those epitopes, the individual isozymes bear.

Five distinct anti-myosin MAbs, which react to five distinct myosin heavy chain epitopes, were used in this study (Table 1, page 34). Three separate anti-myosin immunoaffinity columns were prepared using MAb-F22, MAb-F36, and MAb-S84. These three columns are expected to selectively bind isozymes which bear the F22, F36, and S84 epitopes, respectively. The two remaining MAbs, MAb-S95 and MAb-25, were for use in the hetero-isotypic sandwich ELISAs. The two epitopes characteristic of slow-contracting myosin are S84 and S95. If the S84 and S95

epitopes can be separated from one another on an anti-S84 column then two distinct isozymes of slow-contracting myosin from adult rat skeletal muscle will have been identified, each isozyme bearing a single, characteristic slow epitope. Similarly, the two epitopes characteristic of fast-contracting myosin are F22 and F36. If the F22 and F36 epitopes can be separated from one another on either an anti-F22 or an anti-F36 column then two distinct isozymes of fast-contracting myosin from adult rat skeletal muscle will have been identified, each isozyme bearing a single, characteristic epitope. If the epitopes co-exist on one isozyme then those multiple-epitope isozymes will be bound by more than one column.

Figure 19 shows an example of one theoretical scenario for using anti-F22 and anti-F36 immunoaffinity columns in parallel. In this example, the hypothetical myosin sample contains three possible isozymes: those that bear only the F36 epitope (F36+/F22-), only the F22 epitope (F36-/F22+), or both epitopes together (F36+/F22+). The existence of these various isozymes could be determined by using parallel MAb-F22 and MAb-F36 columns. For the sake of simplicity in this example, only the two fast myosin epitopes are considered; the two slow myosin epitopes would be completely non-retained and elute in the  $V_{0s}$  of both of these anti-fast columns.

If this sample were applied to a MAb-F36 immunoaffinity column (an 'anti-F36' column), F36+ isozymes would be retained while F36- isozymes would be excluded and so elute in the  $V_0$ . Similarly, applying the sample to an anti-F22 column, only F22- isozymes would appear in the  $V_0$ . A hetero-isotypic sandwich ELISA would be used to analyze the original sample, the  $V_e$ , and the  $V_0$  from each column individually for the presence of the F22 and F36 myosin epitopes.



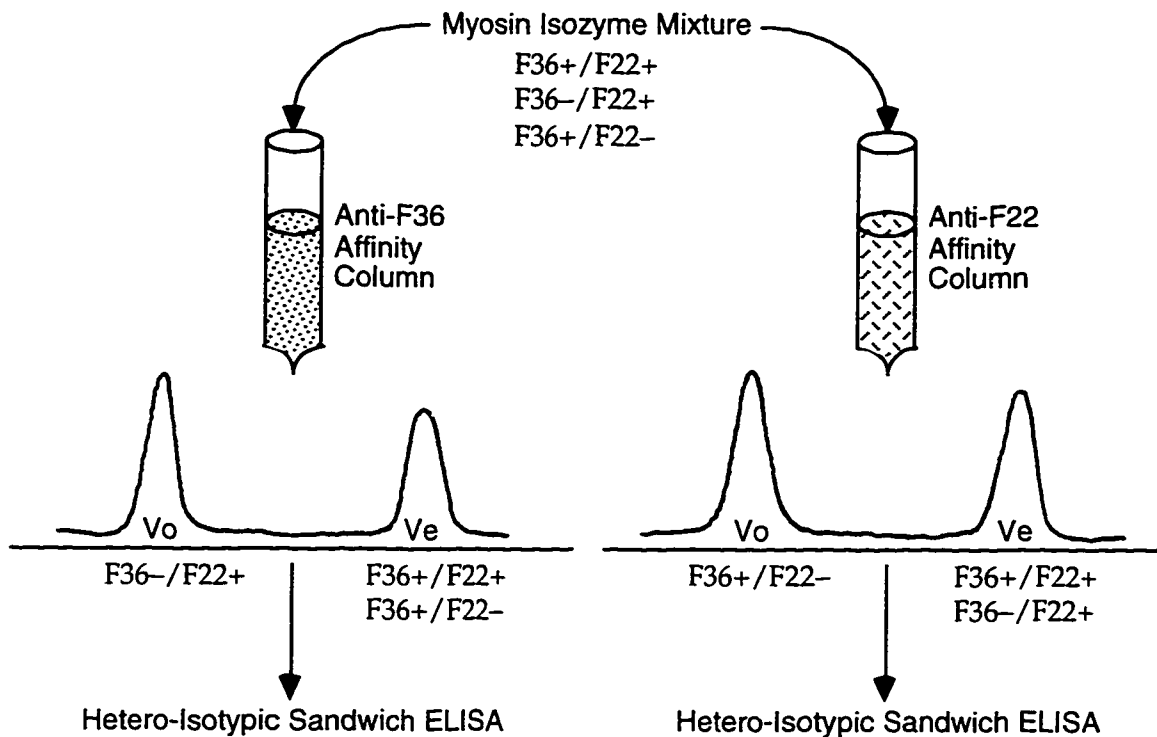


Figure 19. One theoretical scenario of a myosin sample applied to parallel immunoaffinity columns. Each matrix has one MAb bound to it: MAb-F36 or MAb-F22. All F36- isozymes present in the mixed population of myosin isozymes applied to the anti-F36 column will pass through into the void volume ( $V_0$ ), while all F36+ isozymes will be retained on the column until they are removed by elution ( $V_e$ ). Similarly, for the anti-F22 column the  $V_0$  will contain all F22- isozymes. (All slow myosin isozymes would elute in the  $V_0$ s of both of these anti-fast columns.)

Alternatively, these two columns could be used in series, as shown in the theoretical scenario in Figure 20. The mixed isozyme sample is first applied to the anti-F22 column. If F22+/F36- and F22+/F36+ isozymes both exist, they will both be retained on this column; any F22-/F36+ isozymes will pass into the  $V_0$  ( $V_{0F22}$ ). If F22-/F36- and F22+/F36+ isozymes both exist, then hetero-isotypic sandwich ELISAs on the  $V_{0F22}$  will be F22- and F36+, and on the  $V_e$  of the anti-F22 column ( $V_{eF22}$ ) will be F22+ and F36+. The  $V_{0F22}$  is then loaded onto the anti-F36 column. If F22-/F36+ isozymes exist, they will be retained on the anti-F36 column. Hetero-isotypic sandwich ELISAs on the  $V_0$  of the anti-F36 column ( $V_{0F36}$ ) will be F22- and F36-, and on the  $V_e$

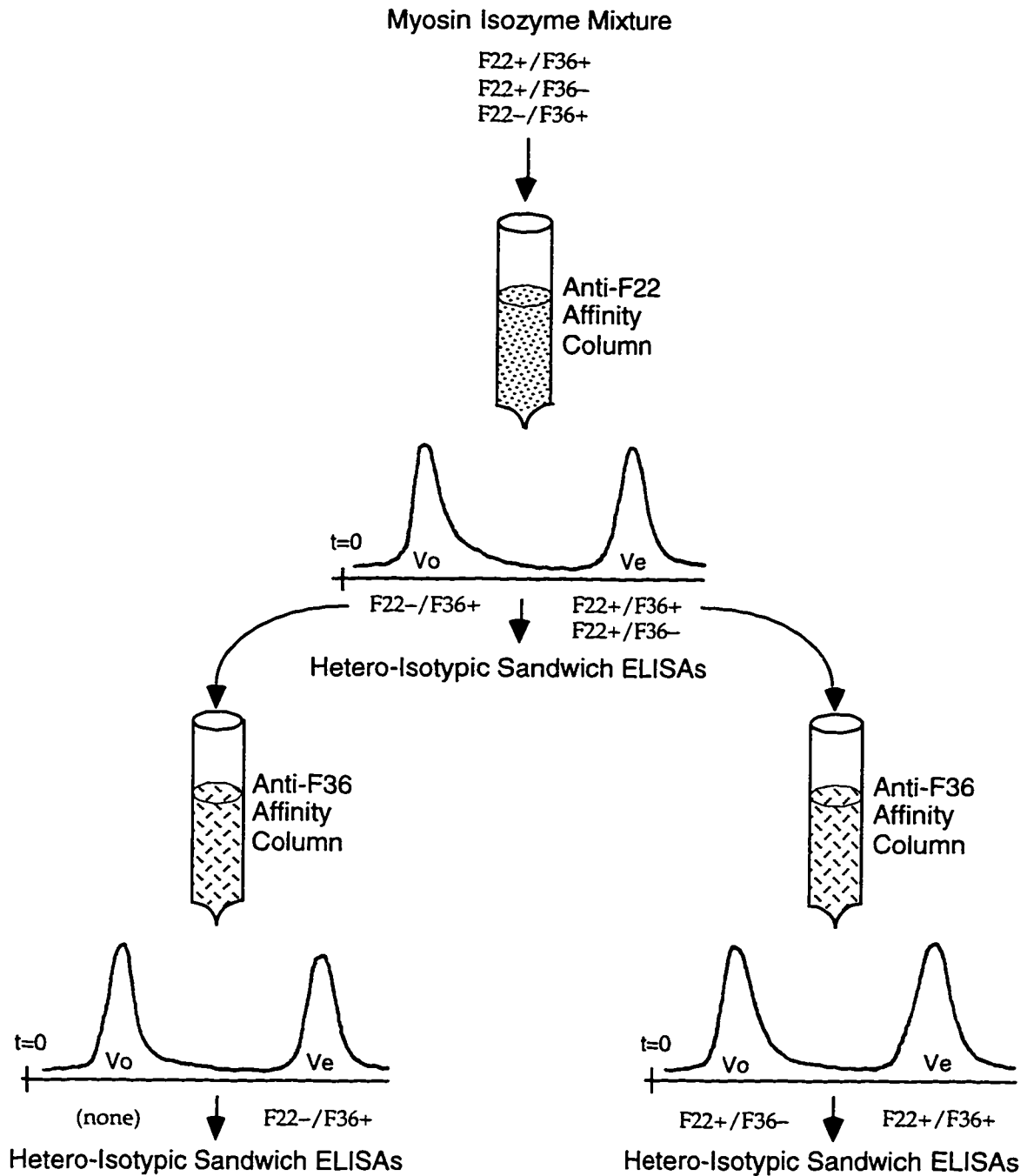


Figure 20. An alternate way to demonstrate the presence of multiple-epitope isozymes involves using two anti-myosin immunoaffinity columns in series. If F22+/F36+ isozymes exist, they will be retained on both anti-F22 and anti-F36 columns and the hetero-isotypic sandwich ELISAs on the  $V_e$ s from both of these columns would show the presence of both epitopes. If F22+/F36- and F22-/F36+ isozymes also exist, they would be detected by hetero-isotypic sandwich ELISAs on the  $V_0$  from each column.

of the anti-F36 column ( $V_{eF36}$ ) will be F22- and F36+. Finally, the  $V_{eF22}$  is loaded onto the anti-F36 column. If F22+/F36+ isozymes exist, they will be retained on the anti-F36 column. Hetero-isotypic sandwich ELISAs on the  $V_{oF36}$  will be F22- and F36-, and on the  $V_{eF36}$  will be F22- and F36+.

## Study Goals and Approach

*Overview.* The goals of this study are to separate putative distinct isozymes of myosin using immunoaffinity chromatography, and to determine if individual myosin molecules carry only one type of epitope, or if different epitopes can co-exist on one myosin molecule. Distinct isozymes of myosin ought to be separable on anti-myosin immunoaffinity columns that are reactive to specific epitopes (Chizzonite et al., 1982; Komuro et al., 1986; Silberstein, 1979; Silberstein and Lowey, 1981). Additionally, by using multiple columns in combination (each with a different anti-myosin specificity), the presence or absence of multiple epitopes on the distinct isozymes can be determined. The preparation and characterization of the affinity columns must precede any chromatography performed, and a reliable analytical method to detect the epitopes in the chromatographic peaks is necessary.

*Goals and Objectives.* The goals of this study were to separate putative distinct isozymes of myosin using anti-myosin immunoaffinity chromatography, and to determine if distinct isozymes bear only a single type of heavy chain epitope or if any isozymes carry combinations of epitopes.

Three specific objectives were accomplished in pursuit of the goals:

- purification of monodisperse myosin from adult vertebral striated skeletal muscle;
- production and purification of monoclonal antibodies reactive to myosin epitopes; and,
- preparation of anti-myosin immunoaffinity matrices by coupling anti-myosin monoclonal antibodies to an inert matrix.

Two additional objectives were pursued:

- development of a method for detecting and analyzing myosin found in column peaks; and,
- development of hetero-isotypic sandwich ELISAs to analyze column peaks for myosin heavy chain epitopes.

*Approach.* Figure 21 summarizes the approach taken to pursue the stated goals of the study. First, to prepare the immunoaffinity columns, anti-myosin monoclonal antibodies were produced and purified. A highly concentrated source of MAbs was produced as an ascites fluid in Balb/c mice by injection of monoclonal hybridoma cell lines that secrete the anti-myosin MAbs. The MAb-rich ascites fluid was collected and purified with saturated ammonium sulfate precipitation, as per the procedure of Heide and Schwics (cited in Hockfield et al., 1993), followed by size exclusion chromatography (SEC) to remove serum albumin, the major contaminating protein in the ascites (Hockfield et al., 1993; Coligan et al., 1994). The MAbs were covalently coupled to an inert matrix using an activated cyanogen bromide reaction such that each batch of immunoaffinity matrix has a known load of a specific anti-myosin MAb (Robyt and White, 1987). The coupled matrices were packed into columns.

The myosin is extracted from adult rat leg muscle as per the procedure of Holtzer and Lowey (Holtzer and Lowey, 1959). The final myosin sample resulting from this procedure contains partially aggregated and/or damaged myosin which is removed by size exclusion chromatography, since the myosin applied to the immunoaffinity columns must be non-aggregated, or 'monodisperse' (Holtzer and Lowey, 1959; Silberstein, 1979). The yield, purity, and quality of the myosin sample is determined before it is applied to the immunoaffinity columns. The myosin prepared by this procedure is a mixed population of isozymes.

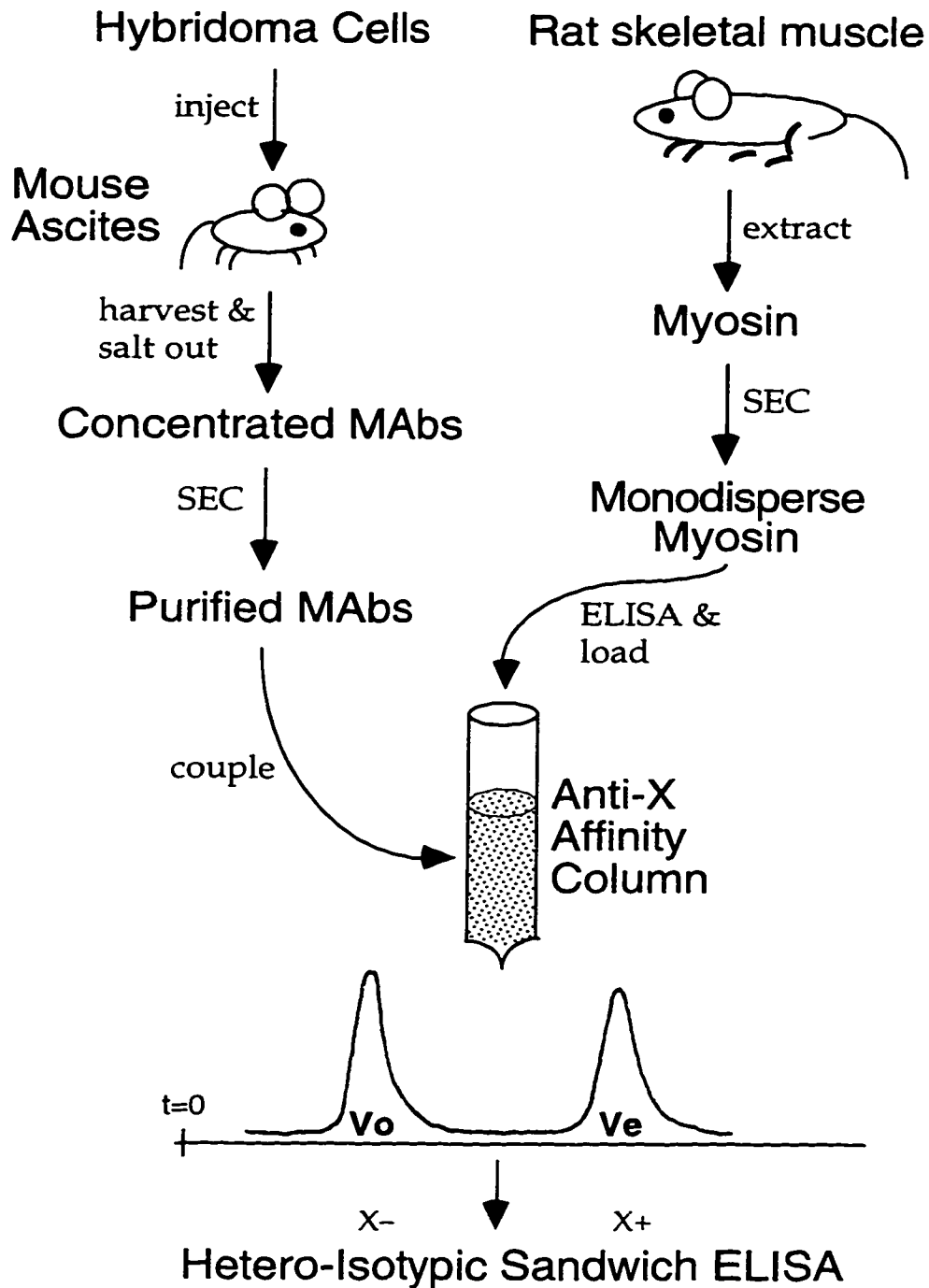


Figure 21. Outline of the approach taken in this study. Purified, monodisperse myosin will be applied to anti-myosin immunoaffinity columns produced from purified anti-myosin MABs. Hetero-isotypic sandwich ELISAs are used to determine the presence or absence of a specific epitope in pre-column samples as well as in column peaks. In this diagram, 'Anti-X' refers to an immunoaffinity column that binds isozymes bearing the generic epitope X.

Application of this isozyme mixture to the anti-myosin immunoaffinity columns should allow the separation of isozymes based on the epitopic specificity of the individual column. Isozymes which bear the epitope recognized by the column will be retained on the column while all others will pass freely through. Hetero-isotypic sandwich ELISAs can be used to detect the presence of specific epitopes in the column peaks (see *Results*).

*Methods Development for Hetero-Isotypic Sandwich ELISAs.* Both false positive and false negative results are possible for the hetero-isotypic sandwich ELISAs. For example, possible sources of false positive results on the hetero-isotypic sandwich ELISAs, designed to detect the F22 myosin heavy chain epitope are: a) if the anti-F22 column capacity is exceeded, allowing F22+ isozymes to pass through the column into its  $V_0$ ; b) if aggregated myosin is applied to the anti-F22 column, allowing F22+ isozymes to avoid being bound to the column and passing into the  $V_0$ ; c) if MAb-F22 bleeds off the anti-F22 column, carrying F22+ isozymes into its  $V_0$ ; and, d) if MAb-F36 bleeds off the anti-F36 column, carrying putative F36+/F22+ isozymes into the  $V_0$ .

Possible sources of false negative results on the F22 hetero-isotypic sandwich ELISA are: a) if the concentration of F22+ isozymes are too low to detect; or b) if the F22 epitope on the myosin molecules is damaged or blocked by aggregated myosin thus rendering it unrecognizable to the MAb-F22 used in the ELISA.

Some of these false results would be relatively easy to address. A homo-isotypic sandwich ELISA to detect IgM in the  $V_0$  peak would address the concern about MAb bleeding off the column since this is the only possible source of an IgM-class MAb in the  $V_0$ . To determine that a column is overloaded, a hetero-isotypic sandwich ELISA on  $V_0$  would detect the presence of the epitope that should have been retained on the column. The detection limit for each epitope could be pre-determined by a hetero-isotypic sandwich ELISA in which known dilutions of myosin are used to

construct a standard curve. From such an ELISA, the lower limit of detection for that epitope could be determined, thus defining the level of certainty for reported results.

Aggregated or damaged myosin presents a greater problem. For example, if aggregated myosin is loaded onto the anti-F22 column a false positive result could be obtained. If the aggregation has occurred in such a way that the F22 epitope is shielded, these isozymes would not be retained on the anti-F22 column and would inappropriately appear in the  $V_0$  of the anti-myosin column. To test for the presence of aggregation a hetero-isotypic sandwich ELISA using two different anti-myosin MAbs, each of which reacts to either only fast isozymes or only slow isozymes of myosin, can be used.

Figure 22 shows a diagram of the sandwich ELISA to detect aggregated myosin on the plate. The  $V_0$  from the anti-F22 column is added to a plate coated with MAb-S95, (an IgG-class, anti-slow MAb); only S95+ isozymes should bind to this plate. Immunohistochemical studies have indicated that isozymes bearing both fast and slow myosin heavy chain epitopes (e.g., S95+/F22+) do not exist (Hughes et al., 1993). Therefore, adding a layer of MAb-F22 CSN (an IgM-class, anti-fast MAb) can only produce a positive result on the hetero-isotypic sandwich ELISA if F22+ myosin is retained on the plate by aggregation to the S95+ myosin. Any MAb-F22 on the plate is detected with the  $\alpha$ mIgM-HRP, which binds to the IgM-class MAb-F22 but not to the IgG-class MAb-S95.

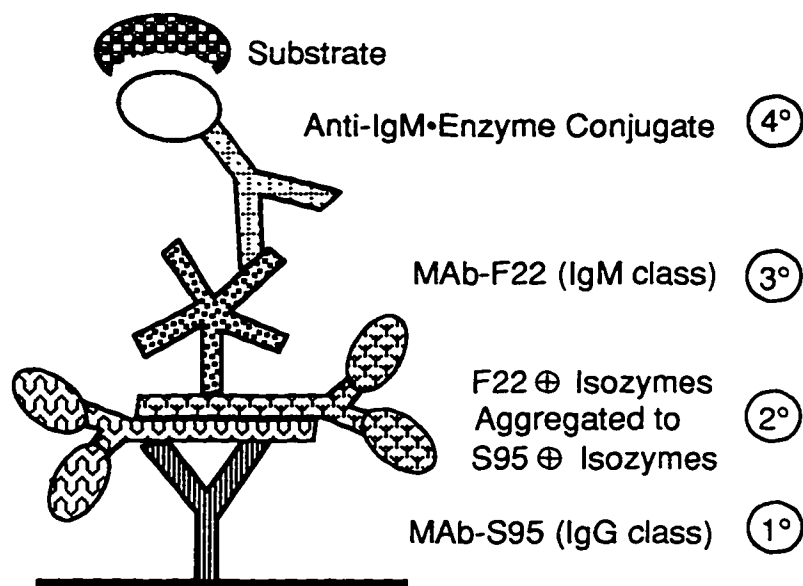


Figure 22. Diagram of the interactions of the individual molecules in the layers of the hetero-isotypic sandwich ELISA designed to detect the presence of aggregated myosin. 1° layer = MAb-S95; 2° layer = peak from immunoaffinity column; 3° layer = MAb-F22 CSN; 4° layer =  $\Gamma$  anti-IgM•HRP. The MAb-S95 on the plate will bind any slow isozymes present. If those IgG-class slow isozymes have any IgM-class F22+ isozymes aggregated to them they will be detected by binding the  $\Gamma$  anti-IgM•HRP and the resultant color change will reveal that aggregated F22+ myosin is present on the plate.

Ideal behavior of the sample and the chromatographic system is necessary for reliable results.

Bleeding of MAb off the matrix, sample overloading, and aggregation or degradation of the

myosin are all unacceptable; if any of these non-ideal behaviors occur, the results of both the

chromatography and the hetero-isotypic sandwich ELISAs would be ambiguous. Various

technical difficulties encountered in methods development for the hetero-isotypic sandwich

ELISAs were found to complicate analysis of the column peaks to such a degree that at the time of

this writing the separation of isozymes has not yet been achieved,<sup>4</sup> however, the theoretical basis

of the approach is sound (Chizzonite et al., 1982; Komuro et al., 1986; Silberstein, 1979;

Silberstein and Lowey, 1981).

<sup>4</sup> See *Results* for a complete description of the complications encountered.



Separation of myosin isozymes would enable comparative studies of their detailed chemical characteristics, both structural and functional. Examination of characteristics such as amino acid sequences of both the heavy and light chains, protein folding, ATP and actin binding sites, as well as ATPase activity of distinct isozyme types could be performed. Such studies could then be extended to include isozymes from various developmental stages and/or disease states and from different species. Ultimately, information gathered in such studies could further our understanding of normal developmental of muscle as well as aberrant or disease processes, and the evolution of myosin and muscle.

## MATERIALS AND METHODS

### Analyses and Assays

*Determination of Protein Concentrations by Protein Assay Kit.* A commercially available assay kit (BioRad #500-0111 DC Protein Assay Kit), based on a modified Lowry assay (Lowry et al., 1951), was used for some determinations of total protein concentration. A Bovine Serum Albumin (BSA) standard provided with the assay kit, diluted to 0.1-1.0 mg/mL in the same buffer in which the samples were diluted, was used as the standard. As per the assay kit instructions, 5  $\mu$ L of diluted sample or standard was added to 25  $\mu$ L of 'Reagent A' (1-5% sodium hydroxide, <1% sodium tartrate, <0.1% copper sulfate), followed by 200  $\mu$ L of 'Reagent B' (<1% of each of the following: lithium sulfate, sodium salt of tungstic acid, sodium salt of molybdic acid, hydrochloric acid, phosphoric acid). Mixing, reaction, and absorbance readings were carried out on 96-well tissue culture plates (Linbrow #IS-FB-96-TC). Absorbance readings were taken at 650 nm on a Molecular Devices V<sub>max</sub> Microplate Reader at a known time at least 15 min after adding Reagent B to the plate. Data was analyzed using the Softmax v. 2.02 software package for Macintosh. Protein concentrations in the samples were determined using Beer's Law based on the linear BSA standard curve.

*Determination of Protein Concentrations by Absorbance Spectra.* Some determinations of total protein concentration were made by reading the absorbance spectra as per the procedure of Margossian and Lowey, 1978. UV absorbance spectra of protein samples were read from 230 to 390 nm (Hewlett Packard Diode Array Spectrophotometer driven by a Hewlett Packard Vectra ES/12 computer with 89531A MS-DOS UV-VIS Operating Software, Revision A.03.00). Protein concentrations were calculated by applying Beers' Law to the A<sub>280</sub> values using the following extinction coefficients ( $\epsilon$  <sup>1%</sup><sub>280nm</sub>): 5.0 mL/mg-cm for myosin (Margossian and Lowey, 1978;

Silberstein, 1979); 13.3 mL/mg-cm for IgM-class immunoglobulins (Silberstein, 1979); 14 mL/mg-cm for IgG-class immunoglobulins (Hochfield et al., 1993); 10.0 mL/mg-cm for ascites (Silberstein, 1979); and 5.8 mL/mg-cm for albumin (Robyt and White, 1987). Absorbance values were corrected for  $A_{260}$  due to nucleic acid contamination, as per the method of Warburg and Wharton (as described in Robyt and White, 1987). Additionally, baseline corrections were made for high  $A_{340}$  (Grant, 1995). The ratio of  $A_{340}/A_{280}$  was used to monitor for the presence of aggregated material for both myosin and immunoglobulin samples (Slater, 1970). When values of  $(A_{340}/A_{280}) \times 100$  exceeded 10% the sample was considered too turbid for a reliable absorbance reading (Silberstein, 1979) and was clarified by centrifugation for 5 min at ~15 krpm (maximum speed, Eppendorf Model 5415 Microfuge).

*Electrophoresis on SDS-PAGE Gels.* Electrophoresis was performed on commercially available denaturing, non-gradient polyacrylamide gels. Following the classical Laemmli procedure (described in Harris and Angal, 1994), samples and standards were diluted to 1-5 mg/mL total protein in 2X SDS Sample Buffer (10% (v/v) sodium dodecyl sulfate, 125 mM Tris hydrochloride at pH 6.8, 0.02% (w/v) bromphenol blue, 0.05% (w/v) pyronin Y, 20% (v/v) glycerol, 4 mM dithiothreitol), dosed with 1  $\mu$ L  $\beta$ -mercaptoethanol, and placed quickly into a boiling water bath for 3-5 min. Boiled samples were removed to an ice bath and immediately loaded onto the gel at 2-10  $\mu$ L per well. Samples were quickly re-frozen to minimize damage to the proteins from proteolysis. Gels were run at 20-25 mAmps constant current (BioRad Mini-Protean II Dual Slab Electrophoresis Cell) using 0.192 M glycine, 0.025 M Tris-base, 0.1% (v/v) SDS as the Gel Running Buffer. All gels used were of the mini slab gel format (8 x 10 cm, 0.75 mm thick). For samples from the IgM purifications, custom 12.5% denaturing non-gradient gels from Jule Biotechnology (#12.5 D.75BMC-10G; resolving: 12.5%T, 2%C; stacking: 6%T, 3%C) were used. To separate IgM and albumin on these gels the total run time used was 50% longer than the

amount of time required for the tracking dye to reach the bottom of the gel (a so called '150% run'). Standards used for IgM gels were Mineral Oil-Induced Plasmocytoma Originated IgM (MOPC, Sigma #M3273), BSA (Nutritional Biochemicals, Fraction V), and a high molecular weight mixture of six proteins (Sigma Biochemicals #SDS-6H). Gels used for myosin purification samples were denaturing non-gradient 7.5% Jule gels (#7.5 D.75BMC-10P); the standard was the same high molecular weight mixture described above. Gels were fixed for 20 min at RT in Gel Fix (10% (v/v) acetic acid), stained in Gel Stain (0.25% (w/v) Coumassie Brilliant Blue G250, 50% (v/v) methanol, 12.5% (w/v) trichloroacetic acid) overnight at RT, destained in Gel Destain (5% (w/v) trichloroacetic acid) for 5-10 min at RT, and finally stored in 7% (v/v) acetic acid until a permanent record was made by electronic scan with an image scanner (Hewlett-Packard ScanJet 4c Color Scanner with Adobe Photoshop v. 3.0 run on a Macintosh IICI) followed by drying the gel.<sup>5</sup>

*Determination of Concentration of Total Immunoglobulin.* The concentration of total immunoglobulin in MAb preparations and cell supernatants was determined by homo-isotypic sandwich Enzyme Linked Immunosorbent Assays (ELISAs). The procedure used was modified from the titration ELISAs described in Hockfield et al., 1993. To assay IgM-class MAbs, 96-well ELISA microtiter plates (Corning #25801) were coated at 100  $\mu$ L/well with goat anti-mouse-IgM (G $\alpha$ mlgM, CalTag #M31500) as the primary antibody diluted to 1  $\mu$ g/mL in ELISA Plate Coating Buffer (0.1 M sodium bicarbonate at pH 9.5); plates were coated in batches and stored at -20 °C. The previously coated plates were thawed at RT, washed three times with ELISA Wash Buffer (EWB; 0.5 M sodium chloride, 10 mM sodium phosphate at pH 7.4, 0.05% (v/v) Tween 20), then blocked against non-specific binding by incubation at 4 °C for 30 min with 100  $\mu$ L Blocking Buffer (PBS-blotto; 0.15 M sodium chloride, 20 mM sodium phosphate at pH 7.4, 5% (v/v) powdered milk solution) per well. Starting at 10  $\mu$ g/mL, 1:2 serial dilutions of each standard and sample were

---

<sup>5</sup> Scanning performed by W. Acevedo.

prepared in Blocking Buffer; the standard for these IgM-class MAb assays was MOPC (Sigma #M3273). The Blocking Buffer was removed from the plate with three washes of EWB, then 100  $\mu$ L-aliquots of the dilutions of the MOPC and each sample were added to the plate in duplicate wells. After a 1-h incubation at 4 °C, three washes with EWB were used to remove excess sample or standard. A 1:1,000 dilution of goat anti-mouse-IgM conjugated to the enzyme horseradish peroxidase ( $\alpha$ mIgM•HRP, CalTag #M31507) was prepared in Blocking Buffer.  $\alpha$ mIgM•HRP was added to each well in 100- $\mu$ L aliquots followed by incubation at 4 °C for 1–2 h; an aliquot of diluted  $\alpha$ mIgM•HRP solution was saved at 4 °C for a reactivity 'spot test' with HRP's substrate, ABTS (2,2'-azino-bis-(3-ethylbenz-thiazoline-6-sulfonic acid), Sigma #A1888). After incubation, a freshly prepared ELISA Substrate Solution (2 mM ABTS in 0.1 M sodium citrate at pH 4.2, 0.03% (v/v) hydrogen peroxide), was spot tested against the saved aliquot of  $\alpha$ mIgM•HRP solution. If the dark green color, characteristic of the HRP/ABTS reaction, developed in the spot test within 15-30 sec, the excess  $\alpha$ mIgM•HRP solution was removed from the plate with three washes of EWB and the substrate solution was added to the plate at 100  $\mu$ L per well, then incubated in the dark at RT. (If color development did not occur as expected for the spot test, a fresh solution of ABTS was prepared and tested). The incubated plate was read in the microplate reader (Molecular Devices  $V_{max}$  Microplate Reader) at 405 nm at 5-min intervals until absorbance readings reached 0.5-4.0 AU for the positive controls on the plate. A standard curve was constructed relating absorbance to IgM concentration. IgM concentrations in the samples were calculated based on the standard curve. Data analysis was performed with Softmax v. 2.02 software.<sup>6</sup> To assay IgG-class MAbs the procedure was identical except that the IgG standard used was mouse IgG (Sigma #I-8765); the primary antibody was  $\alpha$ mIgG (CalTag #M30000); and the antibody-enzyme conjugate reagent was  $\alpha$ mIgG•HRP (CalTag #M30107).

---

<sup>6</sup> Some homo-isotypic ELISAs were performed by K. Nguyen and L. Khan.

*Detection of Specific Myosin Epitopes.* Hetero-isotypic sandwich ELISAs were used to analyze the anti-myosin immunoaffinity column samples for the presence of specific myosin epitopes. 96-well ELISA microtiter plates (Corning #25801) were coated at 100  $\mu$ L/well with MAb-25.<sup>7</sup> The MAb-25 was coated onto the plates at 10  $\mu$ g/mL in ELISA Plate Coating Buffer and incubated overnight at  $-20$   $^{\circ}$ C. The plates were thawed at RT, washed three times with Sepharose Column Buffer with Tween-20 (SCB-Tween; 0.5 M potassium chloride, 50 mM potassium phosphate at pH 7.2, 0.25 mM EGTA, 0.05% (v/v) Tween-20), and blocked by incubation at 4  $^{\circ}$ C for 30 min with 100  $\mu$ L Blocking Buffer per well. (The composition of the Blocking Buffer varied; see *Results*, for details). The Blocking Buffer was removed from the plate with three washes of SCB-Tween, then 100  $\mu$ L of each myosin sample, diluted in Blocking Buffer pre-chilled to 4  $^{\circ}$ C, was added to the plate in duplicate; the Blocking Buffer alone served as the blank. The plate was incubated overnight at 4  $^{\circ}$ C. Three washes with SCB-Tween pre-chilled to 4  $^{\circ}$ C were used to remove excess sample from the plate, then 100  $\mu$ L of neat anti-myosin IgM-class cell supernatant (i.e., MAb-F22 CSN, MAb-F36 CSN, or MAb-S84 CSN), pre-chilled to 4  $^{\circ}$ C, was added to the plate. After incubating overnight at 4  $^{\circ}$ C a 1:1,000 dilution of stock  $\Gamma$ αIgM•HRP (CalTag #M31507) in Blocking Buffer was added to each well. (An aliquot of diluted  $\Gamma$ αIgM•HRP solution was saved at 4  $^{\circ}$ C for the spot test with substrate). After incubation at 4  $^{\circ}$ C for 1–2 h, the spot test was performed with a freshly prepared ABTS (Sigma #A1888) solution and if the color development was satisfactory the excess  $\Gamma$ αIgM•HRP solution was removed from the plate with three washes of SCB-Tween.<sup>8</sup> The ABTS solution was then added to the plate at 100  $\mu$ L per well and the plate was incubated in the dark at RT. The plate was read in the microplate reader (Molecular Devices  $V_{\max}$  Microplate Reader) at 405 nm at 5-min intervals until absorbance readings reached 0.5–4.0 AU for the positive controls. Data analysis was performed with Softmax v. 2.02 software.

---

7 MAb-25 is an IgG-class monoclonal antibody which binds to all myosin heavy chain isozymes.

8 See *Determination of Concentration of Total Immunoglobulin* for details.

## Myosin Preparation

*Extraction of Myosin from Muscle.* Myosin was purified in a 5-day process as per Holtzer and Lowey (Holtzer and Lowey, 1959) by alternately precipitating and solubilizing the myosin relative to other proteins present. Sprague-Dawley rats (~400 g males) were CO<sub>2</sub>-euthanized and guillotined.<sup>9</sup> Thigh muscle was collected at RT and immediately wrapped in plastic wrap and packed under ice for 30-60 min. From this point on, all work was done in a coldroom at 4 °C with pre-chilled purified water (10-18 megaohms<sup>-1</sup> cm<sup>-1</sup>) from a Millipore MilliQ<sup>®</sup> Water Purification System ('MQ H<sub>2</sub>O'), buffers, solutions, glassware, and equipment. The chilled muscle was passed twice through a meat grinder that had been pre-rinsed with 0.2 M EDTA. The ground muscle was weighed (typically, 40 g of ground muscle was collected from each rat); a small amount of the ground muscle was set aside for SDS-PAGE samples. ATP Extraction Buffer (0.3 M potassium chloride, 0.15 M potassium phosphate at pH 6.7, 0.02 M EDTA, 5 mM magnesium chloride, 5 mM adenosine triphosphate) was added to the ground muscle (2 L/kg muscle) and the slurry was stirred gently with a glass rod for 15 min. The slurry was then diluted in half with MQ H<sub>2</sub>O and the extracted muscle mince was removed by filtration through four layers of cheesecloth. The filtrate was decanted in equal aliquots of known volumes into Florence flasks and MQ H<sub>2</sub>O was slowly added with constant swirling until each aliquot was diluted six-fold. The diluted slurries were left on ice in the coldroom overnight. The next day, the flasks contained a clear pale pink supernatant over a flocculent white precipitate. The supernatant was aspirated away and discarded. Once the majority of the supernatant was decanted, the remaining precipitate slurry was centrifuged at 8 krpm for 30 min at 4 °C (IEC B20 Refrigerated Centrifuge, Rotor 872). The off-white 'crude myosin' pellets were collected and a small amount was set aside for SDS-PAGE samples; the balance of the pellet was gently resuspended in a minimum volume of Pellet Dispersion Buffer #1

---

<sup>9</sup> All animal work was performed in strict adherence to the San Jose State University Institutional Animal Care and Use Committee (IACUC) *Protocol for Animal Use, Academic Senate Policy #S87-3*.

(1.0 M potassium chloride, 50 mM potassium phosphate at pH 6.7, 20 mM EDTA). The viscous 'crude myosin' solution was dialyzed (Spectra/Por molecular porous membrane tubing #25225-228) against Myosin Buffer (0.6 M sodium chloride, 10 mM sodium phosphate at pH 7.0, 10 mM EDTA) in the coldroom overnight. The dialyzed 'crude myosin' suspension was collected and diluted twofold by slow addition of MQ H<sub>2</sub>O (over the course of 15 min with constant, gentle swirling) to precipitate any contaminating actin/myosin (actomyosin) co-aggregates present. The resultant slurry was then centrifuged at 8 krpm for 30 min at 4 °C (IEC B20 Refrigerated Centrifuge, Rotor 872) and the supernatant was further clarified by centrifugation at 20 krpm for 1 h at 4 °C (Beckman L8-M Ultracentrifuge, Rotor Type SW 41T1-41,000 RPM, Class C, D, F, G, H). The myosin-containing supernatant was divided into aliquots of known volume in Florence flasks and then diluted eight-fold by slow addition of MQ H<sub>2</sub>O with constant, gentle swirling. The diluted myosin was left overnight on ice at 4 °C on ice to re-precipitate the myosin. The next day the flasks contained a fine white precipitate which was collected by first aspirating off the bulk of the supernatant then centrifuging the remaining slurry at 8 krpm for 30 min at 4 °C (IEC B20 Refrigerated Centrifuge, Rotor 872). The pure white pellets containing re-precipitated myosin were collected, a small amount of the pellet was set aside for SDS-PAGE samples, and the balance of the pellet was resuspended in an absolute minimum volume (<1 mL PDB #2 per 1 mL of pellet) of Pellet Dispersion Buffer #2 (PDB #2, 3.0 M potassium chloride, 50 mM potassium phosphate at pH 6.7). The viscous, slightly opalescent re-suspended pellets of myosin were dialyzed against Myosin Buffer in the coldroom overnight. On the final day, the dialyzed (Spectra/Por molecular porous membrane tubing #25225-228) material was clarified by centrifugation at 20 krpm for 2 h at 4 °C (Beckman L8-M Ultracentrifuge, Rotor Type 70T1/70.1T1, 70,000 RPM). Any floating layer of fat was aspirated off and any pellet of aggregated myosin and/or actomyosin was left behind. The clear, almost colorless supernatant containing purified myosin was collected and a small amount was set aside for SDS-PAGE samples and total protein



concentration determination by absorbance spectra. The balance of the supernatant was then diluted twofold with glycerin by thoroughly but very gently folding small aliquots of glycerol into the purified myosin until a homogeneous solution was attained. The glycerinated myosin was stored at  $-20\text{ }^{\circ}\text{C}$ .

*Size Exclusion Chromatography of Myosin.* To ensure that the myosin applied to the immunoaffinity columns is monodisperse (i.e., non-aggregated), the extracted myosin was chromatographed by size exclusion with a procedure modified from Silberstein, 1979. All work was done in a coldroom at  $4\text{ }^{\circ}\text{C}$  with pre-chilled buffers, solutions, glassware, and equipment. A  $1.5 \times 80$ -cm column of Sepharose 2B (Sigma #2B-300), was poured and conditioned with a run of 1 mL of neonatal calf serum (NCS, Sigma #N0515) loaded at 5 mg/mL, followed by a run of 0.5 mL of Blue Dextran (Sigma #D5751) at 5 mg/mL to determine the void volume of the column. The column buffer used for all runs was Sepharose Column Buffer (SCB; 0.5 M potassium chloride, 50 mM potassium phosphate at pH 7.2, 0.25 mM EGTA). The column was eluted at 5.4 mL/h (Tris Series 1610-008 Peristaltic Pump) and effluent was monitored at 280 nm; a chart recorder (ISCO Type 6 Optical Unit with 0.5-cm Flow Cell; ISCO UA-5 Absorbance/ Fluorescence Detector and Chart Recorder) traced the chromatogram of eluting peaks. To chromatograph myosin, glycerinated myosin was dialyzed (Spectra/Por molecular porous membrane tubing #25225-228) overnight at  $4\text{ }^{\circ}\text{C}$  against SCB, diluted to 5 mg/mL with SCB, and loaded as a 4-mL aliquot onto the column by laying it onto a moist bed (method described in Harris and Angal, 1994). The column was eluted at 5 mL/h with SCB; 1-mL fractions were collected (ISCO Retriever II Fraction Collector). The absorbance spectra of key fractions were taken to determine protein concentration and to identify the peak containing monodisperse myosin; SDS-PAGE was performed on the peaks to monitor purity.

## Monoclonal Antibody Preparation

*Cell Culture.* Hybridoma cell lines known to produce monoclonal antibodies (MAbs) to a variety of myosin heavy chain epitopes were produced and provided by L. Silberstein. Cell lines of interest were thawed, grown, and re-frozen as needed (following procedures described in Hockfield et al., 1993). All work with cells was done under sterile conditions at RT. Vials of cells were thawed in a 37 °C water bath. The cells (~0.3 mL of frozen cell suspension) were transferred from cryovials (Nalge Cryovial #5000-0012) into a sterile tube with Cell Growth Media (CGM; see below) then centrifuged at 2 krpm for 5 min at RT (IEC Model HN-SNII, Benchtop Clinical Centrifuge; IEC 958 Rotor with 305 sleeve); the supernatant was discarded and the cells were gently resuspended in CGM. The newly thawed cells were counted on a hemacytometer (American Optical Bright Line Hemocytometer), their viability checked via trypan blue dye exclusion, and their concentration determined. The cell suspension was diluted with CGM to high ( $4 \times 10^5$  cells/mL), medium ( $2 \times 10^5$  cells/mL), and low ( $1 \times 10^5$  cells/mL) concentrations. Cells were transferred to plastic tissue culture well plates (Linbrow #IS-FB-96-TC) and incubated at 37 °C, 97% humidity, 5% CO<sub>2</sub> (Forma Scientific HEPA filtered IR Incubator). Growing cells were checked daily for density, morphology, and viability. Cells were 'fed' (i.e., media was replaced) and 'split' (i.e., contents of wells were subdivided) as needed to maintain vigorous growth. Cells were grown in one of two compositions of CGM: 89% (v/v) Dulbecco's Modified Eagle's Medium (DMEM, Sigma #D5530) and 1% (v/v) glutamine with either 5% (v/v) Fetal Calf Serum (FCS, Sigma #F4010) and 5% (v/v) Hyclone™ (Hyclone Laboratories #A6165L) or 10% (v/v) FCS. Spent media collected out of the culture plates were pooled and centrifuged at 2 krpm for 10 min at RT (IEC Model HN-SNII, Benchtop Clinical Centrifuge; IEC 958 Rotor with 305 sleeve); the clarified cell supernatant (CSN) was transferred to a new sterile tube and stored at 4 °C for use as a dilute source of MAbs; the few pelleted cells were discarded in autoclaved trash. Cells were frozen when viability was  $\geq 85\%$  as determined by trypan blue dye exclusion. Cells were collected by

centrifugation at 2 krpm for 5 min at RT (IEC Model HN-SNII, Benchtop Clinical Centrifuge; IEC 958 Rotor with 305 sleeve) and resuspended to a density  $\geq 5 \times 10^6$  cells/mL in Cell Freezing Media (90% (v/v) FCS, 10% (v/v) dimethylsulfoxide) and dispensed into ~0.3-mL aliquots in cryovials. The vials were wrapped in cotton gauze and transferred to overnight storage at  $-80^\circ\text{C}$  within 15 min of resuspension in Cell Freezing Media. Finally, the vials were transferred into a liquid nitrogen cell bank (Taylor Wharton 8K Auto-filling Liquid Nitrogen Cell bank) for long-term storage.<sup>10</sup>

*Ascites Production.* Balb/c mice (12-13 weeks old) were primed for ascites production by intraperitoneal injection with 0.5 mL of pristane 10 and 4 days prior to injection with cells, following the procedure described in Hockfield et al., 1993.<sup>11</sup> Each mouse was injected with 0.5 mL of a suspension of DMEM- or PBS-washed hybridoma cells containing  $10^6$  cells in DMEM. Once the mice showed significant tumor growth (as evidenced by abdominal swelling) they were 'tapped' every other day. The abdomen was cleaned with ethanol and a 23-gauge needle was inserted into the peritoneal cavity without any syringe attached. The expelled fluid was collected drop-by-drop into sterile tubes and left to stand at RT for 20 min to clot, then centrifuged at 2 krpm for 10 min at RT (IEC Model HN-SNII, Benchtop Clinical Centrifuge; IEC 958 Rotor with 305 sleeve). The unclotted supernatant was collected and stored at  $-20^\circ\text{C}$  in sterile tubes. The collected ascites were stored at  $-20^\circ\text{C}$ .<sup>12</sup>

---

10 Cell work was performed as a team with J. Huebenthal, K. Seitz, L. Frey, and K. Nguyen.

11 All animal work was performed in strict adherence to the San Jose State University Institutional Animal Care and Use Committee (IACUC) *Protocol for Animal Use, Academic Senate Policy #S87-3*.

12 The ascites for two hybridoma cell lines was produced by this investigator. All others were manufactured for use in this study by Sierra BioSource (Gilroy, California) using hybridoma cell lines provided to them by the Silberstein laboratory and following a similar procedure.

*Saturated Ammonium Sulfate Precipitation of Immunoglobulin.* Purification of class M immunoglobulins (IgMs) was accomplished in two steps beginning with precipitation with a Saturated Ammonium Sulfate solution. Following the procedure of Heide and Schwics (as described in Hockfield et al., 1993), frozen ascites was thawed in a 37 °C bath then filtered through three layers of cheesecloth into an Erlenmeyer flask on ice. A 50- $\mu$ L aliquot of the filtrate was set aside at 4 °C for SDS-PAGE, protein assays, and homo-isotypic ELISAs. The volume of remaining filtrate was determined. Saturated Ammonium Sulfate solution (SAS; 528 g/L ammonium sulfate, 0.25 mM EDTA, pH 7.2) pre-chilled to 4 °C was added to the ice-cold ascites, drop-by-drop over the course of 30 min, with constant gentle stirring, until the desired concentration of SAS was reached (30 to 50% (v/v); see *Results*). After all the SAS was added, the slurry was left to stand overnight at 4 °C on ice. The next day, the slurry was centrifuged at 10 krpm (IEC B20 Refrigerated Centrifuge, Rotor 870) for 30 min at 4 °C. The supernatant was decanted and stored at 4 °C for analysis. The white pellet of IgM precipitate was resuspended by gentle swirling in a minimum volume of Borate Saline Buffer (BSB; 150 mM sodium chloride, 20 mM sodium borate at pH 8.2) pre-chilled to 4 °C. The resuspended pellet and a ~5 mL aliquot of the supernatant were dialyzed (Spectra/Por molecular porous membrane tubing #132-676) over two nights at 4 °C against 2 L of BSB pre-chilled to 4 °C, with one change of dialysate in that time. The dialyzed material was stored on ice at 4 °C. The dialyzed pellet and supernatant were analyzed by SDS-PAGE, protein assay, and homo-isotypic ELISA.

*Size Exclusion Chromatography of Precipitated Immunoglobulins.* The primary contaminating protein in the purified IgM after the SAS precipitation is albumin, which was removed by size exclusion chromatography. Following the procedure adapted from Silberstein, 1979, a 1.5 x 80-cm Sephacryl S300-HR column (Sigma #S-300-HR) was poured at RT and conditioned with a run of 5 mL NCS (Sigma #N0515), then washed with 20-column volumes of BSB. A run of

Blue Dextran (Sigma #D5751) at 5 mg/mL was used to determine the void volume of the column and the elution time of albumin was determined using BSA (Nutritional Biochemicals, Fraction V) at 15 mg/mL. The column buffer used for all runs was BSB; all runs were performed at RT. The column was eluted at 9.0 mL/h (Tris Series 1610-008 Peristaltic Pump) and effluent was monitored at 280 nm; a chart recorder (ISCO UA-5 Absorbance/ Fluorescence Detector and Chart Recorder) traced the chromatogram of eluting peaks. A dialyzed, resuspension of IgM precipitated with SAS was then loaded onto the column in 1-mL aliquots and eluted at 9 mL/h with BSB; 1.5-mL fractions (ISCO Retriever II Fraction Collector) were collected. Fractions for the two eluted peaks (IgM and albumin) were collected and pooled separately and the total volume of each pool was measured. A 50- $\mu$ L aliquot of each pool was stored at 4 °C for analysis by SDS-PAGE, protein assay, and homo-isotypic ELISA. The pooled IgM and albumin peaks fractions were re-concentrated approximately 10-fold by dialysis (Spectra/Por molecular porous membrane tubing #25225-228) against dry Sephadex G-200 (Pharmacia #G-200). The change in weight of the dialysis bags was monitored to determine when the approximate desired fold re-concentration was reached. The re-concentrated peak pools were dialyzed (Spectra/Por molecular porous membrane tubing #132-676) over two nights at 4 °C against 2 L of BSB pre-chilled to 4 °C, with one change of dialysate in that time. A 50- $\mu$ L aliquot of each dialyzed, re-concentrated peak (IgM and albumin) was set aside at 4 °C for protein assays, SDS-PAGE, and homo-isotypic ELISAs. The balance of each dialyzed, re-concentrated IgM peak was stored on ice at 4 °C.

*Purification of Immunoglobulins by Affinity Chromatography.* Class G immunoglobulins (IgGs) were purified by chromatography on a Protein A affinity column (Pierce Chemical Co. #44667, ProSep™ Protein A, High Capacity Matrix) by G. Alegre following the manufacturer's instructions (Alegre and Silberstein, unpublished results). Column-eluted IgG fractions were analyzed for total protein concentration by reading  $A_{280}$  ( $\epsilon$   $^{1\%}_{280\text{nm}}$  of 14.0 mL/mg-cm for IgG-

class immunoglobulins) and for total IgG concentration by homo-isotypic sandwich ELISA. Sodium azide at 0.02% (v/v) was added to the pooled MAbs and they were stored at 4 °C.<sup>13</sup>

## Immunoaffinity Chromatography

*Preparation of Immunoaffinity Matrix.* Preparation of the immunoaffinity matrix is a four-step process: activation of the coupling sites on the inert matrix, coupling of the MAb to the inert matrix, blocking of uncoupled activated sites, and washing of the coupled matrix to remove any uncoupled IgM. All MQ H<sub>2</sub>O, buffers, reagents, solutions, and glassware were pre-chilled to 4 °C. All work with cyanogen bromide (CNBr) was performed in a chemical fume hood. All filtrates containing CNBr were saved and later pooled and neutralized with an 0.3 M solution of iron sulfate, for disposal as hazardous waste. The coupling procedure followed was adapted from Axén et al., 1967; Harris and Angal, 1994; and Goding, 1986. The MAb to be coupled was dialyzed (Spectra/Por molecular porous membrane tubing #132-676) overnight at 4 °C against Coupling Buffer (0.5 mM sodium chloride, 50 mM sodium phosphate at pH 7.4) and brought to the desired coupling concentration in that same buffer. Pre-swollen Sepharose CL 4B (Sigma #CL-4B-200) was washed with 10-bed volumes of MQ H<sub>2</sub>O on a coarse sintered glass funnel. Then a 1:1 (v/v) slurry of the washed matrix was made with MQ H<sub>2</sub>O and placed in an ice bath with constant stirring and a pH electrode. Aliquots of 2-M sodium hydroxide were added to bring the slurry to pH 10.5-11. Cyanogen bromide (CNBr) at 200 mg CNBr/mL of matrix to be activated was dissolved in acetonitrile (~3 g CNBr/5 mL) and added to the cold matrix slurry in ~1-mL aliquots with constant stirring.<sup>14</sup> The change in pH per unit volume CNBr added was measured to monitor the rate of activation. Also, since the reaction is exothermic, the temperature was monitored to

---

13 CAUTION: Sodium azide is highly poisonous. Refer to manufacturers' MSDS for further information.

14 CAUTION: CNBr quickly sublimates and the vapors are highly irritating and very poisonous; also impure CNBr tends to explode. Refer to manufacturers' MSDS for further information.

ensure the mixture was maintained at 4-8 °C. After each addition of CNBr, 2 M sodium hydroxide was added drop-wise to titrate the matrix slurry back to pH 10.5-11. All of the CNBr was added within 5 min of the first addition. After the activation reaction proceeded for 15 min, the activated matrix was quickly washed with 20-bed volumes of MQ H<sub>2</sub>O followed by 20-bed volumes of Coupling Buffer, then immediately transferred from the sintered glass funnel and combined in a sterile snap-cap test tube (Fisher Scientific #14-956-1J) with an equal volume of MAb solution diluted in Coupling Buffer. This slurry was incubated overnight at 4 °C on a rocker (Labquake Shaker Model T400-110). After the incubation, the matrix was allowed to settle and the A<sub>280</sub> of the clarified supernatant was measured to determine the concentration of any uncoupled MAb. The coupled matrix was washed with three bed volumes of Coupling Buffer and the A<sub>280</sub> of each filtrate was measured to track removal of any MAb. To block any uncoupled activated sites the matrix was incubated at RT for 1-2 h on a rocker with 3-bed volumes of 0.5 M ethanolamine at pH 9. Finally the matrix was washed three times alternately with 7-bed volumes each time of High- and Low-pH Wash Buffers (High = 0.5 M sodium chloride, 0.1 M sodium borate at pH 9.0; Low = 0.5 M sodium chloride, 0.1 M sodium acetate at pH 3.5), as per Goding, 1986. The A<sub>280</sub> of the washes was measured to track any protein lost. The final matrix was stored at 4 °C as a 1:1 (v/v) slurry in Affinity Matrix Storage Buffer (150 mM sodium chloride, 20 mM sodium borate at pH 8.3, 0.02% (w/v) sodium azide).

*Immunoaffinity Matrix Stability.* The stability of the coupled matrices (i.e., the matrix-MAb crosslinks) to the immunoaffinity column 'stripping' eluants was determined (see *Results*). A low pH stripping eluant (0.5 M potassium chloride, 50 mM potassium phosphate, 0.25 mM EGTA at pH 2.0) and a high salt concentration stripping eluant (3.0 M potassium chloride, 50 mM potassium phosphate, 0.25 mM EGTA at pH 7.2) were used. The coupled matrices were washed with three-bed volumes of each immunoaffinity column eluant. The filtrate from each wash was collected and

monitored for protein content by reading the UV absorbance spectra, individually and after pooling the three filtrates for each different eluant.

*Stability of Myosin to Immunoaffinity Chromatography Eluants.* The stability of myosin in the immunoaffinity column eluants, with respect to aggregation, was tested. All sample preparation was done at 4 °C with pre-chilled buffers. Glycerinated myosin was dialyzed (Spectra/Por molecular porous membrane tubing #25225-228) overnight at 4°C against Sepharose Column Buffer (SCB; 0.5 M potassium chloride, 50 mM potassium phosphate at pH 7.2, 0.25 mM EGTA). The absorbance spectra of the dialyzed sample was read and  $A_{340}/A_{280} \times 100$  was calculated to determine the presence of aggregated material. Three 1-mL aliquots of the dialyzed myosin were diluted twofold separately with each of the three immunoaffinity column 'stripping' eluants (4.0 M guanidine hydrochloride; 0.5 M potassium chloride, 50 mM potassium phosphate, pH 2.0, 0.25 mM EGTA; and 3.0 M potassium chloride, 50 mM potassium phosphate, pH 7.2, 0.25 mM EGTA). A 1-mL aliquot of dialyzed myosin was diluted twofold in SCB as the control. The diluted samples were incubated on ice in a coldroom at 4 °C. The spectra of each of the dilutions was read at RT at 10 min and 60 min after mixing;  $(A_{340}/A_{280}) \times 100$  was used as a measure of the amount of aggregated material in the samples.

*Chromatographic System for Immunoaffinity Columns.* The anti-myosin immunoaffinity column was used in a bench top chromatographic system set up in a 4 °C cold room. Following the procedure described in Silberstein, 1979, the affinity matrices were poured as 1:2 slurries in cold SCB into 0.7 x 5-cm Econo Columns (BioRad #737-0706). A chromatographic system was assembled in a 4 °C cold room, as follows: a column was connected in line with a peristaltic pump (Tris Series 1610-008 Peristaltic Pump) delivering eluant (SCB or 'stripping buffers,' see *Results*) through a three-way valve (Baxter Pharmaseal #K75), for quick eluant switching, and a 70-cm



length of 0.3-cm (i.d.) low pressure silicone tubing (BioRad #731-8209) to serve as a pulse dampener, and finally into the column at 15 mL/h. A second three-way valve (Baxter Pharmaseal #K75) served as the sample loading port at the top of the column and allowed the sample to be loaded directly onto the moist column bed as per the procedure in Harris and Angal, 1994. Effluent from the column was delivered directly into an 0.5-cm flow cell monitored at 280 nm (ISCO UA-5 Absorbance/ Fluorescence Detector and Chart Recorder; ISCO Type 6 Optical Unit with 0.5-cm Flow Cell); 0.25-mL fractions were collected into tubes containing 50  $\mu$ L of SCB (ISCO Retriever II Fraction Collector).

## RESULTS

### **Myosin Preparation**

*Overview.* Myosin was purified in a five-day process that begins with its solubilization from rat skeletal muscle followed by a step-wise separation from other muscle proteins. Once the myosin was relatively pure, size exclusion chromatography was used to separate monodisperse myosin from aggregated and/or damaged myosin. SDS-PAGE (sodium dodecylsulfate polyacrylamide gel electrophoresis) was used both to monitor the progress of the myosin purification and the effectiveness of the chromatography. Absorbance spectroscopy was used to determine the yield and quality of the extracted myosin.

*Extraction of Myosin from Muscle.* The extraction of myosin from muscle is based on the differential solubility of myosin and other muscle proteins as a function of ionic strength,  $\Gamma$ .

Table 2 summarizes the results of the eight myosin preparations showing the final myosin yields. Typically, 40 g of thigh muscle was collected from each 350-400 g rat. Myosin yields ranged from 0.53 mg to 17.4 mg of myosin per gram of muscle. Yield varied as modifications were made to the procedure and as unexpected problems arose (see *Discussion and Conclusions*).

Preparation #	g Muscle Used	Total mg Myosin Collected	Yield (mg Myosin per g Muscle)	Total mL Glycerinated Myosin	mg/mL Glycerinated Myosin
S1	145	406	2.8	29	14
S2	160	60.0	0.375	10	6.0
S3 extracted w/1 mM ATP	188	108	0.52	18	5.4
S3 extracted w/5 mM ATP	188	113	0.60	20	5.6
S4 forelimbs	25	59.1	2.4	4.0	15
S4 hind limbs	63	673	11	36	19
S5 §	48	836	17.4	44	19
S6 extracted w/ ATP §	51	27	0.53	9.0	7.8
S6 extracted w/ PP <sub>i</sub> §	51	53	1.0	8.0	11
S7 §‡	158	0	0	0	0
S8 'grind only' §‡	106	102	0.96	20	5.1
S8 'grind & homogenize' §‡	106	104	0.98	18	5.8

Table 2. Summary of yields from myosin preparations. (§ Indicates those which were done with S. Grant; ‡ indicates those which were done with G. Alegre.) "Total mg Myosin Collected" reported for each preparation is for glycerinated myosin prior to size exclusion chromatography to remove aggregated material.

Over the course of the extraction and purification, aliquots were removed to determine protein concentration and the presence of aggregated material (using absorbance spectra), and to determine myosin purity using SDS-PAGE.

*Determination of Myosin Yield and Purity.* The protein concentration of myosin samples was determined by absorbance spectroscopy.  $A_{280}$  is converted into protein concentration (mg/mL) through Beer's Law using an extinction coefficient for myosin of  $\epsilon^{1\%_{280nm}} = 5.0 \text{ mL/mg-cm}$

(Silberstein, 1995). Corrections were made for the presence of aggregated material and any nucleic acid contamination (see *Introduction and Theory*).

Table 3 shows the complete absorbance data for preparation S8. In this preparation, two different methods of breaking up the myofibril structure, prior to the initial extraction, were compared: passing the muscle twice through a meat grinder (preparation S8-G), versus following this double grinding with homogenization of an ice-cold slurry of the mince in a Virtus™ blender (preparation S8-H). The absorbance spectra of the final products of preparation S8 show that homogenization did not increase the yield of myosin; 102 mg of myosin were collected for Prep S8-G and 104 mg for Prep S8-H (see Table 2). However, it did increase the contamination by nucleic acids as shown by the ratio of  $A_{280}$  to  $A_{260}$ ; for S8-G this ratio was found to be 1.39 while for S8-H it was 0.986 (see Table 3). These ratios translate into 0.75% nucleic acid content in S8-G and 3.4% nucleic acid content in S8-H.<sup>15</sup>

	Prep S8-G	Prep S8-H
$A_{340}$ (AU)	0.0166	0.0103
$A_{280}$ (AU)	0.231	0.185
$A_{260}$ (AU)	0.167	0.187
$(A_{340}/A_{280}) \times 100$	7.2%	5.6%
$A_{280}/A_{260}$	1.39	0.986
% Nucleic Acid	0.75%	3.4%

Table 3. Absorbance data (AU) on the parallel S8 preparations.  $A_{280}/A_{260}$  values indicate that homogenization of muscle mince after grinding (S8-H) results in a greater contamination of nucleic acid in the final myosin than only grinding (S8-G).

<sup>15</sup> See Robyt and White, 1987, p. 234.

The values of  $(A_{340}/A_{280}) \times 100$ , which indicates the presence of aggregated material, for the two preparations are 7.2% for S8-G and 5.6% for S8-H. These low values indicate low amounts of aggregated material are present in both preparations, with S8-H having slightly less than S8-G. So S8-H was seen to have higher nucleic acid contamination than S8-G, but less aggregated material.

*SDS-PAGE to Monitor Myosin Purification.* To track the myosin extraction process, aliquots were taken at various stages and analyzed by the Laemmli method of SDS-PAGE to visualize the proteins present. For example, Figure 23 shows a 7.5% denaturing non-gradient SDS-PAGE

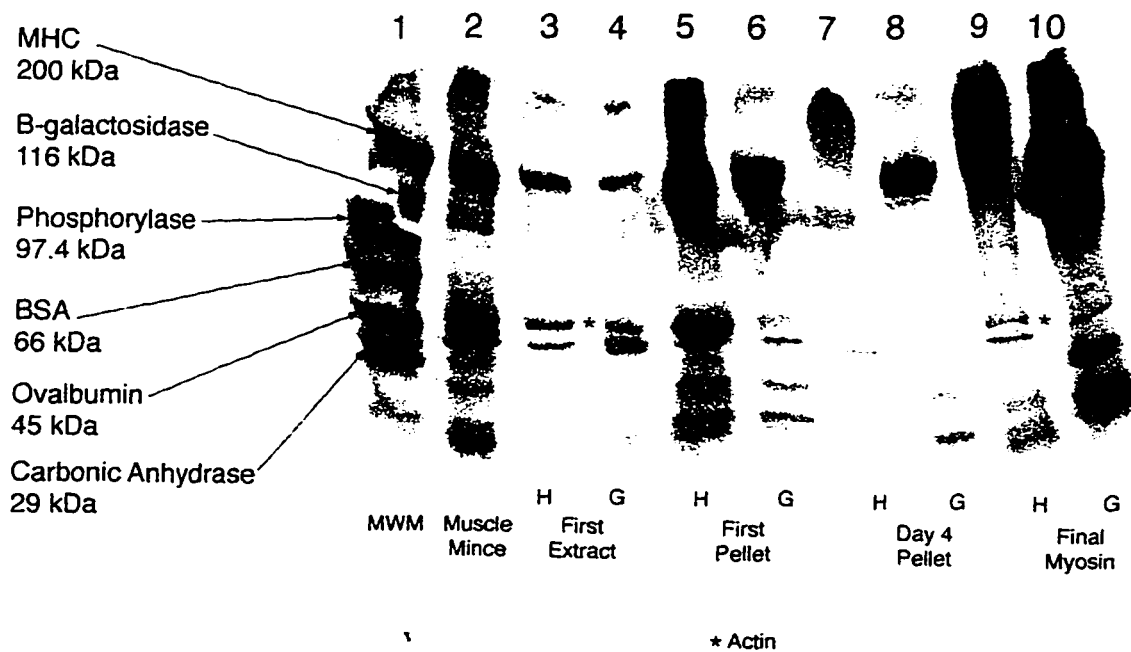


Figure 23. SDS-PAGE analysis of the major stages of the myosin preparation S8. The actin contamination remaining at the end of preparation S8-H can be seen in Lane 9 (at the ★), but is not present in S8-G. Lane 1: molecular weight markers; Lane 2: minced muscle; Lane 3: Day 1 extract from minced, homogenized preparation (H); Lane 4: Day 1 extract from minced muscle preparation (G); Lane 5: first pellet, H; Lane 6: first pellet, G; Lane 7: Day 4 pellet, H; Lane 8: Day 4 pellet, G; Lane 9: final myosin, S8-H; Lane 10: final myosin, S8-G. (7.5% denaturing, non-gradient SDS-PAGE gel run at 25 mAmps constant current.)

(Jule Biotechnology #7.5 D.75BMC-10P) which was run on samples taken at various stages during the parallel S8 preparations, S8-G and S8-H. This gel qualitatively shows the increasing purity of the myosin, in particular the removal of actin. A strong actin band is seen in both the S8-G and S8-H Preps on day 1 in the extract of the minced muscle (lanes 3 and 4, respectively). By comparing lanes 9 and 10, the final products from Preps S8-G and S8-H, respectively, it can be seen that this actin band has disappeared from S8-G but remains in S8-H. The final myosin collected from S8-H contains actin, while the final myosin collected from the portion of S8-G apparently contains no actin.

*Size Exclusion Chromatography of Myosin.* Since the myosin must be monodisperse when applied to the anti-myosin immunoaffinity columns, any aggregated material was removed by Size Exclusion Chromatography (SEC). The SEC matrix used was Sepharose 2B, a beaded agarose with a fractionation range of 70 to 40,000 kDa (Smith, 1988).

Figure 24 shows a sample chromatogram from the Sepharose 2B column. The sample is an aliquot of glycerinated myosin Prep S8-H that had been dialyzed to remove the glycerol. The peaks were identified by their absorbance spectra, using  $(A_{340}/A_{280}) \times 100$  as an indicator of the presence of aggregated material, and by SDS-PAGE. Peak 2, with  $(A_{340}/A_{280}) \times 100 = 1.01\%$ , was identified as containing the monodisperse myosin. Peaks 1 and 3, with  $(A_{340}/A_{280}) \times 100 = 31.9\%$  and  $3.81\%$ , respectively, were identified as different types of aggregated materials (see *Discussion and Conclusions*).

## Size Exclusion Chromatography of Myosin

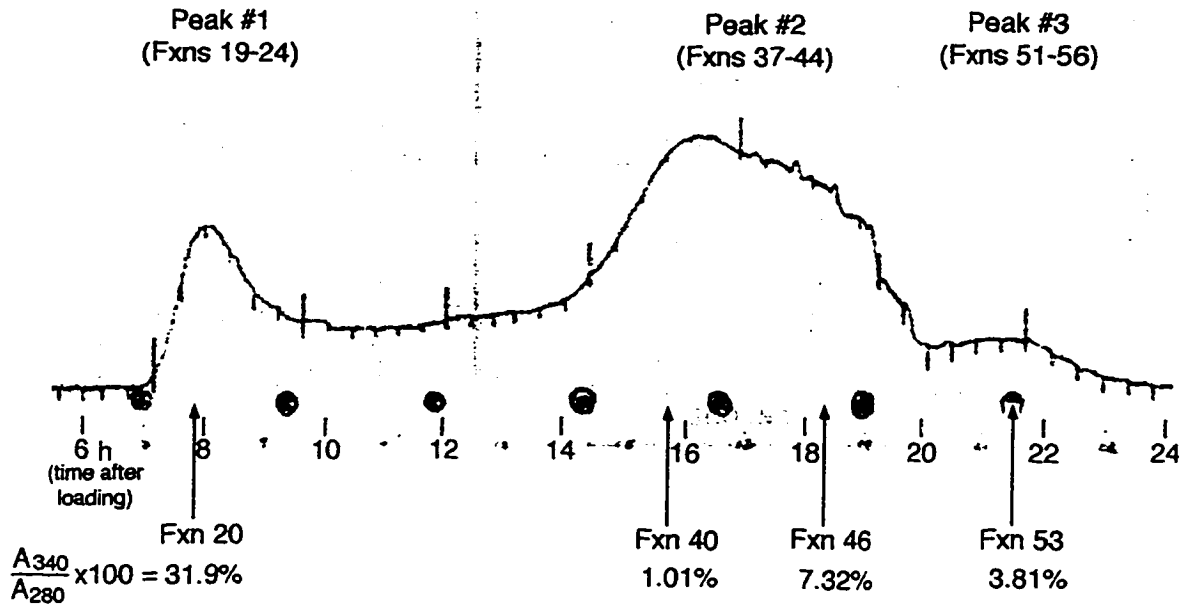


Figure 24. Chromatogram of myosin from preparation S8-H run on a 1.5 x 80-cm Sepharose 2B size exclusion column. A 4-mL aliquot of dialyzed myosin was loaded at 5 mg/mL. The column void volume,  $V_o$ , was pre-determined using Blue Dextran (MW = 2,000 kDa). Flow rate = 5.1 mL/h at 4 °C; eluant = SCB, Sepharose Column Buffer = 0.5 mM KCl, 50 mM  $KP_i$  @ pH 7.2, 0.25 mM EGTA; flow cell monitored at 280 nm with 0.2 AUFS.

Denaturing, non-gradient SDS-PAGE was performed on the Sepharose 2B peaks to identify the proteins in the three peaks, to check the myosin for signs of degradation, and to check for the presence of contaminating proteins.

Table 4 lists the molecular weights for typical contaminating proteins and characteristic degradation products that might be present. Pure, non-degraded myosin should appear on the gel as just two bands corresponding to the heavy and light chains at 230 and 16-25 kDa, respectively. Degraded myosin would be expected to show additional bands representing several characteristic head and tail fragments (see \* in Table 4): heavy meromyosin (150 kDa), light

meromyosin (70 kDa), S1 heads (95 kDa), and S2 fragments (55 kDa) (Garrett and Grisham, 1995; Offer et al., 1973). Also, this purification procedure is not expected to produce completely pure myosin, so some contaminating proteins may be visible.

Protein or Polypeptide	Approx. Mol Wt in kDa
Myosin heavy chain	230
M Protein	165
Heavy meromyosin *	150
C Protein	135
S1 head *	95
Light meromyosin *	70
S2 fragment *	55
Actin	42
Tropomyosin sub-units	33
Myosin light chains	16-25

Table 4. The most likely contaminating proteins and polypeptides and characteristic myosin degradation products (marked by \*) found in glycerinated myosin, and their corresponding molecular weights in kilodaltons (Excerpted from Garrett and Grisham, 1995; Offer et al., 1973.)

Figure 25 shows a diagram of the SDS-PAGE performed on peaks eluted from the Sepharose column. The sample loaded onto the column was the final product from myosin preparation S8-H, which is shown in lane II. The myosin heavy chains are visible at 230 kDa but the light chains are not seen on this gel since the sample was under-loaded and the normally faint myosin light chain bands were not made visible with the Coomassie stain. The band at 42 kDa is presumed to be actin. The band at ~30 kDa is consistent with the typical migration position for the three identical sub-units of the muscle protein tropomyosin.



I Molecular Weight Markers		II Myosin as loaded onto SEC column	III SEC Peak 1	IV SEC Peak 2	V SEC Peak 3
rabbit myosin heavy chains	205 kDa				
$\beta$ -galactosidase	116 kDa				
phosphorylase b	97 kDa				
BSA	66 kDa				
ovalbumin	45 kDa				
carbonic anhydrase	29 kDa				

Figure 25. Diagram of the SDS-PAGE performed on the three peaks eluted from S8-H myosin chromatographed on a 1.5 x 80-cm Sepharose 2B column. Lane I = molecular weight markers; Lane II = myosin preparation S8-H as loaded onto the Sepharose column; Lane III = peak 1 off the SEC column; Lane IV = peak 2; and Lane V = Peak 3. Peak 2 contains the desired monodisperse myosin. (7.5% denaturing, non-gradient gel run at 25 mA constant current.) (Diagram drawn from the original gel which was inadvertently damaged before scanning.)

There does seem to be some degradation in this myosin sample as indicated by the appearance of a band at 95 kDa; this corresponds to the expected position for the migration of the myosin fragments designated 'S1 heads.' The accompanying degradation product, the tail, may be represented at 125 kDa in the trio of bands just below the myosin heavy chains. This trio of bands is of particular interest since it might also represent contamination by M protein (165 kDa) and C protein (135 kDa). The presence of these two proteins in the myosin sample are of particular concern since they are myofibrillar scaffolding proteins and so would be expected to facilitate the undesirable aggregation of myosin (Offer et al., 1973).

The band pattern for peak 1 (lane III) shows a band at 42 kDa, which is probably actin, and myosin heavy chains at 230 kDa. Peak 1 on the SEC chromatogram showed the highest degree of aggregation in the absorbance data (31.9%, Figure 24). The results of this gel, the absorbance data, and the SEC elution profile combine to indicate that Peak 1 contains actomyosin as well as homo-aggregates of myosin (see *Discussion and Conclusions*).

Peak 2 is found in lane IV; here the gel shows myosin heavy chains with the trio of minor bands. The absorbance data which indicate that Peak 2 has the least aggregation (1.01%, Figure 24), thus, Peak 2 contains monodisperse myosin. If the trio of bands just below the myosin heavy chain does represent M protein and C protein, the absorbance data indicate that they are not causing the myosin to aggregate.

Finally, Peak 3 is in lane V showing the tropomyosin sub-units (~30 kDa), the S1 heads (95 kDa), and one unidentified high molecular weight band (>230 kDa). The lack of any complete myosin heavy chains in this lane combined with the presence of the S1 heads and the absorbance data indicating some aggregated material present (3.81%, Figure 24), seems to indicate that this late-eluting peak contains compact aggregates of degraded myosin heavy chains. This is consistent with the elevated value for  $A_{340}/A_{280} \times 100$  and the expected SEC elution order of the material in Peak 3 (see *Discussion and Conclusions*).

## **Monoclonal Antibody Preparation**

*Overview.* The monoclonal antibodies (MAbs) used in this study fall into two immunoglobulin classes: IgM and IgG. Hybridoma cell lines designated MHC-F22, MHC-F36, MHC-S84, MHC-S95, and MHC-25, were previously shown to produce MAbs which bind unique myosin heavy chain epitopes (Silberstein and Blau, 1986). Fresh quantities of these MAbs were produced as supernatants from MAb-secreting hybridoma cells and as an 'ascites' fluid. The MAbs were

purified in a two-step procedure consisting of precipitation from the ascites fluid followed by size exclusion chromatography to remove the major contaminating protein, serum albumin. The IgGs were purified by a single-step procedure involving adsorption onto a 'Protein A' column.<sup>16</sup>

*Cell Culture.* Five hybridoma cell lines known to secrete anti-myosin monoclonal antibodies, each with binding specificity to a unique myosin heavy chain epitope, were maintained. Table 5 shows a summary of the hybridoma cell lines maintained, the immunoglobulin class of the MAb they produce, and the myosin contractile type and specific myosin heavy chain epitope to which the MAb reacts (see also Table 1, page 34).

Hybridoma Cell Line	Ig Class of MAbs	Myosin Epitope Recognized by MAb	Myosin Contractile Type
MHC-F22	IgM	F22	Fast
MHC-F36	IgM	F36	Fast
MHC-S84	IgM	S84	Slow
MHC-S95	IgG	S95	Slow
MHC-25	IgG	25	All

Table 5. The five monoclonal hybridoma cell lines each secrete a unique MAb. Each MAb reacts with a unique myosin epitope; they either react with a fast-contracting type myosin isozyme or a slow-contracting type myosin isozyme, except for MAb-25 which reacts with all myosin isozymes. (See also Table 1, page 34.)

The hybridoma cells were thawed from long-term liquid nitrogen storage and brought to the log-phase of their growth cycle. The cells were maintained at this stage of growth and the cultures were expanded in volume until they were found to be growing sufficiently vigorously and densely as to be secreting up to 10 µg/mL of the MAb of interest. At this point, aliquots of cells were

---

<sup>16</sup> IgG purification using Protein A column was performed by G. Alegre (unpublished data).

returned to liquid nitrogen for storage. This process was repeated multiple times for each different cell line to collect sufficient cells and cell supernatants (CSNs) for further use in the study.

Table 6 summarizes typical health data recorded for cell lines over the course of freeze/thaw cycles. Viability is defined as the ratio of live cells to total cells (Hochfield et al., 1993), expressed as a percent. It is preferable that the cells be  $\geq 85\%$  viable upon freezing as there is some loss of viability during cold storage. The cells' ability to survive cold storage varies with cell line, density of storage, and length of storage. For example, note that the cells of the MHC-S95 cell line went from 89% viable at freeze to 50% viable upon re-thaw ~2 months later, while cells of the MHC-25 cell line maintained essentially all of their viability after ~6 months in liquid nitrogen storage.

Cell Line	Freeze	Thaw	Freeze
MHC-S95	August 13 $1.58 \times 10^6$ cells/mL 89% viable	October 6 $1.54 \times 10^6$ cells/mL 50% viable	November 10 $1.3 \times 10^6$ cells/mL 86% viable
MHC-25	July 14 $3.83 \times 10^5$ cells/mL 92% viable	January 11 $3.4 \times 10^5$ cells/mL 88% viable	January 20 $1.58 \times 10^6$ cells/mL 94% viable

Table 6. Typical viability results upon freezing and subsequent thawing of hybridoma cell lines. (Unpublished data compiled from cell culture done by L. Silberstein, B. Godden, J. Hubenthal, and S. Acevedo).

While actively growing, these cells secrete MAbs into the media in which they are grown. This is an easily collected, though dilute source of MAbs; typical concentrations of MAbs in these 'cell supernatants' (CSNs), as determined by homo-isotypic sandwich ELISA are shown in Table 7.

MAb	IgM in Cell Supernatant (mg/mL)	IgM in Ascites (mg/mL)
MAb-F22	0.00226	1.45
MAb-F36	0.0147	3.26
MAb-S84	0.0531	1.53

Table 7. The concentration of total IgM in the cell supernatants and ascites as determined by homo-isotypic sandwich ELISA.

*Ascites Production.* In order to acquire more concentrated solutions of MAbs, 'ascites' were produced (see *Introduction and Theory*). The ascites that contain IgM-class MAbs (MAb-F22, MAb-F36, and MAb-S84) were analyzed by homo-isotypic sandwich ELISAs to determine total IgM concentration. As can be seen in Table 7, the ascites typically contain much higher concentrations of IgM than the CSNs.

*Determination of Total Concentration of Immunoglobulin.* The total concentration of immunoglobulin in a sample was determined by homo-isotypic sandwich ELISAs (see *Materials and Methods* and *Introduction and Theory*).

Table 8 shows the data (average absorbance values for duplicate wells, without blanks subtracted) from one homo-isotypic sandwich ELISA. This ELISA was performed to determine the concentration of IgM in cell supernatants (CSNs) from the three cell lines (MHC-F22, MHC-F36, and MHC-S84) which produce IgM-class anti-myosin MAbs. On this 96-well plate, the standard was MOPC, the samples were CSNs from the three IgM-class MAbs. CSN from the cell line that produces the IgG-class MAb-25 was used as a negative control; PBS-blotto was used as the diluent and blank. The data from the MOPC standard were used to construct a linear standard

curve relating absorbance to IgM concentration. Using this curve, the absorbance data from the samples were converted into concentration of IgM in each CSN.

	Absorbance at 405 nm (AU)						MOPC ng/mL
	Blanks	F22 CSN	F36 CSN	S84 CSN	MAB-25	MOPC	
A	0.083	0.492	1.413	1.525	0.077	0.777	1,000
B	0.091	<b>0.344</b> <b>0.264</b>	1.144	1.377	0.079	0.681	500
C	0.073	<b>0.207</b> <b>0.127</b>	0.800	1.294	0.063	0.554	250
D	0.074	<b>0.146</b> <b>0.066</b>	0.496	0.938	0.072	0.331	125
E	0.078	0.103	<b>0.325</b> <b>0.245</b>	0.653	0.065	0.246	62.5
F	0.082	0.096	<b>0.202</b> <b>0.122</b>	<b>0.398</b> <b>0.318</b>	0.073	0.178	31.3
G	0.193	0.095	<b>0.138</b> <b>0.058</b>	<b>0.260</b> <b>0.180</b>	0.070	0.118	15.6
H	0.065	0.071	0.098	0.130	0.059	0.115	7.8

— 2.26 14.7 53.07 — —  
 $\mu\text{g/mL IgM}$   $\mu\text{g/mL IgM}$   $\mu\text{g/mL IgM}$

<— calculated IgM concentrations —>

Table 8. Raw absorbance readings (average AUs for duplicate wells; blanks not subtracted) from a homo-isotypic sandwich ELISA to determine IgM concentrations in cell supernatants from the cell lines (MHC-F22, MHC-F36, and MHC-S84) that produce IgM-class anti-myosin MAbs. 1° layer =  $\text{G}\alpha\text{mIgM}$  at 1  $\mu\text{g/mL}$ ; 2° layer = CSNs diluted 1:2 serially down the plate (i.e. A, B, C, etc.) in PBS-blotto (starting at a 1:10 dilution of neat CSN), IgG-class MAb-25 CSN diluted 1:2 serially down the plate in PBS-blotto as a negative control, PBS-blotto as blanks, and MOPC as the IgM standard at dilutions shown; 3° layer = 1:1,000 dilution of stock  $\text{G}\alpha\text{mIgM}\cdot\text{HRP}$ . The samples outlined in heavy borders are those used to calculate the IgM concentrations for each sample shown at the bottom of the table; the absorbance values in bold have the average blank subtracted (see text).

Typically, the final value of IgM concentration in a given sample is calculated as an average from a subset of all the dilutions of that sample. This is because some of the dilutions are too concentrated in IgM and some too dilute to produce reliable absorbance readings. The wells which have been included in the calculation for this example are shown outlined in heavy black in Table 8; for these samples, the absorbance values with the average blank subtracted are shown in bold. The samples have been diluted twofold in each successive row down the plate (A, B, C, etc.), and the average absorbance values (with blanks subtracted) drop approximately in half in each successive row. This halving is indicative of which dilutions produced data reliable for use in calculating the final IgM concentrations. For each CSN, the reported IgM concentration at the bottom of Table 8 is the average of the values calculated from the data shown in the outlined boxes.

*Saturated Ammonium Sulfate Precipitation of Immunoglobulin from Ascites.* IgM is just one of the proteins present in ascites. The amount of IgM in the ascites used in this study, as determined by homo-isotypic sandwich ELISAs, ranged from 7-16% of the total protein (Table 9).

Ascites	mg/mL Protein	mg/mL IgM	% IgM/Protein
MAB-F22	14.2	1.45	10.2%
MAB-F36	20.4	3.26	16.0%
MAB-S84	21.5	1.53	7.12%

Table 9. Concentrations of total protein and total IgM in the original ascites. Protein concentrations were determined by BioRad DC Protein Assay kit (for MAb-F22) or absorbance at 280 nm (for MAB-F36 and MAB-S84;  $\epsilon^{1\%_{280\text{nm}}} = 10.0 \text{ mL/mg-cm}$ ); total IgM concentrations were determined by homo-isotypic sandwich ELISA (see *Materials and Methods*, for details).

The IgM was separated away from the bulk protein in the ascites by precipitation with Saturated Ammonium Sulfate (SAS). The MAb-F22 was the first ascites precipitated; a flow chart of the precipitation protocol is shown in Figure 26.

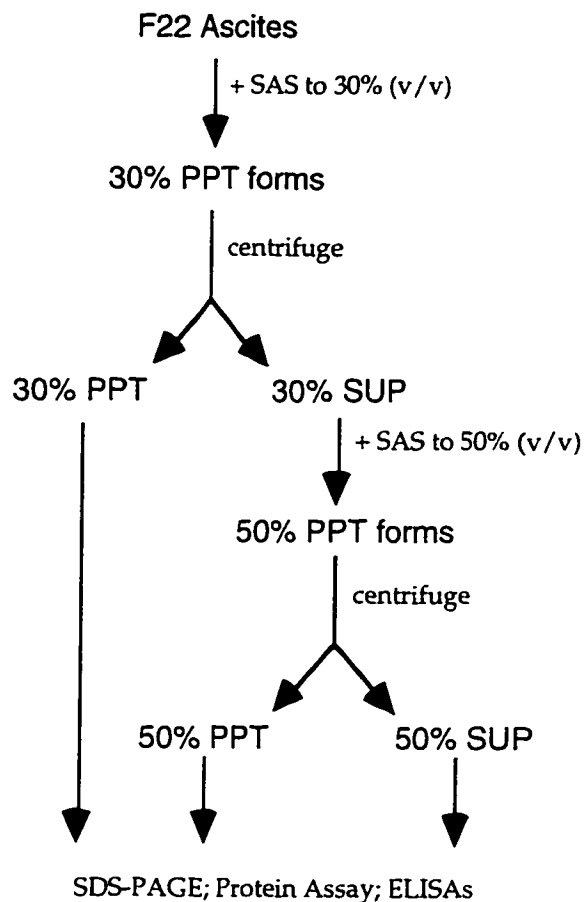


Figure 26. Flow chart for the SAS precipitation protocol for F22 ascites. The final three stages: F22<sub>30%SAS</sub> PPT, F22<sub>50%SAS</sub> PPT, and F22<sub>50%SAS</sub> SUP, are then analyzed for content and purity of both total protein and IgM by SDS-PAGE, homo-isotypic sandwich ELISAs, and protein assays.

The MAb-F22 was precipitated at two SAS concentrations to determine the best concentration to use. SAS was added to the ascites until it reached 30% (v/v) at which point the precipitate designated 'F22<sub>30%SAS</sub> PPT' was collected by centrifugation. Additional SAS was added to the remaining supernatant until the cumulative concentration was 50% (v/v). At this point the



precipitate designated 'F22<sub>50%</sub>SAS PPT' was collected and the remaining supernatant ('F22<sub>50%</sub>SAS SUP') was saved. Each of the two precipitates were resuspended in buffer and chromatographed individually on a Sephacryl S300-HR size exclusion chromatography column (see Figure 27, page 96, and Figure 28, page 97). Assays for total protein and IgM concentration were performed on the starting ascites, the SAS precipitates and supernatants, and the peaks from the SEC column (these data are summarized in Tables 10 through 13).

Table 10 shows the results of the analyses of total protein and total IgM concentrations of the starting ascites and the three stages from the SAS precipitation of F22 ascites (30% (v/v) SAS PPT, 50% (v/v) SAS PPT, and final SUP); the material in the ascites is taken as 100% for all comparisons. The IgM yield approximately doubled in raising the cumulative SAS concentration from 30% (v/v) to 50% (v/v). At 30% (v/v) SAS added, 5.74 mg of IgM was collected (9.90% of available IgM); an additional 4.28 mg of IgM (7.39% of available) was collected by increasing the

Sample	Total Protein		Total IgM		
	mg	% Recovery	mg	% Recovery	% IgM/Protein
MAB-F22 Ascites	1000	=100%	58.0	=100%	5.8%
F22 <sub>30%</sub> SAS PPT	56.2	5.62%	5.74	9.90%	10.2%
F22 <sub>50%</sub> SAS PPT	38.4	3.84%	4.28	7.39%	11.1%
F22 <sub>50%</sub> SAS SUP	444	44.4%	0.87	1.50%	0.20%
Net Recovery	549	54.9%	10.9	18.8%	

Table 10. Yields of 'Total Protein' and 'Total IgM' in the SAS precipitation of IgM from MAB-F22 ascites. Total Protein was determined by BioRad DC Protein Assay kit and Total IgM was determined by homo-isotypic sandwich ELISA. The Total Protein and Total IgM in the original ascites are defined as 100%. '% Recovery' = total amount at that stage relative to amount in ascites; 'Net Recovery' = sum total of Recovery at all stages.

SAS up to a cumulative concentration of 50% (v/v). The material left behind in the supernatant at this point had a high protein content (444 mg) but a very low IgM content (0.87 mg). Thus using greater than 50% (v/v) SAS would not gain much more IgM, but would increase the contamination from other proteins.

Based on the results of the MAb-F22 SAS precipitation it was decided to precipitate the MAb-F36 and MAb-S84 ascites using ~50% (v/v) SAS. MAb-F36 ascites was processed in two batches using 45% (v/v) and 50% (v/v) SAS; MAb-S84 ascites was precipitated in one batch at 50% (v/v) SAS. Analyses for total protein and total IgM were performed at the same stages of the purification as for MAb-F22. The data for MAb-F36 and MAb-S84 are summarized in Table 11. Total IgM Recovered ranged from ~56-66% of the total IgM available in the ascites.<sup>17</sup>

---

<sup>17</sup> For a discussion of the discrepancies shown between total protein and total IgM content, see *Discussion and Conclusions*.

Sample	Total Protein		Total IgM		
	mg	% Recovery	mg	% Recovery	% IgM/Protein
MAB-F36 Ascites	92.8	=100%	14.8	=100%	15.9%
F36 <sub>45%</sub> SAS PPT	17.5	18.9%	9.72	65.7%	55.5%
F36 <sub>45%</sub> SAS SUP	48.3	52.0%	0.169	1.1%	0.35%
Net Recovery	65.8	70.9%	9.89	66.8%	

Sample	Total Protein		Total IgM		
	mg	% Recovery	mg	% Recovery	% IgM/Protein
MAB-F36 Ascites	92.8	=100%	14.8	=100%	15.9%
F36 <sub>50%</sub> SAS PPT	25.4	27.4%	8.4	56.8%	33.1%
F36 <sub>50%</sub> SAS SUP	58.1	62.6%	0.364	2.46%	0.63%
Net Recovery	83.5	90.0%	8.76	59.3%	

Sample	Total Protein		Total IgM		
	mg	% Recovery	mg	% Recovery	% IgM/Protein
MAB-S84 Ascites	249	=100%	17.7	=100%	7.1%
S84 <sub>50%</sub> SAS PPT	45.1	18.1%	11.0	62.1%	24.4%
S84 <sub>50%</sub> SAS SUP	109	3.82%	0.0041	0.023%	0.0038%
Net Recovery	154	61.9%	11.0	62.1%	

Table 11. Yields of total protein and total IgM in the purification of IgM from ascites. MAb-F36 at 45% (v/v) SAS (top); MAb-F36 at 50% (v/v) SAS (middle); and MAb-S84 at 50% (v/v) SAS (bottom). Total protein was determined by absorbance at 280 nm (for ascites  $\epsilon^{1\%}_{280\text{nm}} = 10.0 \text{ mL/mg-cm}$ ; for PPTs  $\epsilon^{1\%}_{280\text{nm}} = 13.3 \text{ mL/mg-cm}$ ; for SUPs  $\epsilon^{1\%}_{280\text{nm}} = 10.0 \text{ mL/mg-cm}$ ); total IgM was determined by homo-isotypic sandwich ELISA. The total protein and total IgM in the ascites are defined as 100%.

*Size Exclusion Chromatography of Precipitated Immunoglobulins.* The main contaminating protein that is carried into the SAS precipitated IgM is serum albumin (Hockfield et al., p 370, 1993; Andrew and Titus, 1994). Because of the great size difference between IgM (~900 kDa) and albumin (66 kDa) Size Exclusion Chromatography (SEC) can be used to remove the albumin. After resuspension and dialysis, the SAS-precipitated IgMs were applied to a 1.5 x 80-cm column of Sephacryl S300-HR (fractionation range of 10-1500 kDa). In the following chromatograms (Figures 27-31) IgM elutes first, followed by albumin.<sup>18</sup>

### Size Exclusion Chromatography of F22<sub>30%</sub>SAS PPT

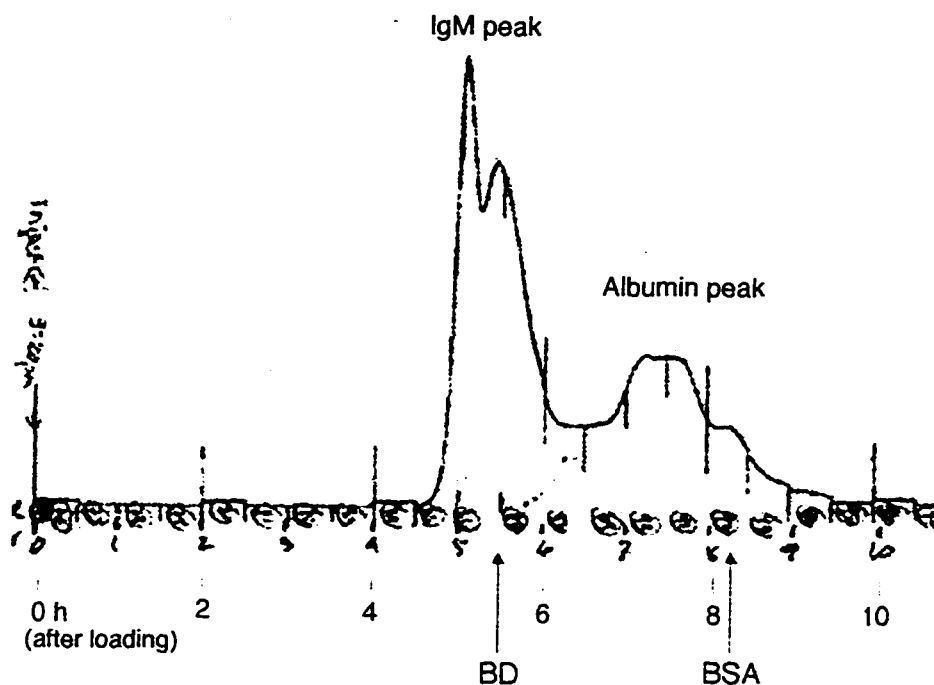


Figure 27. Size exclusion chromatography of the 30% (v/v) SAS precipitation of F22 ascites (F22<sub>30%</sub>SAS PPT) on a 1.5 x 80-cm Sephacryl S300-HR column to remove albumin from IgM. Flow rate = 9 mL/h at RT; eluant = 20 mM sodium borate, 150 mM NaCl @ pH 8.2; flow cell monitoring effluent @ 280 nm, 1.0 AUFS. (Elution times of blue dextran ('BD') and BSA ('BSA') were pre-determined in a separate run.)

<sup>18</sup> The column void volume,  $V_0$ , was pre-determined using Blue Dextran (MW = 2,000 kDa); the elution volume for albumin,  $V_{alb}$ , was pre-determined using BSA (MW = 66 kDa).

These SEC chromatograms clearly show that the different percentages of SAS resulted in slightly different proportions of albumin to IgM in the precipitate. For example, compare the chromatogram for MAb-F36 precipitated with 45% (v/v) SAS (Figure 29) to that for which 50% (v/v) SAS was used (Figure 30). The relative peak heights of Alb:IgM are 1:3.33 for the 45% (v/v) SAS precipitation but decrease to 1:1.75 for the 50% (v/v) SAS precipitation. A similar effect was seen on the chromatograms for MAb-F22 at 30% (v/v) (Figure 27) and 50% (v/v) SAS (Figure 28). Thus, slightly elevating the concentration of SAS used to precipitate the IgM caused a greater amount of albumin to be co-precipitated. Despite this increased albumin contamination, the higher percentage of SAS was preferred since, as previously discussed, a greater fraction of the total IgM present in the ascites was recovered, and the albumin is readily removed by SEC.

#### Size Exclusion Chromatography of F22<sub>50%SAS</sub> PPT

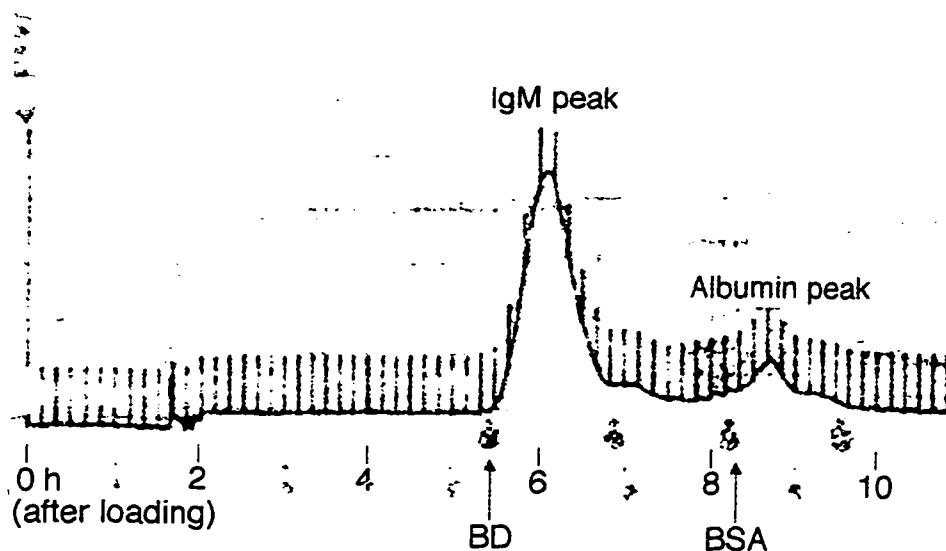


Figure 28. Size exclusion chromatography of the 50% (v/v) SAS precipitation of F22 ascites (F22<sub>50%SAS</sub> PPT) on a 1.5 x 80-cm Sephacryl S300-HR column to remove albumin from IgM. Flow rate = 9.8 mL/h at RT; eluant = 20 mM sodium borate, 150 mM NaCl @ pH 8.2; flow cell monitoring effluent @ 280 nm, 0.5 AUFS. (Elution times of blue dextran ('BD') and BSA ('BSA') were pre-determined in a separate run.)

### Size Exclusion Chromatography of F36<sub>45%</sub>SAS PPT

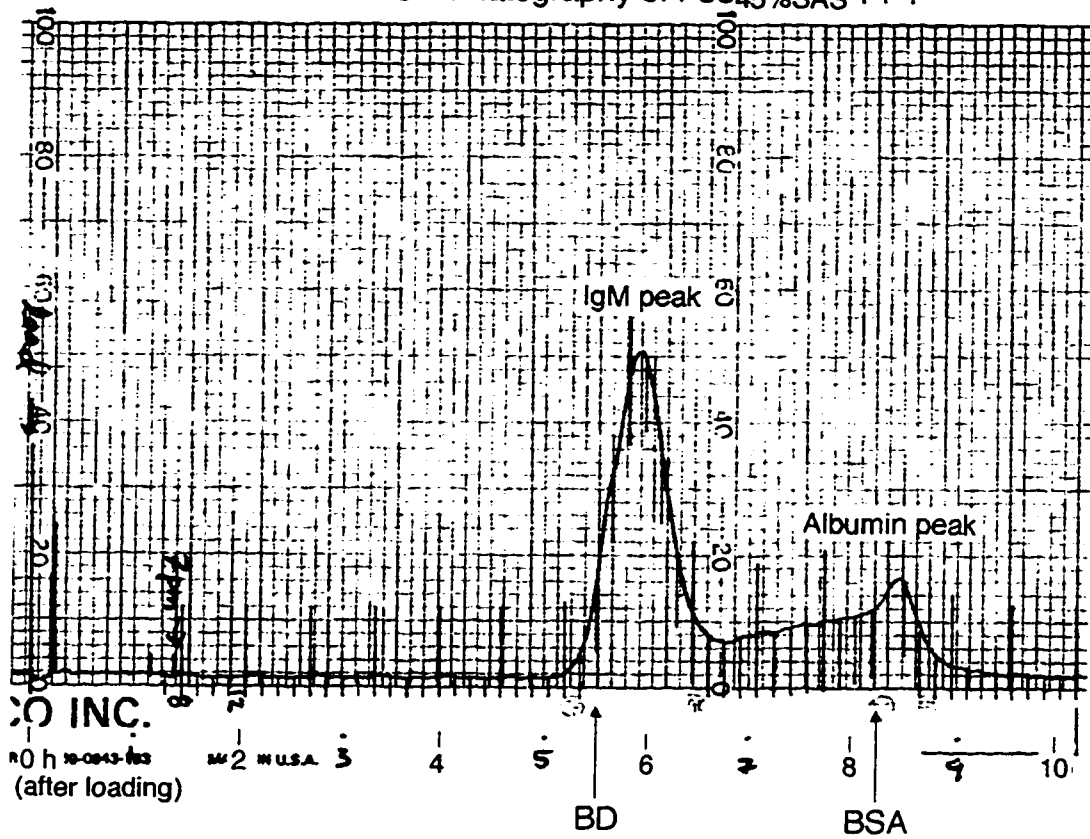


Figure 29. Size exclusion chromatography of the 45% (v/v) SAS precipitation of F36 ascites (F36<sub>45%</sub>SAS PPT) on a 1.5 x 80-cm Sephacryl S300-HR column to remove albumin from IgM. Flow rate = 9 mL/h at RT; eluant = 20 mM sodium borate, 150 mM NaCl @ pH 8.2; flow cell monitoring @ 280 nm, 1.0 AUFS. (Elution times of blue dextran ('BD') and BSA ('BSA') were pre-determined in a separate run.)

### Size Exclusion Chromatography of F36<sub>50%</sub>SAS PPT

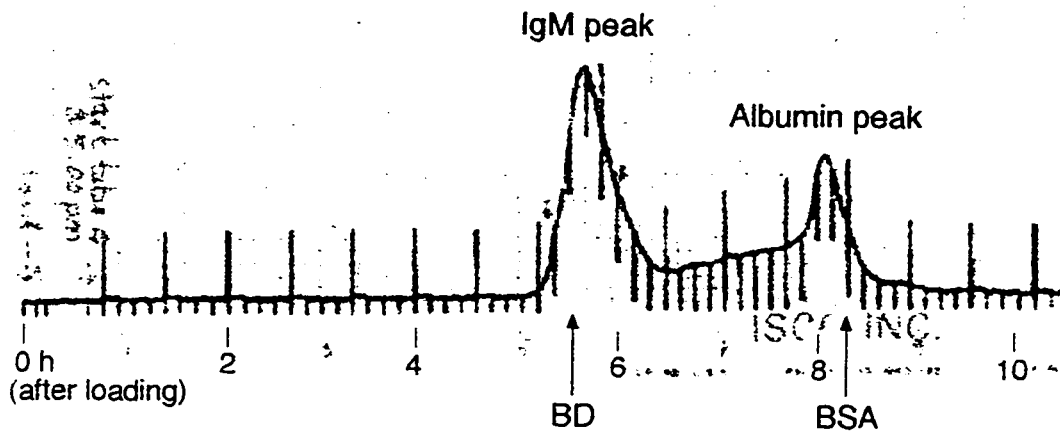


Figure 30. Size exclusion chromatography of the 50% (v/v) SAS precipitation of F36 ascites (F36<sub>50%</sub>SAS PPT) on a 1.5 x 80-cm Sephacryl S300-HR column to remove albumin from IgM. Flow rate = 9 mL/h at RT; eluant = 20 mM sodium borate, 150 mM NaCl @ pH 8.2; flow cell monitoring @ 280 nm, 1.0 AUFS. (Elution times of blue dextran ('BD') and BSA ('BSA') were pre-determined in a separate run.)

### Size Exclusion Chromatography of S84<sub>50%</sub>SAS PPT

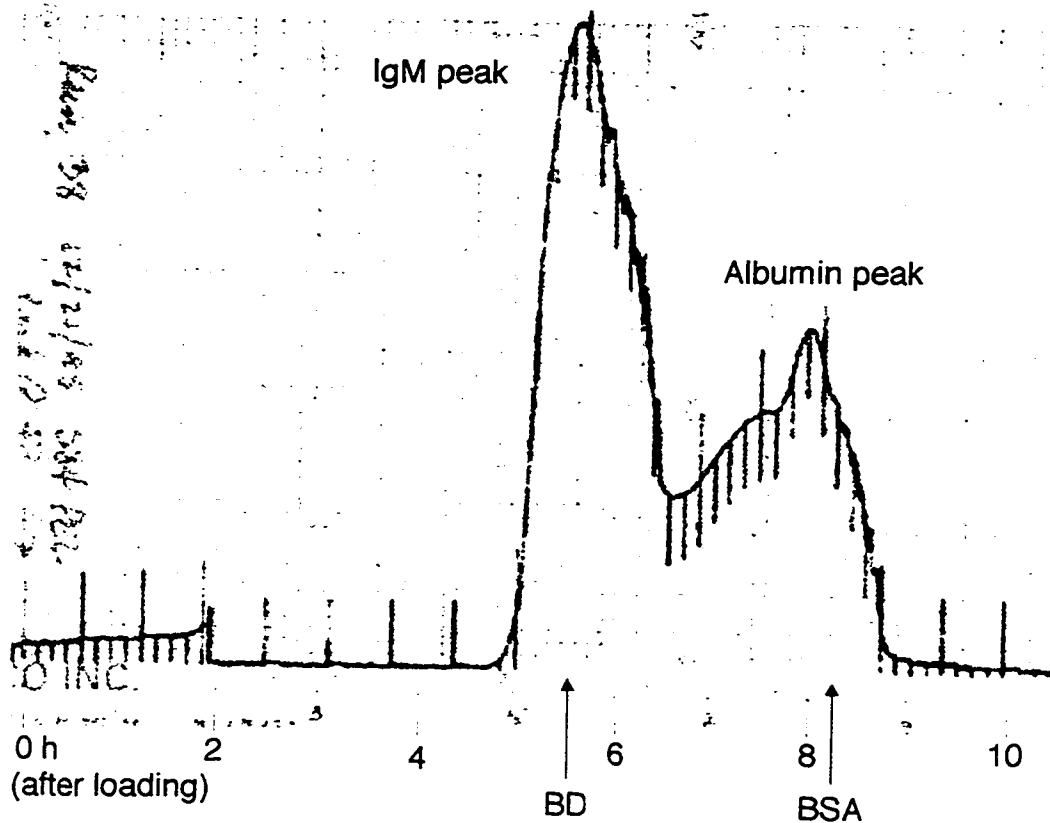


Figure 31. Size exclusion chromatography of S84<sub>50%</sub>SAS PPT on a 1.5 x 80-cm Sephacryl S300-HR column to remove albumin from IgM. Flow rate = 9 mL/h at RT; eluant = 20 mM sodium borate, 150 mM NaCl @ pH 8.2; flow cell monitoring @ 280 nm, 1.0 AUFS. (Elution times of blue dextran ('BD') and BSA ('BSA') were pre-determined in a separate run.)

After the peaks were collected from the Sephacryl columns the IgMs were found by  $A_{280}$  to have been diluted about 10-fold (data not shown). The samples were re-concentrated by dialysis against dry Sephadex G200 (Harris and Angal, 1994). These final purified, re-concentrated IgMs were analyzed by homo-isotypic sandwich ELISA, SDS-PAGE, and absorbance spectra. (The results for protein analyses and homo-isotypic sandwich ELISAs on the ascites and the SAS precipitates have been shown in Tables 10 through 13).



Table 12 shows the results of the analyses for total protein and total IgM in the re-concentrated peaks from chromatographing the resuspended F22 SAS precipitates (F22<sub>30%</sub>SAS PPT and F22<sub>50%</sub>SAS PPT) on the Sephacryl S300-HR column. At both concentrations of SAS, the peak identified as the IgM peak contained much higher yields of total IgM than the peak identified as albumin (peak identification by SDS-PAGE and homo-isotypic sandwich ELISA). Also, the IgM peak was seen to be enriched in IgM relative to the SAS precipitate loaded onto the Sephacryl column. For example, for the F22<sub>50%</sub>SAS PPT the percent of IgM to total protein is 11.1% (Table 10, page 93), but in the IgM peak resulting from chromatographing an aliquot of this sample on the Sephacryl S300-HR column, the percent of IgM to total protein is 28.5% (the peak contained 1.88 mg IgM in 6.60 mg total protein). Similar enrichment was seen for the MAb-F36 and MAb-S84 SAS precipitates chromatographed on the Sephacryl S300-HR column (compare data for IgM content before and after SEC in Table 11, and in Table 13 below).

Sample Loaded	Peak	Total Protein (mg)	Total IgM (mg)	% IgM/Protein
F22 <sub>30%</sub> SAS PPT	IgM Peak	12.8	6.54	51.1%
F22 <sub>30%</sub> SAS PPT	Albumin Peak	1.17	0.0041	0.35%
F22 <sub>50%</sub> SAS PPT	IgM Peak	6.60	1.88	28.5%
F22 <sub>50%</sub> SAS PPT	Albumin Peak	5.90	0.017	0.28%

Table 12. Yields of total protein and total IgM in the 'IgM peak' and 'albumin peak' from the size exclusion chromatography of SAS precipitates of MAb-F22 ascites on Sephacryl S300-HR column. (See chromatograms in Figure 27, page 96 and Figure 28, page 97.) (Total protein was determined by BioRad DC Protein Assay kit; total IgM was determined by homo-isotypic sandwich ELISA.)

The fractions from the tail of the IgM peak from the elution of F36<sub>45%</sub>SAS PPT on the Sephacryl S300-HR column (labeled 'IgM Peak Tail' in Table 13) were pooled and analyzed to see how much IgM was being lost due to a conservative choice of fractions to pool. The data in Table 13 show that not a great deal of IgM was lost in these tail fractions; 0.356 mg of IgM was found in a pool of four tail fractions versus 7.04 mg in the main IgM peak; the IgM in the tail represents ~5% of the IgM in peak.

Sample Loaded	Peak	Total Protein (mg)	Total IgM (mg)	% IgM/Protein
F36 <sub>45%</sub> SAS PPT	IgM Peak	4.3	7.04	163%
F36 <sub>45%</sub> SAS PPT	IgM Peak 'Tail'	0.60	0.356	59.3%
F36 <sub>45%</sub> SAS PPT	Albumin Peak	2.8	0.0039	0.14%

Sample Loaded	Peak	Total Protein (mg)	Total IgM (mg)	% IgM/Protein
F36 <sub>50%</sub> SAS PPT	IgM Peak	3.32	5.28	159%
F36 <sub>50%</sub> SAS PPT	Albumin Peak	2.38	0.0019	0.08%

Sample Loaded	Peak	Total Protein (mg)	Total IgM (mg)	% IgM/Protein
S84 <sub>50%</sub> SAS PPT	IgM Peak	11.9	7.84	65.8%
S84 <sub>50%</sub> SAS PPT	Albumin Peak	13.5	0.0038	0.03%

Table 13. Yields of total protein and total IgM in the 'IgM peak' and 'albumin peak' from the size exclusion chromatography of SAS precipitates of MAb-F36 and MAb-S84 ascites. (See Figures 29 and 30 for chromatograms of F36 precipitates and Figure 31 for chromatogram of S84 precipitate.) 'Total Protein' was determined by absorbance at 280 nm (for IgM peak,  $\epsilon^{1\%}_{280\text{nm}} = 13.3$  mL/mg-cm; for Alb peak,  $\epsilon^{1\%}_{280\text{nm}} = 5.8$  mL/mg-cm). 'Total IgM' was determined by homo-isotypic sandwich ELISA.

*SDS-PAGE to Monitor IgM Purity.* SDS-PAGE analyses were used to track the purification of the IgMs precipitated from ascites.

The gel in Figure 32 shows the results of the precipitation of IgM from MAb-F22 ascites with 30% (v/v) and 50% (v/v) SAS. Lane 2 has the IgM standard (MOPC), lane 3 the albumin standard (BSA); protein bands in the sample lanes are identified by comparison of their migration to these two standards. Lanes 5 and 6 are two different sample loads on the gel of the F22<sub>30%SAS</sub> PPT;

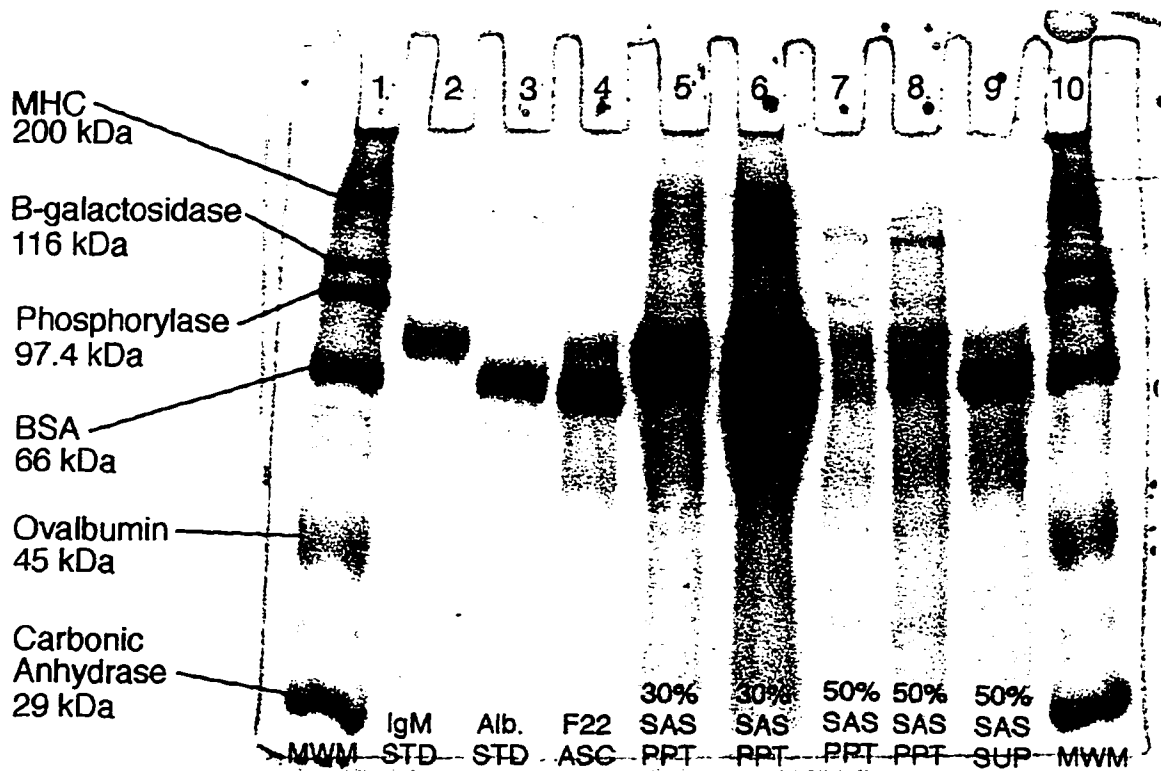


Figure 32. SDS-PAGE analysis to track the SAS precipitation of IgM from F22 ascites. 'MWM' = molecular weight markers; 'IgM STD' = MOPC; 'Alb. STD' = BSA; '30% SAS PPT' = F22<sub>30%SAS</sub> PPT (loaded at 1.2  $\mu$ g and 2.4  $\mu$ g of protein); '50% SAS PPT' = F22<sub>50%SAS</sub> PPT (loaded at 1.2  $\mu$ g and 2.4  $\mu$ g of protein); '50% SAS SUP' = F22<sub>50%SAS</sub> SUP. (Custom 12.5% denaturing, non-gradient gels were loaded with 1-4  $\mu$ g protein in each well and the gels were run for '150% time;' see text for details).

lanes 7 and 8 are two different sample loads of the F22<sub>50%</sub>SAS PPT. In the MAb-F22 ascites (lane 4) the proportion of albumin to IgM is qualitatively observed to be much greater than in either of the SAS precipitates (lanes 5-8). So in the range of 30-50% (v/v) SAS there was a preferential precipitation of IgM over albumin. From these gels, it appears that the F22<sub>30%</sub>SAS PPT has a greater concentration of IgM than the F22<sub>50%</sub>SAS PPT, but homo-isotypic sandwich ELISAs to determine the IgM concentration (Table 10, page 93) showed that the F22<sub>50%</sub>SAS PPT contained a higher concentration of total IgM. Lane 9 shows the supernatant remaining (F22<sub>50%</sub>SAS SUP) after the precipitates have been collected by centrifugation. It can be seen that the amount of IgM left behind in the supernatant was much less than in the original ascites while the bulk of the albumin from the ascites, has been left behind in the supernatant.

The gel in Figure 33 compares the IgM precipitated from the MAb-F22 ascites, at the two different SAS concentrations used, before and after the precipitates have been chromatographed on the Sephacryl SEC column. Lanes 2 and 3 show the IgM and BSA standards. The F22<sub>30%</sub>SAS PPT and F22<sub>50%</sub>SAS PPT are in lanes 4 and 7, respectively. The two lanes following after each of these samples are the IgM peak (lanes 5 and 8) and albumin peak (lanes 6 and 9) off the Sephacryl column run of the resuspended precipitates. Clearly the Sephacryl does a beautiful job of separating the remaining albumin from the IgM.

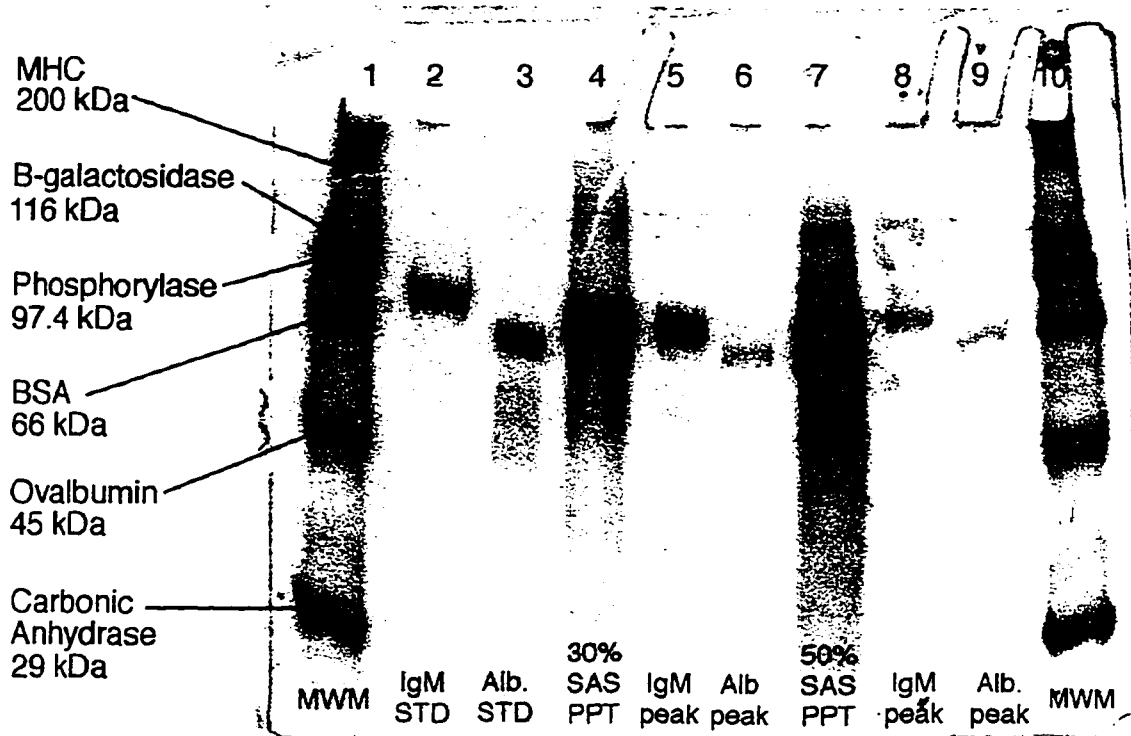


Figure 33. SDS-PAGE analysis to track the removal of albumin from IgM by size exclusion chromatography on the SAS precipitates of MAb-F22. 'MWM' = molecular weight markers; 'IgM STD' = MOPC; 'Alb. STD' = BSA; '30% SAS PPT' = F22<sub>30%</sub>SAS PPT; '50% SAS PPT' = F22<sub>50%</sub>SAS PPT; 'IgM peak' = peak #1 off SEC column; 'Alb. peak' = peak #2 off SEC column. (Custom 12.5% denaturing, non-gradient gels were loaded with 1-4  $\mu$ g protein in each well and the gels were run for '150% time;' see text for details).

The gel shown in Figure 34 tracks the purification of MAb-F36 and the gel shown in Figure 35 tracks the purification of MAb-S84; in both cases, ~50% (v/v) SAS was used. The results of these gels are parallel to those seen for the gels run on MAb-F22 samples. The IgM and albumin standards are in lanes 2 and 3, respectively, on each gel. The starting MAb-F36 and MAb-S84 ascites, with their large amounts of albumin, are in lane 4 on each gel. The SAS precipitates are seen in lane 5 on each gel to have diminished but still noticeable amounts of albumin, compared to the ascites. Lane 6 on each gel shows that the majority of the remaining albumin was left behind in the supernatants after SAS precipitation. Lanes 7 (IgM peak) and 8 (albumin peak) on each gel

show that running the resuspended SAS precipitates on the Sephacryl SEC column completely separates the albumin from the IgM. The MAb-S84 gel also shows that tailing of the IgM peak into the albumin peak (see chromatogram, Figure 31, page 100) leaves a small contamination of IgM in the albumin.

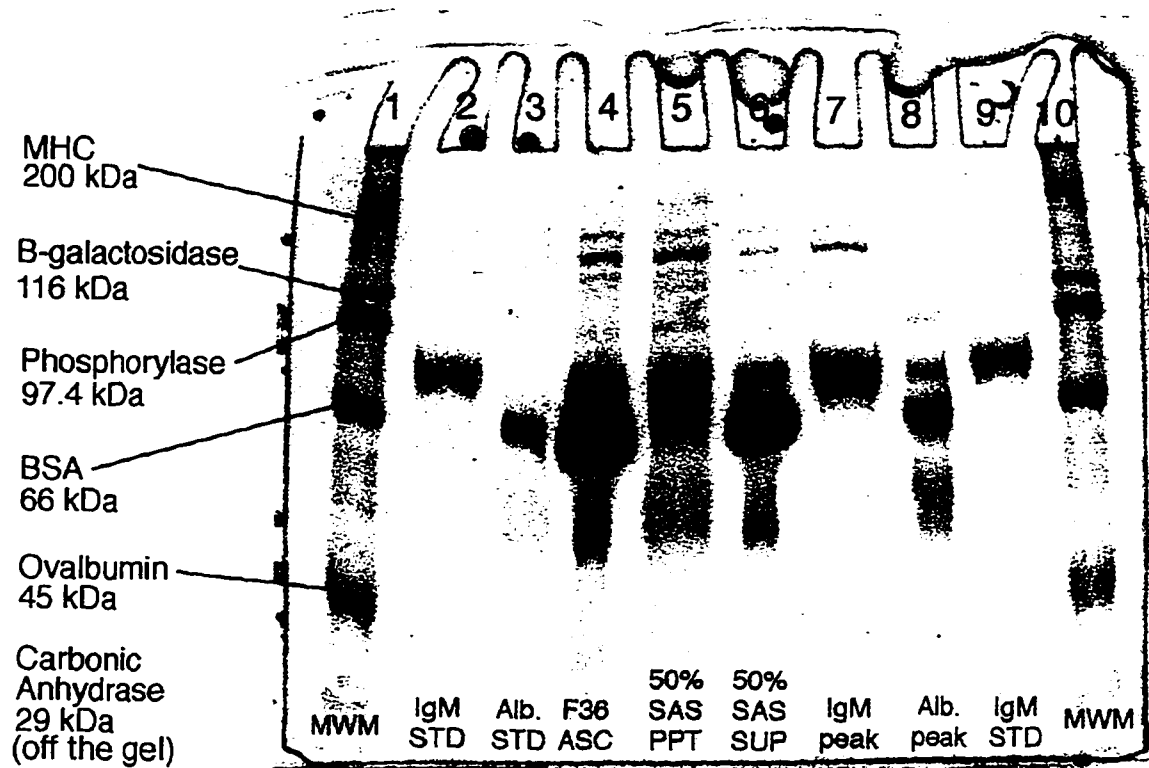


Figure 34. SDS-PAGE analysis to track the purification of MAb-F36. 'MWM' = molecular weight markers; 'IgM STD' = MOPC; 'Alb. STD' = BSA; 'F36 ASC' = F36 ascites; '50% SAS PPT' = F3630%SAS PPT; '50% SAS SUP' = F3650%SAS SUP; 'IgM peak' = peak #1 off SEC column; 'Alb. peak' = peak #2 off SEC column. (Custom 12.5% denaturing, non-gradient gels were loaded with 3  $\mu$ g protein in each well and the gels were run for '150% time;' see text for details).

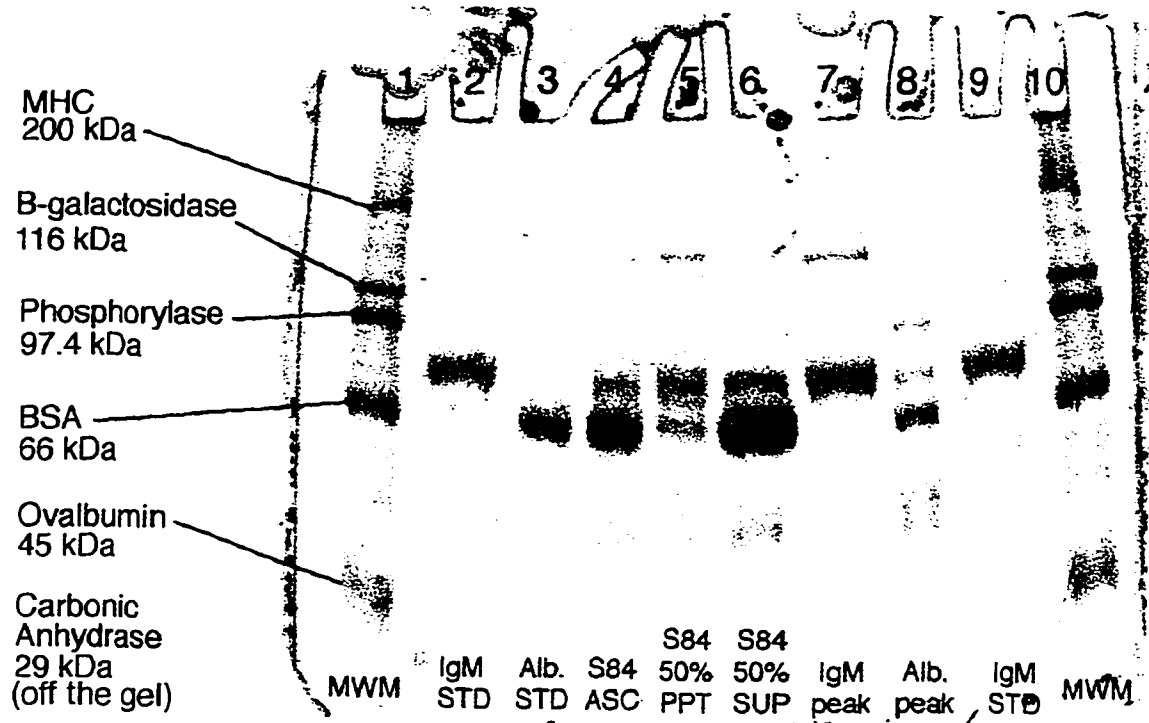


Figure 35. SDS-PAGE analysis to track the purification of MAb-S84. 'MWM' = molecular weight markers; 'IgM STD' = MOPC; 'Alb. STD' = BSA; 'S84 ASC' = S84 ascites; '50% SAS PPT' = S84<sub>50%</sub>SAS PPT; '50% SAS SUP' = S84<sub>50%</sub>SAS SUP; 'IgM peak' = peak #1 off SEC column; 'Alb. peak' = peak #2 off SEC column. (Custom 12.5% denaturing, non-gradient gels were loaded with 3  $\mu$ g protein in each well and the gels were run for '150% time' (see text for details).

*Purification of Immunoglobulins by Affinity Chromatography.* Two of the MAbs used in this study were IgG-class immunoglobulins. MAb-25 and MAb-S95 (specific to myosin epitopes MHC-25 and MHC-S95, Table 1, page 34), are of the immunoglobulin class G, subclass  $\gamma_{2b}$ .<sup>19</sup> The ascites from these two MAbs were purified using a 'Protein A' affinity chromatography column according to the manufacturers' instructions (Pierce ImmunoPure IgG purification kit #44667) by G. Alegre. The ascites were loaded onto the Protein A column without prior SAS precipitation. Protein A, a protein isolated from *Staphylococcus aureus* cultures, has a high affinity for IgGs of

<sup>19</sup> G. Alegre and L. Silberstein, unpublished results.

many mammalian species (Pharmacia LKB Biotechnology, 1986). The affinity is greatest at alkaline pH and a sudden drop in pH between the binding buffer (pH ~8) and the elution buffer (pH ~3) disrupts the IgG-Protein A binding, allowing the IgG to elute off the column (Pharmacia, 1986).

The protein concentrations of the eluted IgGs were determined by absorbance at 280 nm ( $\epsilon^{1\%_{280\text{nm}}} = 14 \text{ mL/mg-cm}$ , Hockfield et al., 1993). The IgG concentrations were determined by homo-isotypic sandwich ELISAs. The results of these two assays are shown in Table 14 and are compared to the protein and IgM concentrations of MAb-F22, MAb-F36, and MAb-S84 which had been purified by SAS precipitation followed by SEC (for comments on the discrepancies between protein and IgM concentrations shown in Table 14, see *Discussion and Conclusions*).

MAb	Ig Class	Protein Conc. (mg/mL)	Ig Conc. (mg/mL)
MAb-25	IgG	1.9	1.99
MAb-S95	IgG	1.5	3.60
MAb-F22 <sub>30%SAS</sub>	IgM	1.71 §	0.966
MAb-F22 <sub>50%SAS</sub>	IgM	0.50 §	2.27
MAb-F36 <sub>45%SAS</sub>	IgM	4.10	6.52
MAb-F36 <sub>50%SAS</sub>	IgM	3.91	6.40
MAb-S84 <sub>50%SAS</sub>	IgM	3.72	2.45

Table 14. Concentrations of protein and Ig in the final purified MAbs. MAb-25 and MAb-S95 are IgG-class MAbs purified from ascites by Protein A affinity chromatography (G. Alegre, unpublished results). MAb-F22, MAb-F36, and MAb-S84 are IgM-class MAbs purified by SAS precipitation of ascites followed by SEC on Sephacryl S300-HR. (Data for re-concentrated IgM peaks collected from SEC runs). § = protein concentrations determined using the BioRad DC Protein Assay kit, otherwise, by  $A_{280}$  (see *Materials and Methods*).



The two IgG-class MAbs, MAb-25 and MAb-S95, were to be used in hetero-isotypic sandwich ELISAs to detect myosin heavy chain epitopes in the peaks from the anti-myosin immunoaffinity columns; more than sufficient MAb-25 and MAb-S95 had been purified for use in these ELISAs. Additionally, sufficient quantities, of good purity, of each of the three IgM-class anti-myosin MAbs (MAb-F22, MAb-F36, and MAb-S84) were purified to produce small immunoaffinity columns with each MAb.

### **Anti-Myosin Immunoaffinity Columns**

*Overview.* The concentrated MAbs were covalently bound to an inert chromatographic matrix resulting in three anti-myosin immunoaffinity matrices. Each coupled matrix has the binding specificity of the MAb which it carries. In this study, MAbs to myosin epitopes F22, F36, and S84 were individually coupled to matrices. These matrices are expected to bind myosin isozymes which bear the F22, F36, and S84 myosin heavy chain epitopes, respectively. The binding specificity of these immunoaffinity columns should allow the separation of sub-populations of myosin molecules (i.e., isozymes) based on which epitopes, or combinations of epitopes, the myosin molecules bear. Hetero-isotypic sandwich ELISAs are used to detect the presence of specific epitopes in the column peaks. Complications can arise in three major areas: instability of the coupled matrix in the form of loss or degradation of the MAbs on the matrix, irreversible aggregation of myosin, and false positive or false negative results in the hetero-isotypic sandwich ELISAs on the column peaks.

*Preparation of Immunoaffinity Matrix.* Preparation of the immunoaffinity matrix involves covalently binding the MAbs onto an inert polymeric support (see *Introduction and Theory*). The inert matrix used was Sepharose CL-4B, a cross-linked beaded agarose. The first step was to activate the matrix with cyanogen bromide (CNBr); this reaction proceeds best at highly alkaline pH (Axén et al., 1967). As each aliquot of CNBr was added to the matrix slurry the pH dropped as

protons were released from the C6 hydroxyl group on the agarose. With the initial addition of CNBr the pH immediately dropped to 9.4. A sodium hydroxide solution was used to bring the pH back to 11 and the next aliquot of CNBr was added. This process was repeated until either the rate of the drop in pH with each addition of CNBr diminished markedly, indicating that the activation reaction was complete, or a total of 15 minutes had elapsed since the initial addition of CNBr, whichever occurred first. For the activation reactions reported here, the rate of change in pH was steady at a decrease of one pH unit over 15 seconds for each of the last 5 additions of CNBr (data not shown).

A summary of the preparation of five coupled matrices from the three IgM-class anti-myosin MAbs is shown in Table 15. MAb-F22 and MAb-F36 were each coupled at low (~1 mg MAb/mL matrix) and high (~2 mg MAb/mL matrix) concentrations of MAb, and MAb-S84 at one concentration (~1 mg MAb/mL matrix); approximately 2 mL of each coupled matrix was prepared.

Column	AU 'Initial' Coupling Sol'n	AU 'Spent' Coupling Sol'n	AU Washes	AU Remaining	% MAb Coupled
MAb-F22 'lo'	1.07	0.0075	0.026	1.04	96.8%
MAb-F22 'hi'	1.63	0.0066	0.030	1.59	97.7%
MAb-F36 'lo'	0.955	0.0082	0.032	0.914	95.8%
MAb-F36 'hi'	1.33	0.0153	0.036	1.28	96.1%
MAb-S84	1.60	0.034	0.034	1.53	95.8%

Table 15. Absorbance readings at 280 nm were used to track percent coupling of MAbs to activated matrix. The sum of the protein in the 'spent' coupling solution and the washes represents that protein which did not couple onto the matrix.

After the coupling reaction was complete, the spent IgM solution was collected from the matrix slurry and the matrices were washed with ~10-bed volumes of Coupling Buffer. The absorbance spectra of the spent solution and pooled washes were each measured separately. The percent MAb coupled was calculated based on the amounts of MAb found remaining in the spent solution and in the washes after coupling, compared to that available in the initial solution. As shown in Table 15, coupling occurred such that >95% of all the available IgM molecules were cross-linked to the activated matrix.

Table 16 shows that, based on the calculated percent-coupled values shown in Table 15 and the known starting concentrations of IgM in the coupling solutions, the matrices were coupled at between 0.88 and 1.78 mg MAb per milliliter of matrix.

Column	Coupling Solution Initial mg/mL	% MAb Coupled	mg MAb per mL Coupled Matrix
MAb-F22 'lo'	0.91	96.8%	0.88
MAb-F22 'hi'	1.82	97.7%	1.78
MAb-F36 'lo'	0.91	95.9%	0.87
MAb-F36 'hi'	1.82	96.2%	1.75
MAb-S84	0.91	95.8%	0.87

Table 16. Final concentration of MAbs on the coupled immunoaffinity matrices based on the starting concentration of IgM in the diluted MAb solutions and the percent coupled as determined in Table 15.

*Stability of Coupled Matrix.* After blocking, each matrix was washed to remove any non-covalently bound MAb. Alternately washing the newly coupled matrices with low and high pH Wash Buffers (low pH buffer = 0.5 M sodium chloride, 0.1 M sodium acetate at pH 3.5; high pH buffer = 0.5 M sodium chloride, 0.1 M sodium borate at pH 9.0) maximized the release of any non-

covalently bound MAb from the matrices (Goding, 1986). The  $A_{280}$  values for these washes on the coupled and blocked matrices were measured to monitor for any loss of protein. Based on these readings, essentially no protein ( $\ll 1\%$ ) was lost from the matrices during these washes (data not shown).

Two additional concerns were loss of coupled MAbs from the matrix or degradation of the MAbs coupled to the matrix while the column is in use; either of these would result in degradation of column performance. These events can occur with use of strong 'stripping' eluants, by irreversible binding of myosin to the MAb, or by bacterial contamination with subsequent degradation of the MAbs through proteolysis.

A 'stripping' eluant is used to remove the retained myosin from the column. This eluant disrupts the non-covalent interactions between the MAb and myosin, allowing collection of the bound myosin for analysis and repeated use of the column. Since the myosin eluted from the column was to be analyzed by hetero-isotypic sandwich ELISA it was necessary to use a stripping eluant that did not denature the myosin.

A 'low pH' stripping eluant (0.5 M potassium chloride, 50 mM potassium phosphate, 0.25 mM EGTA at pH 2.0) and a high salt concentration, ('high [salt]') stripping eluant (3.0 M potassium chloride, 50 mM potassium phosphate, 0.25 mM EGTA at pH 7.2) were first tested to see if they induced loss of coupled MAb from the matrix.<sup>20</sup> The MAb-F36 'lo' coupled matrix (0.87 mg/mL MAb-F36) was washed alternately with three-bed volumes of each of these two eluants, the filtrates collected, and absorbance spectra read; this was repeated three times.

---

<sup>20</sup> It had been previously observed that myosin shows greater resistance to aggregation in potassium-based buffers than in sodium-based buffers (data not shown); therefore potassium-based buffers were used in these tests.

Table 17 shows that less than 1% of the coupled MAb was lost from the MAb-F36 lo-coupled matrix as a result of washes with these stripping eluants. For example, if all the IgM had been lost from the F36 column in the first 'high [salt]' wash, its concentration would have been 0.87 mg IgM in ~6 mL wash, or 0.15 mg/mL. The absorbance of this solution would be expected to be 0.19 AU (using the extinction coefficient of 13.3 mL/mg-cm for pure IgM). The absorbance of the first 'high [salt]' wash was 0.000259 AU, which represents only 0.14% of the total IgM on the F36 'lo' coupled matrix. This was the highest absorbance value observed, therefore, the coupled matrices were considered stable to the stripping eluants with respect to loss of coupled MAb.

Wash	A <sub>280</sub> (AU)
Hi [Salt] #1	0.000259
Low pH #1	-0.00433
Hi [Salt] #2	-0.00111
Low pH #2	-0.00595
Hi [Salt] #3	-0.00314
Low pH #3	-0.00533

Table 17. Washes of the MAb-F36 'lo' coupled matrix with 'hi [salt]' (3 M KCl @ pH 7.2) and 'low pH' (0.5 M KCl @ pH 2.0) 'stripping' eluants showed essentially no loss of protein (<1% relative to the amount coupled), therefore, the coupled matrices were deemed stable to these stripping eluants.

*Myosin Stability.* Tests were also made of the stability of myosin in these two stripping eluants, and one additional potential eluant, guanidine hydrochloride (Gdn•HCl), a strong chaotropic reagent commonly used to 'strip' retained proteins from affinity columns.

Myosin samples were diluted in half with each of the three eluants and the absorbance spectra read after 10 and 60 minutes.<sup>21</sup>  $(A_{340}/A_{280}) \times 100$  values were used to monitor the stability of myosin, with respect to aggregation, in each eluant. The potassium-based Sepharose Column Buffer (SCB) was used as a control since this was also used as the Affinity Column Equilibration Buffer and the myosin would be loaded onto the immunoaffinity columns in this buffer. Table 18 shows the resultant  $(A_{340}/A_{280}) \times 100$  values.

Eluant used to Dilute Myosin	$(A_{340}/A_{280}) \times 100$	
	@ 10 min	@ 60 min
Column Buffer (SCB)	5.39%	5.71%
Low pH Stripping Eluant	29.4%	43.3%
High [salt] Stripping Eluant	9.00%	48.0%
Gdn•HCl Stripping Eluant	8.93%	62.4%

Table 18. As shown by an increase in aggregation over time, the myosin was not stable in any of the three 'stripping' eluants. Samples were diluted in half in the subject eluant then incubated on ice at 4 °C until read. The  $(A_{340}/A_{280}) \times 100$  of the myosin sample was 2.52% prior to any of these dilutions.

The monodisperse myosin collected off the Sepharose SEC column had been found to be quite stable when stored at 4 °C. The  $(A_{340}/A_{280}) \times 100$  of the monodisperse myosin peak from chromatographing S8-G on Sepharose was 2.52% two days after elution and 2.63% six days after elution (data not shown). However, as shown in Table 18, upon simply diluting an aliquot of this monodisperse myosin in half with any of the three potential stripping eluants, the  $(A_{340}/A_{280}) \times 100$  increased dramatically. Even a simple twofold dilution with the SCB, caused the  $(A_{340}/A_{280}) \times 100$  to essentially double from 2.52% before dilution to 5.39% after dilution. The data from these tests indicated that it would probably not be possible to recover monodisperse myosin in the

<sup>21</sup> Eluants were pre-chilled and diluted samples were kept on ice at 4 °C during incubation.

eluted volume,  $V_e$ , off the immunoaffinity columns in any of these three eluants. The consequence of these results was that it would not be possible to perform hetero-isotypic sandwich ELISAs on the  $V_e$ , since aggregated myosin produces spurious results in the hetero-isotypic sandwich ELISAs (see below).

Unfortunately, the non-retained myosin peaks ( $V_o$ ) from preliminary runs of the F36 'lo' immunoaffinity column were also found to contain aggregated material. The minimum value of  $(A_{340}/A_{280}) \times 100$  observed for  $V_o$  peaks was 10.9% (data not shown). It is clear that monitoring for aggregation is of the utmost importance since even gentle handling of the myosin may not be sufficient to prevent aggregation. If the myosin in the immunoaffinity column peaks is aggregated, the hetero-isotypic sandwich ELISAs to analyze for myosin epitopes in the peaks would be adversely affected.

## **Detection of Myosin Epitopes**

*Overview.* The presence of specific myosin epitopes was to be determined by hetero-isotypic sandwich ELISAs. Before proceeding with any myosin runs on the immunoaffinity columns, methods development for the hetero-isotypic ELISAs was done. This methods development included determination of the appropriate concentrations of reagents to use in the various layers on the plate and pre-testing for potential false positive and false negative results. Unexpected results in the methods development for the sandwich ELISAs prevented the analyses of any  $V_o$  peaks from the anti-myosin immunoaffinity columns.

*Methods Development for Hetero-Isotypic Sandwich ELISAs.* Both false positive and false negative results are possible for the hetero-isotypic sandwich ELISAs. Aggregation and proteolysis of myosin were of particular concern.

Verifying the structural integrity of the epitopes on the myosin molecules in the  $V_0$  is quite important. If the epitopes have been damaged the ELISAs could be falsely negative. Such damage could occur through proteolysis. A blocking buffer with a protein source such as Bovine Serum Albumin (BSA), milk, or Neonatal Calf Serum (NCS), is used to 'block' the plate after the primary layer is coated onto the plate. The proteins in the blocking buffer fill any non-specific binding sites on the coated plate and stabilize the protein of interest at the extreme dilutions that are typically made for ELISA samples. The blocking buffer is also used as the diluent for the samples, standards, and the antibody-enzyme conjugate reagent (i.e.,  $G\alpha mIgM\bullet HRP$ ). In all homo-isotypic sandwich ELISAs PBS-blotto (which contains 5% (v/v) milk) was used as the blocking buffer.

Unfortunately, the blocking proteins can contain proteases, which might cause proteolysis damage to the myosin. This is of particular concern in the hetero-isotypic sandwich ELISAs for myosin since proteolysis could result in aggregation of myosin on the plate or damage to the characteristic epitope of interest.

*Proteolysis ELISA.* A hetero-isotypic sandwich ELISA designed to test for proteolysis (a 'proteolysis ELISA') was investigated to determine whether any of the three blocking buffer proteins that are typically used (BSA, milk, or NCS) cause proteolysis of the myosin. In the process of running this ELISA unforeseen problems were encountered, as described below.

In the proteolysis ELISA, MAb-25 was coated onto the plate at a fixed concentration, followed by addition of each of the three ELISA Blocking Buffers of interest (potassium-based Sepharose Column Buffer (SCB) with either 1 mg/mL BSA, or 5% (v/v) milk, or 5% (v/v) NCS) in parallel wells. Separate serial dilutions of myosin, prepared using each of the three blocking buffers, were then added to the plate as the second layer. Neat cell supernatant was added in the third layer as the



source of IgM-class anti-myosin MAb-F22; this was followed by addition of the  $\alpha$ myosin-HRP in the fourth layer. It was anticipated that if any proteolysis of myosin was occurring a diminution of the absorbance signals would be observed.

Both the diluted myosin samples and the blanks of the proteolysis ELISA showed curious absorbance patterns relative to the myosin concentrations; the data are shown in Table 19. It is expected that absorbance is a direct function of myosin concentration. In the samples diluted with the BSA blocking buffer, absorbance was seen to decrease as myosin concentration decreased from 10 to 1.25 mg/mL, but then as myosin concentrations decreased further, the absorbance values began to increase. In the samples diluted with blocking buffers with milk and NCS,

Myosin ( $\mu$ g/mL)	Absorbance (AU) without Blanks Subtracted					
	PBS w/ BSA		PBS w/ Milk		PBS w/ NCS	
	Myosin (AU)	Blank (AU)	Myosin (AU)	Blank (AU)	Myosin (AU)	Blank (AU)
10.0	0.64	0.57	0.25	0.20	0.26	0.30
5.0	0.60	0.52	0.28	0.18	0.27	0.26
2.5	0.47	0.42	0.27	0.25	0.23	0.24
1.25	0.42	0.53	0.29	0.26	0.27	0.32
0.625	0.46	0.60	0.26	0.28	0.28	0.28
0.313	0.72	0.84	0.39	0.32	0.38	0.34
0.156	1.00	0.88	0.60	0.33	0.40	0.37
0.078	1.00	0.85	0.40	0.30	0.44	0.39

Table 19. Raw absorbance readings (AU without blanks subtracted) from the proteolysis ELISA. The myosin samples were diluted in each of three Blocking Buffers; each of the different Blanks contain Blocking Buffer but no myosin. All wells were treated with F22 CSN as the source of IgM-class anti-myosin MAb. (1° layer = MAb-25 at 10  $\mu$ g/mL; 2° layer = diluted myosin as samples with blocking buffers alone as corresponding blanks; 3° layer = F22 cell supernatant, neat; 4° layer = 1:1,000 dilution of stock  $\alpha$ myosin-HRP. All work was done at 4 °C with pre-chilled buffers and reagents.) (See Figure 39, page 125 for a plot of the data shown above for myosin diluted with BSA Blocking Buffer.)

absorbance values start low and actually slightly *increase* over the entire range in which myosin concentration *decreases* - exactly the opposite of the expected result.

In addition to the unusual absorbance values observed for the myosin dilutions, all the absorbance values for the blanks in this ELISA were unusually high. The blanks are wells in which only Blocking Buffer (i.e., no myosin) was added as the second layer. Absorbance values ranged from ~0.2 AU to ~0.9 AU for these blanks, while average values of ~0.06-0.1 AU are typical for blanks (see data for homo-isotypic sandwich ELISAs, Table 8, page 91).

Absorbance values that are high for the blanks and low for the samples raise concerns about the concentration of HRP reagent used and of MAb-25 used to coat the ELISA plates. High blank values (i.e., background absorbance) can occur if the concentration of HRP reagent used was too high,<sup>22</sup> while low sample absorbance values can occur if the plate was insufficiently coated with MAb-25 in the primary layer. At high concentrations of HRP reagent, non-specific binding of the HRP onto the plate can occur, (rather than it only binding to the target IgM-class MAbs). This would result in erroneously high absorbance values in the blanks.

If the plate is not saturated with primary layer (i.e., MAb-25) the ELISA reaction could be limited, resulting in low sample binding and lower than expected absorbance values. Therefore, in coating the primary layer (i.e., MAb-25) onto the plate, it is desirable to attain the maximum adsorption of protein onto the plastic. An unsaturated plate could also allow for non-specific binding of other proteins (i.e., other than MAb-25) onto the plastic which could effect the assay in a number of ways, depending on the reaction of those proteins with subsequent ELISA layers.

---

<sup>22</sup> Product information from the Technical Representative of the HRP reagent manufacturer, Cal Tag Immunodiagnostics, Belmont, California.

In light of the unusual absorbance data collected in the proteolysis ELISA, a conclusion could not be reached regarding proteolysis of myosin by the blocking proteins in the buffers. Furthermore, it was apparent that other aspects of the hetero-isotypic sandwich ELISA method would have to be examined. In particular, the optimal concentration of  $\alpha$ myosin-HRP to use and the concentration of MAb-25 required to saturate the plates would have to be determined. The ELISAs to investigate these two parameters are described in the next two sections.

*Determine Optimal  $\alpha$ myosin-HRP Concentration.* A hetero-isotypic sandwich ELISA was run to examine the effect of concentration of  $\alpha$ myosin-HRP on absorbance values for the blanks, and to determine the optimal concentration of  $\alpha$ myosin-HRP to use. A plate was coated with MAb-25 at 10  $\mu$ g/mL and blocked with PBS-blotto (PBS with 3% (v/v) milk). Myosin, diluted to 20  $\mu$ g/mL with each of the three blocking buffers (BSA, milk, or NCS), was applied to the plate. Neat F22 cell supernatant was applied to the plate as the source of IgM-class anti-myosin MAbs. Finally,  $\alpha$ myosin-HRP, diluted to four different dilutions (1:1,500; 1:3,000; 1:4,500; and 1:6,000-fold dilutions of the  $\alpha$ myosin-HRP stock) in each of the three different blocking buffers was added to different sections of the plate.

The absorbance values for myosin samples diluted in each of the three buffers of interest is 'signal,' while the absorbance of each buffer as a blank is background or 'noise.' The amount of noise relative to signal, R, is calculated as  $(\text{blank}/(\text{signal}-\text{blank})) \times 100$ . Values of R for myosin diluted in each of the three blocking buffers were determined at the four dilutions of  $\alpha$ myosin-HRP. If non-specific binding were occurring, high background would be expected.

A very slight increase in background as a function of the dilution of  $\alpha$ myosin-HRP was observed. More significantly, the sample absorbance was influenced by the blocking protein used. As seen in Figure 36, the blocking buffer with BSA produced the strongest signal and most steady blanks

Comparison of 'Signal' and 'Noise' for Myosin Diluted in Three Blocking Buffers

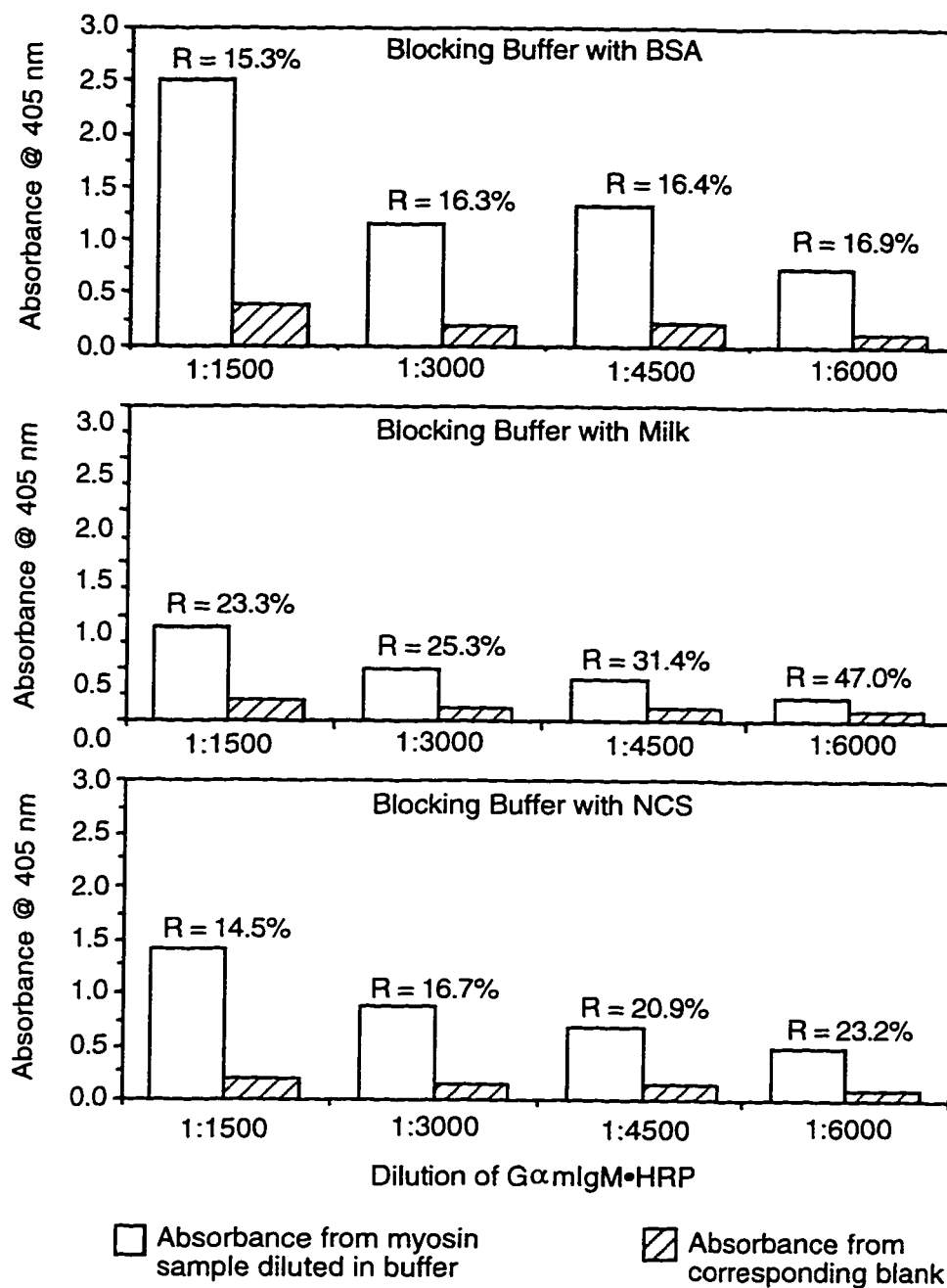


Figure 36. Absorbance values for myosin ('signal') and blank ('noise') samples from a hetero-isotypic sandwich ELISA to determine the optimal concentration of GαmIgM•HRP. The relative amount of noise, R, is calculated as  $(\text{blank}/(\text{signal}-\text{blank})) \times 100$ . 1° layer = MAb-25 at 10 µg/mL; 2° layer = myosin at 20 µg/mL diluted in buffers; or the buffers alone as blanks; 3° layer = neat F22 CSN; 4° layer = GαmIgM•HRP at varying dilutions as shown. (All work was done at 4 °C with pre-chilled buffers and reagents.)

(R ranges from 15.3% to 16.9%) at all concentrations of  $\alpha$ myoglobin-HRP used. Using the buffer with milk, the signal is diminished for all dilutions of  $\alpha$ myoglobin-HRP, relative to that seen for the samples diluted in buffer with BSA, and values for R are significantly increased (R ranges from 23.3% to 47.0%). Using the buffer with NCS the signal is again diminished but values for R are not as poor (R ranges from 14.5% to 23.2%). From these results, it seemed unlikely that the high blanks observed in the proteolysis ELISA were the result of using an inappropriate concentration of  $\alpha$ myoglobin-HRP.

*Determine the Saturating Concentration of MAb-25.* In running the hetero-isotypic sandwich ELISAs it is important to have the plate coated with an excess of primary Ab (i.e., MAb-25) so that it is not a limiting reagent in binding myosin to the assay plate. The concentration at which the primary Ab 'saturates' the plate (i.e., at which it coats the plastic at its maximum carrying capacity for that protein) is determined by a 'saturation ELISA'. In this type of hetero-isotypic sandwich ELISA the plate is coated with varying amounts of Ab in the primary layer, and the absorbance values as a function of this concentration are determined.

MAb-25 was coated onto the plate in serial dilutions of 0.156 to 20  $\mu$ g/mL using the Blocking Buffer containing BSA. After blocking the wells with the BSA Blocking Buffer, myosin, diluted in that buffer, was added at 20  $\mu$ g/mL to all sample wells; the blank wells received only aliquots of the BSA Blocking Buffer without any myosin. Neat F22 cell supernatant, applied to all wells, supplied the anti-myosin IgM.  $\alpha$ myoglobin-HRP, diluted 1:1,000 in the BSA Blocking Buffer, was used to visualize the reaction.

Absorbance as a function of the concentration of MAb-25 applied to the plate is plotted in Figure 37. This saturation curve 'levels off' somewhere between 5-10  $\mu$ g/mL MAb-25 added to the plate. Above this concentration, further addition of MAb-25 does not continue to increase the

absorbance signal, therefore, the plate is saturated somewhere between 5-10  $\mu\text{g}/\text{mL}$  of MAb-25. Since the proteolysis ELISA was performed with 10  $\mu\text{g}/\text{mL}$  MAb-25 in all wells, apparently the plate was saturated with MAb-25, so its concentration should not have been a limiting factor in that ELISA.

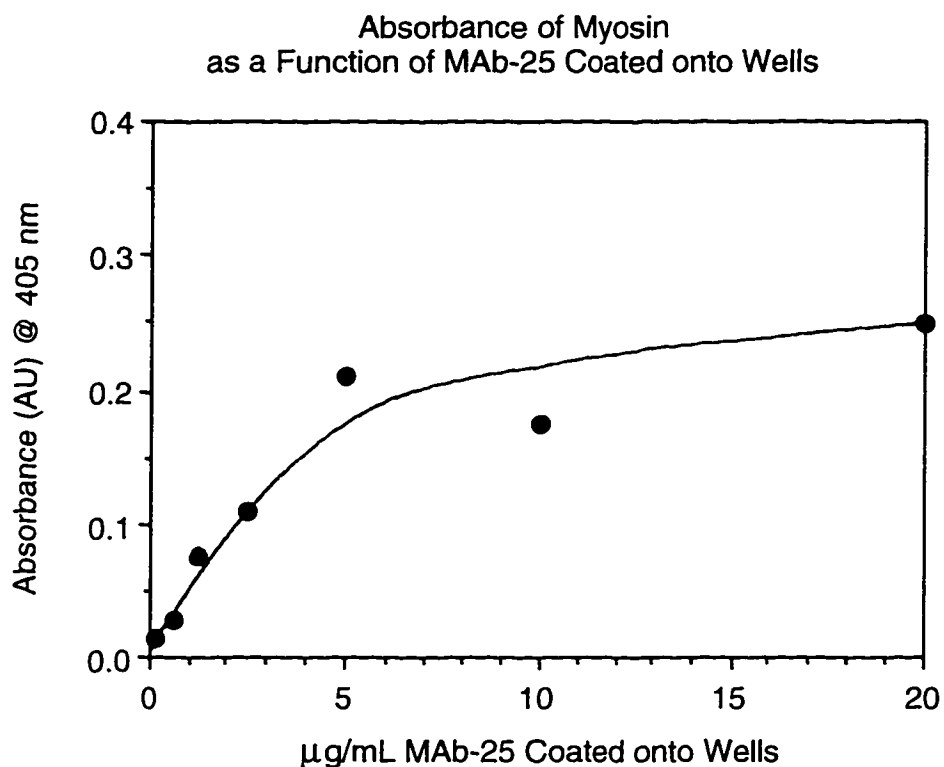


Figure 37. Saturation curve for MAb-25. The absorbance (AU with blanks subtracted) from the MAb-25 levels off between 5 and 10  $\mu\text{g}/\text{mL}$  of MAb applied to the plate, indicating that the saturating concentration is in this range. 1<sup>o</sup> layer = 0.156-20  $\mu\text{g}/\text{mL}$  MAb-25; 2<sup>o</sup> layer = myosin at 20  $\mu\text{g}/\text{mL}$  diluted in the three buffers; or buffers alone, as blanks; 3<sup>o</sup> layer = MAb-F22 CSN neat; 4<sup>o</sup> layer =  $\text{G}\alpha\text{mIgM}\cdot\text{HRP}$ . (All work done at 4  $^{\circ}\text{C}$  with pre-chilled buffers and reagents.)

An interesting observation was made in analyzing the data from the saturation ELISA. In the wells containing myosin, the absorbance values decreased as the concentration of MAb-25 decreased, as expected. However, the absorbance values for the blanks (wells without any myosin),

increased as the concentration of MAb-25 applied to the plate decreased; also the absorbance values from the blanks were again higher than expected. This is similar to the unusual absorbance patterns observed in the proteolysis ELISA.

Figure 38 shows a plot of absorbance values for the blanks, as a function of MAb-25 concentration applied to the wells in the saturation ELISA. All the blanks contain the same concentration of BSA from the Blocking Buffer. Neither the IgG-class MAb-25 nor the BSA should react with the  $\text{G}\alpha\text{mIgM}\cdot\text{HRP}$ , therefore, the absorbance values for all the blanks are expected to

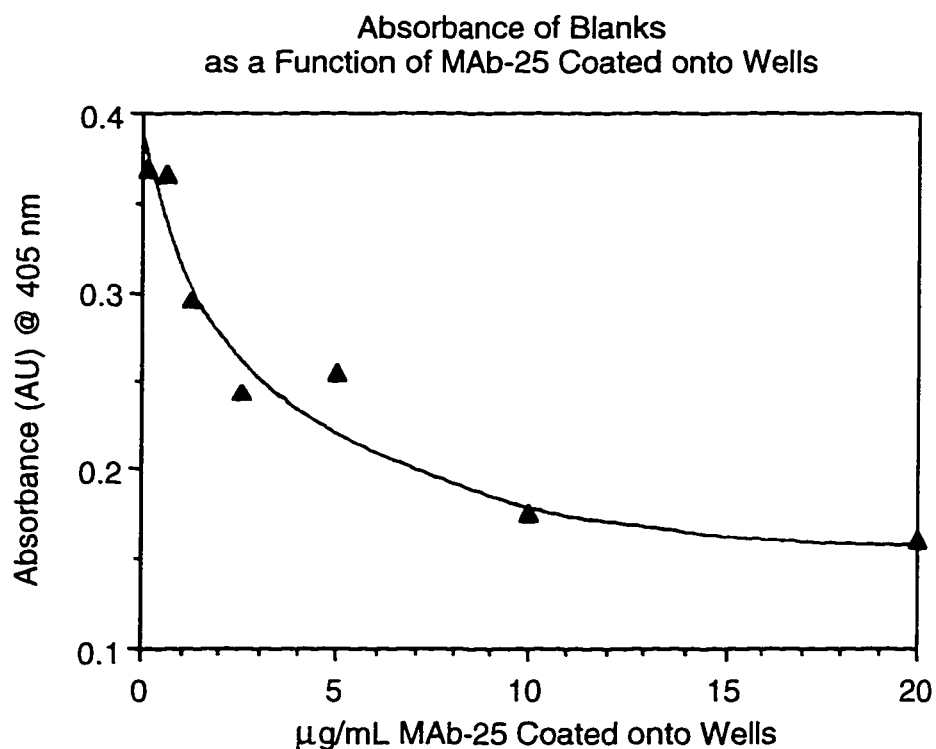


Figure 38. Plot of absorbance values (AU without blanks subtracted) of the blanks as a function of MAb-25 concentration on the plate (data from the MAb-25 saturation ELISA). As the concentration of MAb-25 on the plate decreased, the absorbance of the blanks containing BSA increased, suggesting that the BSA was contaminated with IgM (see text). 1° layer = 0.156-20 µg/mL MAb-25; 2° layer = myosin at 20 µg/mL diluted in the three buffers; or buffers alone, as blanks; 3° layer = MAb-F22 CSN neat; 4° layer =  $\text{G}\alpha\text{mIgM}\cdot\text{HRP}$ . (All work done at 4 °C with pre-chilled buffers and reagents.)

be low and constant. However, as seen in Figure 38, the blanks showed a titratable effect.

Apparently, there was something present in the blanks that the anti-IgM reagent ( $\alpha$ mIgM•HRP) was detecting.

If there is a contaminating IgM in the BSA, then as the MAb-25 applied to the plate decreases, more sites on the plastic become available to bind the contaminating IgM during the blocking step. The absorbance values for the blanks would increase as the concentration of MAb-25 applied to the plate decreased, due to the increasing amount of contaminating IgM from the BSA. This is the pattern shown by the data in Figure 38, suggesting that BSA does have an IgM contaminant. It is not completely unreasonable that the BSA would contain IgM since it is from serum, which can contain IgM, and a high purity of BSA was not being used (see *Discussion and Conclusions*, for further comment).

Absorbance data (AU without subtracting the blanks; Table 19, page 117), for the myosin samples diluted in BSA Blocking Buffer from the 'proteolysis' ELISA to detect are plotted in Figure 39. The shape of this curve is characteristic of a biphasic phenomenon, suggesting that two sources are contributing to the absorbance curve. Given the results of the MAb-25 saturation ELISA this biphasic curve can be explained as follows: when myosin concentrations are high, the absorbance values are the result of the MAb-F22 (IgM-class anti-myosin MAbs from the F22 cell supernatant) bound to F22+ myosin isozymes present on the plate, as expected. However, when the myosin concentrations are low, the elevated absorbance values are due to a contaminating IgM in the BSA which is now able to adsorb onto the plate. This is consistent with the interpretation of the data shown in Figure 38. This possibility was confirmed by running a homotypic sandwich ELISA on the BSA to determine the concentration of IgM it contained. This led to further unexpected information being revealed, as discussed in the next section.



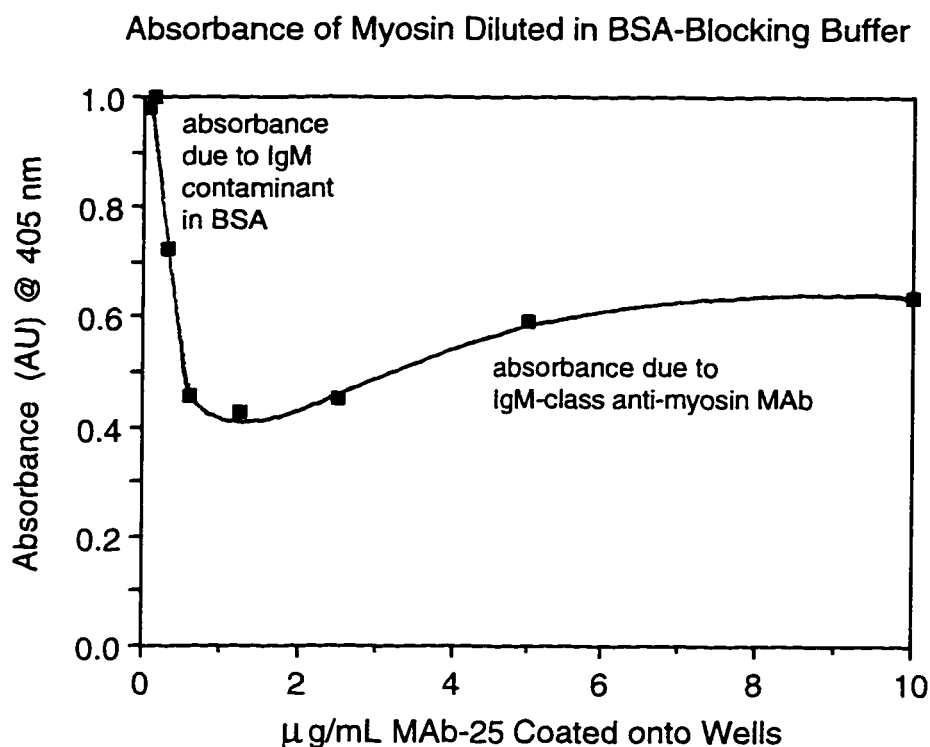


Figure 39. Absorbance (AU without blanks subtracted) of myosin samples diluted in BSA-Blocking Buffer (data from the proteolysis ELISA; see Table 19, page 117). This biphasic ELISA curve is the result of the combined absorbance from two sources (see text). 1° layer = 10  $\mu\text{g}/\text{mL}$  MAb-25; 2° layer = myosin diluted to 0.156-10  $\mu\text{g}/\text{mL}$  in the BSA Blocking Buffer; 3° layer = MAb-F22 CSN neat; 4° layer =  $\text{G}\alpha\text{mIgM}\cdot\text{HRP}$ . (All work done at 4 °C with pre-chilled buffers and reagents.)

*Homo-Isotypic Sandwich ELISA to Determine IgM Concentration in BSA.* A homo-isotypic sandwich ELISA was set up to assay the BSA for IgM content. A plate coated with  $\text{G}\alpha\text{mIgM}$  was blocked with PBS-blotto (PBS with 3% (v/v) milk), then BSA was added as the sample at serial dilutions of 7.8-1,000  $\mu\text{g}/\text{mL}$  in PBS-blotto. MOPC was added as the IgM standard, and the IgG-class purified MAb-25 was added as a negative control. All samples and standards were serially diluted with PBS-blotto; the blank was PBS-blotto alone.  $\text{G}\alpha\text{mIgM}\cdot\text{HRP}$  was added to detect any IgM present. The data are shown in Table 20.

BSA		MAb-25		MOPC		Blank
µg/mL	AU	µg/mL	AU	µg/mL	AU	AU
1,000	0.065	20	0.352	0.500	1.329	0.072
500	0.069	10	0.290	0.250	1.148	0.069
250	0.068	5	0.199	0.125	0.651	0.077
125	0.069	2.5	0.147	0.0625	0.380	0.075
62.5	0.070	1.25	0.114	0.0313	0.241	0.077
31.3	0.068	6.25	0.093	0.0158	0.150	0.070
15.6	0.071	3.13	0.077	0.0078	0.110	0.071
7.8	0.069	1.58	0.075	0.0039	0.089	0.071

Table 20. Absorbance data (AU, blanks not subtracted), from a homo-isotypic sandwich ELISA to determine the concentration of IgM-class Igs in BSA and purified MAb-25. Both BSA and MAb-25 and found to contain an IgM contamination. (1° layer =  $\Gamma$ αmIgM; 2° layer = samples diluted in PBS-blotto; 3° layer =  $\Gamma$ αmIgM•HRP; the blank is PBS-blotto.)

As seen in Table 20, all the BSA sample wells show the same low background absorbance values of ~0.07 AU as the blanks on this plate, which contained only PBS-blotto. This suggests that if the plate is first blocked with PBS-blotto, the milk proteins block the IgM in the BSA from getting onto the plate and adding to the background absorbance. This is consistent with the explanation of the biphasic absorbance curve shown in Figure 39 for the proteolysis ELISA.

Surprisingly, this ELISA also showed that the IgG-class purified MAb-25 contained IgM. The MAb-25 diluted in PBS-blotto had been added to this plate as a negative control since, as an IgG-class MAb, it should not react at all with  $\Gamma$ αmIgM•HRP. However, as the data in Table 20 show, a titratable effect was seen in the wells with the dilutions of the purified MAb-25 (i.e., absorbance values decrease from 0.35 to 0.075 AU). Based on the standard curve constructed from the

absorbance data from the MOPC dilutions on this plate, it was calculated that the purified MAb-25 contains ~1.6 µg/mL IgM. This is in the range of IgM concentration found in the cell supernatants from IgM-producing hybridoma cells (Table 7, page 89). As shown in Table 14 (page 108), the purified MAb-25 had been found by homo-isotypic sandwich ELISA to contain 1.99 mg/mL IgG. Therefore, the IgM contaminant is present at approximately 1 part in 800, relative to the IgG in the purified MAb-25.

*Determine IgM Concentration in All Layers of Hetero-Isotypic Sandwich ELISA.* After seeing these results, a homo-isotypic sandwich ELISA was performed to test the 'reagents' used in all layers of the hetero-isotypic sandwich ELISAs for IgM contamination. This homo-isotypic sandwich ELISA was performed in parallel with sodium- and potassium-based blocking buffers to see if this ion difference contributed to any of the effects seen in prior ELISAs.<sup>23</sup> This plate contained MOPC as a standard, cell supernatants from the three IgM-class cell lines (MHC-F22, MHC-F36, and MHC-S84) as positive controls, cell supernatants from the IgG-class cell lines (MHC-25 and MHC-S95), myosin, and the three different Blocking Buffer proteins (BSA, NCS, and milk). The plate was blocked with PBS-blotto, which also served as the diluent and blank.

The data from this plate are shown in Table 21. It clearly shows that the IgG-class MAb-25 and MAb-S95, when assayed at 10 and 20 µg/mL, respectively, both contain an IgM component. The three blocking buffers (PBS with BSA, or milk, or NCS), myosin, and the IgG cell supernatants all show absorbance values in the range of blanks, as expected.<sup>24</sup> The absorbance is overall slightly elevated when the samples are diluted in the sodium-based PBS-blotto relative to the potassium-based SCB-blotto, but this effect is not large.

---

<sup>23</sup> Typically, homo-isotypic sandwich ELISAs were run with sodium-based buffers, while hetero-isotypic sandwich ELISAs were run with potassium-based buffers to protect the myosin from aggregation.

<sup>24</sup> Note that the absorbance for the BSA is low here since the plate was blocked with PBS-blotto, preventing the IgM in the BSA from binding onto the plate.

Sample	Protein	Concentration	Sample Absorbance (AU)			
			PBS-Blotto w/Na <sup>+</sup>		SCB-Blotto w/K <sup>+</sup>	
			G $\alpha$ MIgM•HRP dilution		G $\alpha$ MIgM•HRP dilution	
			@ 1:1,000 dil'n	@ 1:5,000 dil'n	@ 1:1,000 dil'n	@ 1:5,000 dil'n
MOPC	IgM	0.10 $\mu$ g/mL	1.6	0.77	0.94	0.51
MAB-F22 CSN	IgM	1:50 dil'n of neat	2.5	1.8	2.6	2.2
MAB-F36 CSN	IgM	1:50 dil'n of neat	2.5	1.9	3.7	2.3
MAB-S84 CSN	IgM	1:50 dil'n of neat	2.2	1.9	3.0	2.0
Pure MAb-25	IgG	10 $\mu$ g/mL	0.94	0.57	1.0	0.40
Pure MAb-S95	IgG	20 $\mu$ g/mL	0.33	0.21	0.25	0.15
MAB-25 CSN	IgG	1:2 dil'n of neat	0.094	0.068	0.075	0.074
MAB-S95-CSN	IgG	1:2 dil'n of neat	0.071	0.060	0.066	0.066
BSA	non-Ig	1,000 $\mu$ g/mL	0.073	0.066	0.078	0.079
Milk	non-Ig	3% (v/v)	0.056	0.063	0.065	0.068
NCS	non-Ig	3% (v/v)	0.072	0.069	0.081	0.068
Myosin	non-Ig	20 $\mu$ g/mL	0.076	0.064	0.080	0.065

Table 21. Absorbance data (AU without blanks subtracted), from a homo-isotypic sandwich ELISA performed on the reagents used in all layers of the hetero-isotypic sandwich ELISA. The MAb-25 and MAb-S95 purified from ascites by Protein A affinity column contain significant amounts of IgM. (1° layer = G $\alpha$ MIgM; 2° layer = samples diluted in buffer shown; 3° layer = G $\alpha$ MIgM•HRP at dilutions shown; the plate was blocked with PBS-blotto.)

A color difference was visible in the spot tests between the G $\alpha$ MIgM•HRP and ABTS (the HRP substrate) when the G $\alpha$ MIgM•HRP was diluted in the sodium-based PBS-blotto versus the potassium-based SCB-blotto. The potassium-based SCB-blotto produced a more purple-blue than the teal-green produced by the sodium based PBS-blotto. This shift in color could reflect a

shift in maximum absorbance wavelength and account for the difference in absorbance observed between samples diluted in the two buffers (this possibility was not investigated).

The consequence of these results is that in order to perform effective hetero-isotypic sandwich ELISAs on any peaks from the anti-myosin immunoaffinity columns, the contaminating IgM must be removed from the 'purified' IgG-class MAbs (MAb-25 and MAb-S95). Additionally, a Blocking Buffer protein that does not contain a contaminating IgM must be identified.

## DISCUSSION AND CONCLUSIONS

### Myosin Preparation

*Extraction of Myosin from Muscle.* The myosin extraction is based on the differential precipitation of proteins from muscle as a function of ionic strength. The process is not perfect and individual molecules of different proteins can become aggregated to one another or simply trapped in a precipitate, resulting either in loss of some myosin or inclusion of some undesired proteins. The procedure must be conducted in such a way as to minimize such non-ideal behavior.

Techniques such as making ionic strength changes gradually, maintaining the temperature at 4-8 °C, and handling the proteins gently, minimizes damage to individual molecules and decreases their tendency to non-ideal behavior. Specific steps are included in the procedure to remove the inevitable aggregates that do form. For example, a drop-wise dilution on day 3, in which the ionic strength is lowered from  $\Gamma = 0.6$  M to 0.3 M, is specifically designed to precipitate actomyosin, which is soluble at  $\Gamma = 0.6$  M but not at  $\Gamma = 0.3$  M. Another example is the final ultracentrifugation on day 5 which pellets any myosin homo-aggregates present at that stage. Myosin aggregates formed at this stage are presumably from material which has been damaged in the purification process. A number of changes to various aspects of the procedure were investigated in a preliminary manner and the following observations were made (see also Table 2, page 79).

In preparation S2 the ionic strength of the initial extraction buffer was inadvertently 10-fold too low, resulting in a very low yield. In preparation S3, low and high concentrations of ATP were used in the initial extraction buffer. ATP is well known to reduce the interaction between myosin and

actin (Ebashi and Nonomura, 1973; Szent-Györgyi et al., 1973). The role of ATP in this buffer is to bind to myosin thus minimizing its attachment to actin during the initial extraction, when the most actin is present. This, in turn, minimizes the amount of actin contamination in the final myosin. Little difference in either actin contamination or myosin yield was observed between the two concentrations (1 mM and 5 mM) of ATP used.

In all but one preparation, only thigh muscles were used. Preparation S4 shows the single attempt made to use other muscle groups. The yield of myosin from the forelimbs is significantly lower than that from the hind limbs (i.e., thighs). The exceptionally high yield seen in preparation S4 compared to other preparations may be due to the addition of the protease inhibitors leupeptin and phenylmethyl-sulfonyl fluoride (PMFS) to the initial extraction buffer. A specific comparative test of this was not performed, but these protease inhibitors were also added to the extraction buffers for preparation S5 and these are the two preparations with the highest yields, by far. However, the lack of significant proteolysis of the myosin in any of the preparations, as revealed by SDS-PAGE analyses (Grant, 1995), makes the presumptive role of the protease inhibitors in preparations S4 and S5 obscure.

In preparation S6, sodium pyrophosphate ( $PP_i$ ) was tested as an analog for ATP in the initial extraction buffer. The results of this parallel preparation show that the yield of protein per gram of muscle using the  $PP_i$  extraction buffer is twice that of using the ATP extraction buffer. However, analyses of the final products indicate problems with using the  $PP_i$  buffer. SDS-PAGE gels show a higher amount of actin in the  $PP_i$  preparation. Additionally, absorbance data indicate that the  $PP_i$ -extracted preparation had both more aggregated material ( $(A_{340}/A_{280}) \times 100 = 28\%$  for  $PP_i$ -extracted;  $(A_{340}/A_{280}) \times 100 = 3\%$  for ATP-extracted), and more nucleic acid contamination ( $-4\%$  for  $PP_i$ -extracted;  $<1\%$  for ATP-extracted) (Grant, 1995).

Preparation S7 is an example of the importance of the temperature at which the extraction is performed. The cold room was at 11 °C on the first day of this preparation instead of 4 °C as it usually was. It was observed on the start of day 2 that the amount of precipitate was about 25% lower than usually observed at this stage, and at each successive stage the amounts were lower and the colors and consistencies different than usual (data not shown). Finally, on day 5 a collapse of the ultracentrifuge tube resulted in a complete loss of all material.

In preparation S8 two different methods of breaking up the myofibril structure were compared: passing the muscle twice through a meat grinder (S8-G), versus following the double grinding with homogenization of an ice-cold slurry of that mince in a Virtus™ blender (S8-H). Homogenizing the minced muscle was found to result in slightly less aggregated material than if the muscle is simply put through the meat grinder, but as shown by absorbance and SDS-gel data, it also results in higher contaminations of actin and nucleic acid in the final extracted myosin (see Table 3, page 80, and Figure 23, page 81).

The overall conclusions from these various preparations of myosin are as follows: 1) using buffers of high ionic strength is essential for good yield in the initial extraction of myosin from muscle; 2) keeping the myosin cold (i.e., 4-8 °C at all times) is vital for effective extraction and to prevent aggregation; 3) extremely gentle handling of myosin is required at all times to prevent aggregation; 4) the use of protease inhibitors in the extraction buffers seems to be useful, though for non-obvious reasons; and, 5) homogenization of the minced muscle is not recommended due to the increased amounts of contaminating actin and nucleic acids, despite the slightly lowered amounts of aggregated material in the final extracted myosin.

*Size Exclusion Chromatography of Myosin.* The myosin must be monodisperse when applied to the anti-myosin immunoaffinity columns. Size exclusion chromatography (SEC) to remove



aggregated material from the extracted myosin was very successful. Additionally, it is not a demanding procedure; the main problem encountered was getting the viscous myosin sample diluted homogeneously, without over-handling it, so that it could be loaded onto the column.

Identification of the peak from the SEC column that contained the monodisperse myosin was relatively straightforward using absorbance data and SDS-PAGE gels. Table 22 shows  $((A_{340}/A_{280}) \times 100)$  values for key fractions from one run of myosin on the Sepharose 2B column (see Figure 24, page 83 for chromatogram). Since a high ratio of  $A_{340}$  to  $A_{280}$  indicates the presence of aggregated material, these values clearly show that the second peak, at 1.01%, contains monodisperse myosin, while the first peak, at 31.9%, contains aggregated material. This is consistent with the expected behavior of the monodisperse myosin versus aggregated species

Sample	$(A_{340}/A_{280}) \times 100$ of Sample	Theoretical Stokes' Radius	Model in Figure 40
Preparation S8-G	13.0%	–	–
Fraction 20 (top of Peak 1)	31.9%	2,000-10,000 Å	C
Fraction 40 (top of Peak 2)	1.01%	750-1,500 Å (dynamic)	A
Fraction 46 (tail of Peak 2)	7.32%	800 Å	B
Fraction 53 (top of Peak 3)	3.81%	~200 - 600 Å	D

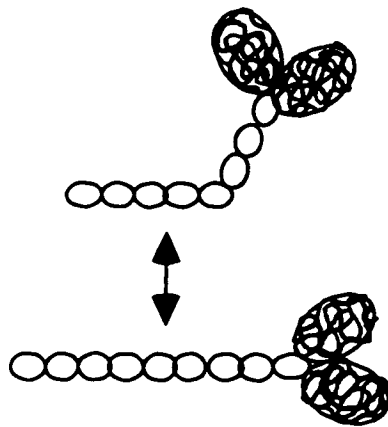
Table 22. Absorbance data for fractions from the Sepharose 2B chromatograph shown in Figure 24 indicate which peaks contain aggregated materials and which contain monodisperse myosin molecules. From this and the results of an SDS-PAGE analysis of the peaks (Figure 23, page 81), the fractions can be correlated to the models (shown in Figure 40) of possible forms in which myosin could exist in the peaks. The desirable, monodisperse myosin is found in peak 2, well-separated from actomyosin and homo-aggregates of myosin, as well as aggregates of fragments of degraded myosin.

on the SEC column, based on their respective sizes. The absorbance ratios also show that the tail of the second peak and an unexpected third peak both have a slightly elevated degree of aggregation.

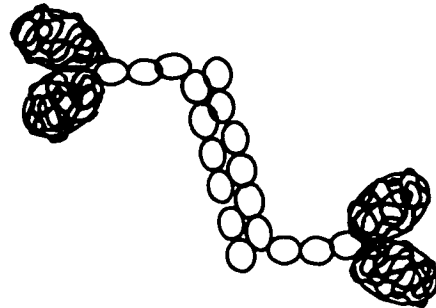
To aid in further interpreting the chromatogram, four models of possible physical conditions of myosin, and their corresponding theoretical Stokes' radii, were considered. These models, shown in Figure 40, are theoretical constructs based on information provided by the SDS-PAGE analyses and absorbance spectra run on the peaks, in combination with the known dynamic structure and behavior of myosin (Lowey and Holtzer, 1958; Holtzer and Lowey, 1958). Model A, with a Stokes' radius of 800-1500Å, incorporates the known dynamic structure of native monodisperse myosin (i.e., bending at the hinge region in the tail).<sup>25</sup> Model B is a suggested dimer with a Stokes' radius of ~800 Å (described in Pollack, 1990). Model C represents two polymeric forms: a bipolar homopolymer of myosin (similar to the arrangement of myosin in a thick filament), and actomyosin aggregates. Native homopolymers of myosin (thick filaments) and of actin (thin filaments) *in vivo*, exist in a wide range of lengths depending on the source (e.g. which animal species or muscle group served as the muscle source), and the state (e.g. contracted or not) in which they are measured; in vertebrates the lengths of thin filaments are typically ~10,000 Å and of thick filaments are typically ~20,000 Å (Pollack, 1990; Dreizen et al., 1984). Non-native *in vitro* polymers such as those that would be found in these samples could be either larger or smaller than the native polymers, but in either case would be larger than monodisperse myosin. A theoretical range of 2,000-10,000Å is used in Model C. If the SEC column had been more finely calibrated a more accurate size range of the species in peak 1 could have been determined. Model D represents possible aggregates of degraded myosin. The SDS-PAGE analysis indicated

---

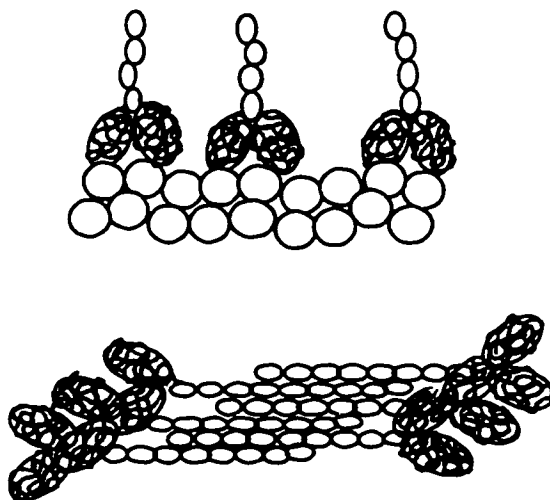
<sup>25</sup> The hinge is approximately one-third of the way along the tail from the head (see *Introduction and Theory*).



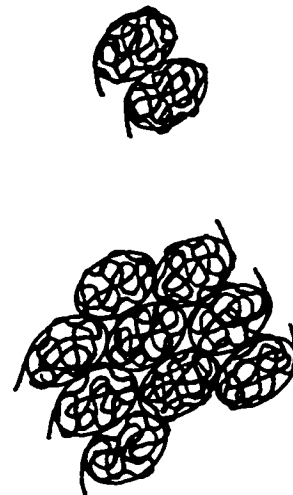
Model A. Native Monomers  
(800 - 1,500 Å)



Model B. Aggregated Dimers  
(~800 Å)



Model C. Polymers and Actomyosin  
(2,000-10,000 Å)



Model D. Aggregated S1 heads  
(200 - 600 Å)

Figure 40. Four models of possible forms in which myosin could exist *in vitro* and their approximate Stokes' radii. Model A shows a monodisperse, native, dynamic myosin molecule. Model B shows aggregated dimers of intact myosin. Model C shows the largest aggregates that myosin forms either with itself or with actin (actomyosin); these aggregates will have a wide range of sizes. Model D shows aggregates of S1 heads, fragments of degraded myosin; these small aggregates will vary in size depending on the type and number of fragments present.

the presence of S1 heads in peak 3, so these aggregates would be at least ~200Å for simple dimers of S1 heads.<sup>26</sup>

The theoretical Stokes' radii of all of these models fall within the fractionation range of Sepharose 2B. Based on these Stokes' radii, monodisperse myosin (model A) would be expected to elute after any large aggregates of actomyosin or homopolymers of myosin (model C) and before any small aggregates of degraded myosin fragments (Model D). This is consistent with the peak identification made based on the SDS-PAGE analysis: actomyosin and myosin homo-aggregates in peak 1, monodisperse myosin in peak 2, aggregates of S1 heads in peak 3. The Sepharose 2B nicely separated the monodisperse myosin from all aggregated material, both large aggregates of myosin and actomyosin as well as small aggregates of degradation products. The monodisperse myosin collected off the Sepharose columns was found to be stable, with respect to aggregation, for up to a week if stored at 4 °C in a potassium-based elution buffer. It was observed that myosin stored in potassium-based buffer was quite a bit more stable to aggregation than when stored in sodium-based buffer.

## **Monoclonal Antibody Preparation**

*Saturated Ammonium Sulfate Precipitation of Immunoglobulin from Ascites.* Ascites is a highly concentrated source of MAb. Addition of Saturated Ammonium Sulfate (SAS) was found to be a very effective method to precipitate immunoglobulin from ascites. The net recovery of IgM from the SAS precipitation shows recoveries of total IgM from MAb-F36 and MAb-S84 ascites to be 56.8 to 65.7% of the total IgM available in the ascites; these are comparable to results reported in the literature (Coppola et al., 1987). MAb-F22 yields were however quite low (9.90% of total IgM at 30% (v/v) SAS and 7.39% of total IgM at 50% (v/v) SAS; see Table 10, page 93), no doubt due to

---

<sup>26</sup> Recall that each S1 head is ~50 x 190 Å (see *Introduction and Theory*).

it being the first SAS precipitation attempted by this investigator. Performing the IgM precipitations at 50% (v/v) SAS was preferred since it was found for MAb-F22 to approximately double the total IgM yield, over using 30% (v/v) SAS.

Yields of IgM (Net Recovery) were lowered by processes not related to the precipitation itself. Significant losses were observed during transfers and handling of these small-volume, highly viscous samples. Sample analyses also accounts for some loss since at every stage of the purification sufficient material was removed to perform multiple analyses multiple times; a significant fraction of the MAb-F36 45% (v/v) precipitate was lost to a spill. Finally, malfunctioning autopipets made many of the measured volumes suspect in retrospect, which adds indeterminate error into all calculated yields. It was shown that only small amounts of IgM (~5%) were lost through conservative pooling of fractions from the Sephacryl S300-HR SEC runs (Table 13, page 102).

*Analyses for Total Protein and Total Immunoglobulin Content.* Discrepancies were seen between the results from analyses of total protein and total Ig concentrations which were never resolved. For example, in Table 13 (see page 102) two of the IgM peaks are seen to contain more than 100% of the total protein present. Similarly, in Table 14 (see page 108), for F22 purified by addition of 50% (v/v) SAS the total protein concentration was determined to be 0.50 mg/mL while the total IgM concentration was found to be 2.27 mg/mL. Obviously discrepancies exist between the results of the analyses for protein and Ig concentration since the total Ig concentration is expected to be the same as or less than the total protein concentration.

For IgM samples, two methods were used to determine protein concentrations, absorbance at 280 nm and the BioRad DC Protein Assay Kit. All protein concentrations for MAb-F22 samples were determined using the Assay Kit. Use of the inaccurate autopipets in running the Protein

Assay Kit assays makes protein concentrations calculated from these data suspect.

For some samples of MAb-F36 and MAb-S84, the total protein concentrations were determined both by absorbance and by Assay Kit. For these samples, the calculated concentrations from the two methods did not match and were not consistently different (data not shown).

All reported values of total protein concentration for MAb-F36 and MAb-S84 samples were based on data from the absorbance spectra, corrected for nucleic acid contamination and aggregation as appropriate (see *Introduction and Theory*).

A problem inherent in relying on the absorbance data is the choice of extinction coefficient ( $\epsilon$ ). An extinction coefficient represents the absorptivity of a pure protein. However, many of these samples are mixtures of proteins and the mixture changes at each step of the purification. Even once the IgM has been eluted from the Sephacryl column it is still not necessarily pure, and the identity and amounts of all the other proteins present are unknown. The extinction coefficients for the major contaminating proteins present after the SAS precipitation, albumin and transferrin, are smaller ( $\epsilon^{1\%_{280\text{nm}}} = 5.8$  and  $11.2$  mL/mg-cm, respectively) than for the value used for IgM-class MAbs ( $\epsilon^{1\%_{280\text{nm}}} = 13.3$  mL/mg-cm). So when these contaminating proteins are present the calculated concentrations of total protein in the IgM samples will be erroneously low. As the SDS-PAGE analyses showed, the ascites contained a high proportion of albumin. So, although an attempt was made to use a value for  $\epsilon^{1\%_{280\text{nm}}}$  appropriate to each specific sample, the true value was not known.

Additionally,  $\epsilon^{1\%_{280\text{nm}}}$  values for IgMs actually range from 10-14 mL/mg-cm. If 13.3 is an erroneously high extinction coefficient, the calculated protein concentration values in the IgM samples will again be erroneously low. All the calculated total protein concentrations shown in

Table 14 (except for MAb-F22 precipitated at 30% (v/v) SAS and MAb-S84) are lower than the Ig concentrations suggesting the extinction coefficient used was high. Therefore, the more significant data for yield analysis are probably the IgM concentrations in ascites and final purified IgM, as determined by ELISA.

While measuring the absorbance spectra of the re-concentrated, purified MAb-F36 and MAb-S84 reversible aggregation was observed. The re-concentrated IgM peaks from the Sephacryl SEC column were initially diluted 60-fold in Sephacryl Column Buffer to bring them into a reasonable concentration range to read the absorbance. At this concentration, the diluted IgMs showed high  $A_{280}$  values and  $(A_{340}/A_{280}) \times 100$  values of 70-80% indicating that the IgMs were greatly aggregated. However upon further dilution of the exact same sample to 100-fold total dilution the ratio dropped to <10% in all cases (data not shown). It may be that in diluting the re-concentrated IgM sample 100-fold, the concentration of the sample was diluted below its critical concentration, the minimum concentration required for aggregation to occur.<sup>27</sup>

*Size Exclusion Chromatography of Precipitated Immunoglobulins.* The main contaminating protein carried into the SAS precipitation of IgM from ascites is serum albumin. Because of the great size difference between IgM (~900 kDa) and albumin (66 kDa), size exclusion chromatography is very effective in separating the albumin away from the IgM.

In the SAS precipitations, although using 50% (v/v) SAS was found to be beneficial over using 30% (v/v) SAS, with respect to total IgM yield, at 50% (v/v) SAS a greater proportion of albumin was co-precipitated than at 30% (v/v) SAS (e.g., compare the relative peak heights for the IgM and albumin peaks between the SEC chromatograms for F36 precipitates in Figures 29 and 30).

---

<sup>27</sup> L. Silberstein, personal communication, 1996

Despite this increased albumin contamination, the higher percentage of SAS was preferred since the IgM yield was so enhanced and the albumin was easily and thoroughly removed by SEC. The SEC method is not difficult and the only drawback is the approximately 10-fold dilution the IgM samples undergo during elution. Thanks to the stability of immunoglobulins, this dilution was readily reversed by dialysis against dry Sephadex.

Sufficient quantities, of good purity, of each of the three IgM-class anti-myosin MAbs (MAb-F22, MAb-F36, and MAb-S84) were collected to produce small immunoaffinity columns with each (see Table 14, page 108).

### **Anti-Myosin Immunoaffinity Columns**

*Preparation of Immunoaffinity Matrix.* The reactions to covalently couple the IgM-class MAbs to the inert chromatographic matrix were very effective. Approximately 2 mL of coupled immunoaffinity matrix was produced from each IgM-class MAb (MAb-F22, MAb-F36, and MAb-S84). Although the number of cross-links between each MAb molecule and the inert matrix is unknown, the matrix activation and coupling reactions were apparently effective since all the reactions produced matrices with >95% of all the available IgM molecules coupled (see Table 15, page 110). Matrices were coupled at ~1 and ~2 mg IgM per milliliter of matrix for MAb-F22 and MAb-F36, and at ~1 mg/mL for MAb-S84 (see Table 16, page 111).

*Stability of Coupled Matrix.* Three eluants (a low pH buffer, a high salt concentration buffer, and guanidine hydrochloride) were candidates for use as the stripping eluant. The stripping eluant would be used to disrupt the non-covalent myosin/MAb interactions and release the bound myosin from the immunoaffinity columns. The coupled, blocked matrices were found to be quite stable to the low pH and high-salt concentration stripping eluants. No loss of coupled MAb was observed upon multiple washes of a MAb-F36-coupled matrix with the low pH and high [salt]



eluants (Table 17, page 113). The matrix stability to guanidine hydrochloride was not tested.

*Myosin Stability.* In addition to the requirement that the coupled matrices be stable to the stripping eluants, the myosin must be too. Unfortunately a simple twofold dilution of myosin in the three candidate stripping buffers showed that significant aggregation occurred only 10 minutes after dilution (Table 18, page 114). Apparently using any of these three stripping eluants would make analysis of  $V_e$  for myosin concentration by absorbance spectra, or for the presence of specific myosin heavy chain epitopes by hetero-isotypic sandwich ELISAs, impossible.

However, the 'high [salt]' and guanidine hydrochloride stripping eluants showed much lower aggregation ( $(A_{340}/A_{280}) \times 100 = 9.00\%$  and  $8.93\%$ , respectively) than the 'low pH' eluant ( $(A_{340}/A_{280}) \times 100 = 29.4\%$ ). Since the amount of aggregation that developed in the Gdn•HCl and 'high [salt]' eluants was less than 10% in 10 min, it is possible that the total protein in the myosin eluted with one of these two eluants could be quantified if measured sooner. A calibrated, low mixing flow cell (Snyder and Kirkland, 1979), with a dual wavelength detector, could be used to analyze the peak for protein concentration ( $A_{280}$ ) and aggregated material ( $A_{340}$ ) simultaneously as it elutes from the immunoaffinity column (i.e., in less than 10 min). Unfortunately, the detector available was not able to be calibrated to an external protein standard and was only able to monitor at a single wavelength.

As there was no reliable method available for spectroscopically measuring either the quantity or condition of the myosin as it eluted from the columns, and as monodisperse myosin would probably not be recoverable from the immunoaffinity columns in the eluted volume ( $V_e$ ) it was concluded that any analyses of the immunoaffinity column runs would have to occur on the void volume ( $V_0$ ) peaks, representing the non-retained isozymes.

## Detection of Myosin Epitopes

*Methods Development for Hetero-Isotypic Sandwich ELISAs.* The assay method for the  $V_0$  peaks was to be hetero-isotypic sandwich ELISAs. These rely on the antibody-enzyme conjugate being able to distinguish between the Ig-class of the anti-myosin MAbs used in the first and third layers on the plate (see Figure 14, page 39). In the process of performing methods development on the hetero-isotypic sandwich ELISAs, spurious results led to the discovery of two sources of IgM contamination in reagents being used. Both the BSA used in the Blocking Buffer and the IgG-class MAbs, MAb-25 and MAb-S95, which had been purified by Protein A affinity chromatography were contaminated with some IgM-class immunoglobulin.

It is not completely unreasonable that the BSA would contain IgM, since BSA is from serum, which can contain IgM, and a high purity of BSA was not being used. The fact that the anti-mouse IgM reagent ( $G\alpha mIgM \cdot HRP$ ) detects the contaminating bovine IgM from the BSA attests to the homology of the IgM between these different species; this cross-species reactivity is not uncommon. It is possible that only a subset of the  $G\alpha mIgM \cdot HRP$  molecules present in the commercial reagent react with the bovine IgM. If this were the case, the  $G\alpha mIgM \cdot HRP$  reagent could be treated by affinity chromatography to remove that fraction which reacts with the bovine IgM. Alternatively, a higher purity of BSA, or a different blocking protein could be identified.

Although the MAb-25 and MAb-S95 had been purified from ascites using a Protein A affinity column they were both found to contain a contaminating IgM (Table 21, page 128). Protein A is generally recommended for purification of IgG-class immunoglobulins based on its specificity for this class, however, it has been shown to bind to some IgMs (Pharmacia LKB Biotechnology, 1986; Fuller et al., 1988). The source of the contaminating IgM would be the original MAb-25 and

MAB-S95 ascites. The immune systems of the mice in which the ascites were produced would have mounted a response to both the injected hybridoma cells and the MABs these cells secrete. Some of this 'endogenous' IgM from the mouse would become mixed into the ascites along with the IgG-class MABs that the hybridoma cells are secreting. Although the Protein A column will primarily bind IgG-class immunoglobulins, some of the endogenous mouse IgM immunoglobulins present in the ascites were apparently retained on this column and carried into the 'purified' monoclonal IgG preparations.

Hetero-isotypic sandwich ELISAs require pure sources of IgG- and IgM-class MABs if  $\alpha$  IgM•HRP is to be used to specifically detect the presence of an IgM-class MAB. Contamination of one class with the other produces a mixed reaction and the spurious signals observed in the blanks of the proteolysis ELISA (see data in Table 19, page 117), and the saturation ELISA performed on the purified MAB-25 (see Figure 37, page 122). It is clear that the contaminating IgM present in the purified IgG-class MAB-25 and MAB-S95 (when these MABs are coated on the plate at 10 and 20  $\mu$ g/mL), gives rise to substantial signals (see Table 21, page 128). The homo-isotypic sandwich ELISA results showed that MAB-25 contains 1.99 mg/mL IgG (Table 14, page 108) with  $\sim$ 1.6  $\mu$ g/mL IgM as a contaminant (see Table 20, page 126). So an IgM contaminant present at  $\sim$ 1 part in 800 relative to the IgG component, was sufficient to interfere with the sandwich ELISAs. The IgM contamination found in the IgG-class MAB-25 prevented the development of a useful hetero-isotypic sandwich ELISA for analysis of the void volume peaks ( $V_0$ ) from the anti-myosin immunoaffinity columns. The hetero-isotypic sandwich ELISA cannot be used for analysis of myosin isozyme epitopes until pure MAB-25 and MAB-S95 can be obtained.

### **Future Work**

The use of immunoaffinity chromatography for the separation of the isozymes of myosin cannot proceed until some reliable analytical methods can be developed for quantifying myosin content

of peaks and for determining the epitopic identity of myosin in either the void volume ( $V_0$ ) or eluted volume ( $V_e$ ) peaks. Specifically, analysis of the peaks from the anti-myosin immunoaffinity columns cannot occur until the problems with aggregation of myosin in the  $V_e$  and contamination of IgG-class MAbs with IgM-class Abs are solved.

Problems related to the rapid aggregation of myosin and the lack of a method to quantitatively monitor myosin peaks as they elute from the immunoaffinity columns must be solved to enable analysis and collection of useful sample peaks off the columns. Keeping myosin monodisperse as it is applied to the columns, chromatographed, collected as separated peaks, and finally applied to the ELISA plates is a major undertaking. However, it would be possible with quick, careful handling and the appropriate chromatographic equipment such as wide-bore, constant flow injection valves and accurate detectors with low-mixing flow cells (Snyder and Kirkland, 1979). A dual-wavelength monitor, able to simultaneously measure the  $A_{280}$  and  $A_{340}$  of the peaks as they elute off the columns, would also be very helpful in determining the amount of myosin in the peak as well as its condition (i.e., degree of aggregation). Without the ability to quantitate the peaks as they elute from the column, the hetero-isotypic sandwich ELISAs was to be relied upon for quantitation. Absence of aggregation in the myosin as it is applied to the plates must be confirmed for any form of hetero-isotypic sandwich ELISA to prove reliable.

Re-purification of the MAb-25 could be pursued. The fractionation range of Sephacryl S300-HR (fractionation range of 10-1500 kDa), should allow separation of the IgM from the IgG MAbs due to the large size difference between them (IgG = ~150 kDa; IgM = ~900 kDa). This assumes that the IgM contaminant exists only in the pentameric form (see Figure 12, page 33), however, many ascites contain monomeric IgM. These  $\mu$ -class monomers are the result of an insufficient supply of the J protein required to bind the monomers into the pentameric form characteristic of IgM-class immunoglobulins. These monomeric IgMs would be essentially identical in size to IgG, therefore

would not be separable from IgG on SEC.

Biotinylation of some of our anti-myosin MABs is a possible alternative analytical method which could be used to detect specific epitopes (Ternynck and Avrameas, 1990; Hochfield et al., 1993). Conjugation of biotin to the available IgM-class anti-myosin MABs would result in reagents that would be highly specific to the myosin heavy chain epitopes of interest, and would not rely on Ig-class differences between the first and third layers of the hetero-isotypic sandwich ELISA. This would avoid the use of 'generic' HRP reagents which are reactive to an entire class of immunoglobulins. Additionally, it is possible that immunoblots (i.e., dot blots or Western blots) would be useful in detecting myosin heavy chain epitopes in the immunoaffinity column  $V_{eS}$ , even with the presence of denatured or aggregated myosin.<sup>28</sup> Any alternative methods would, of course, require a period of methods development.

Eventual separation of myosin isozymes will enable comparative studies of their detailed chemical characteristics, both structural and functional. Examination of characteristics such as amino acid sequences, protein folding, ATP and actin binding sites, as well as ATPase activity of individual isozymes could be performed. Such studies could then be extended to include isozymes from various developmental stages and/or disease states. Ultimately it is hoped that the information gathered in such studies would further our understanding of both normal development and aberrant states of muscle.

---

<sup>28</sup> L. Silberstein, personal communication (1997).

## APPENDICES

### Buffers and Reagents

ABTS	2,2'-azino-bis-(3-ethylbenz-thiazoline-6-sulfonic acid); Sigma #A1888 (see also <i>ELISA Substrate Solution</i> )
Affinity Matrix Coupling Buffer	0.5 M sodium chloride, 50 mM sodium phosphate, pH 7.4
Affinity Matrix Equilibration Buffer	0.5 M potassium chloride, 50 mM potassium phosphate, pH 7.2, 0.25 mM EGTA
Affinity Matrix High pH Wash Buffer	0.5 M sodium chloride, 0.1 M sodium borate, pH 9.0
Affinity Matrix Low pH Wash Buffer	0.5 M sodium chloride, 0.1 M sodium acetate, pH 3.5
Affinity Matrix High Salt Eluant	3.0 M potassium chloride, 50 mM potassium phosphate, pH 7.2, 0.25 mM EGTA
Affinity Matrix Low pH Eluant	0.5 M potassium chloride, 50 mM potassium phosphate, pH 2.0, 0.25 mM EGTA
Affinity Matrix Storage Buffer	150 mM sodium chloride, 20 mM sodium borate, pH 8.3, 0.02% (w/v) sodium azide
Affinity Matrix Chaotropic Eluant	4.0 M guanidine hydrochloride
ATP	adenosine triphosphate, disodium salt; Sigma #A3377
ATP Extraction Buffer	0.3 M potassium chloride, 150 mM potassium phosphate, pH 6.7, 0.02 M EDTA, 5 mM magnesium chloride, 5 mM ATP
$\beta$ -mercaptoethanol	Sigma #M6250
BioRad DC Protein Assay Kit	BioRad #500-0111 (see also <i>Reagent A</i> and <i>Reagent B</i> , below)
Blocking Buffer(s)	see <i>ELISA Blocking Buffer(s)</i>
Blue Dextran	Sigma #D5751
Borate Saline Buffer (BSB)	150 mM sodium chloride, 20 mM sodium borate, pH 8.2
BSA	bovine serum albumin; Nutritional Biochemicals, Fraction V bovine albumin

Cell Freezing Media	90% (v/v) FCS, 10% (v/v) DMSO
Cell Growth Media	89% (v/v) DMEM and 1% (v/v) glutamine with either: 5% (v/v) FCS and 5% (v/v) Hyclone™, or 10% (v/v) FCS (see <i>Materials and Methods</i> )
CNBr	cyanogen bromide; Sigma #C6388
Coomassie Brilliant Blue	Coomassie Brilliant Blue G250; BioRad #161-0406
DMEM	Dulbecco's modified Eagle's media; Sigma #D5530, lot #51H-4600
DMSO	dimethylsulfoxide; Sigma #D5879
DTT	DL-dithiothreitol (Cleland's Reagent); Sigma #D0632
EDTA	ethylenediamine-tetraacetic acid; US Biochemical Corp. #15699
EGTA	ethylene glycol-bis-( $\beta$ -aminoethyl ether) N,N,N',N'-tetraacetic acid; Sigma #E4378
ELISA Blocking Buffer(s)	for homo-isotypic sandwich ELISAs: 150 mM sodium chloride, 20 mM sodium phosphate, pH 7.4, 5% (v/v) powdered milk solution  for hetero-isotypic sandwich ELISAs: 0.5 M potassium chloride, 50 mM potassium phosphate, pH 7.2, 0.25 mM EGTA, with one of the following proteins: 1 mg/mL BSA, or 5% (v/v) milk, or 5% (v/v) NCS (see <i>Results</i> )
ELISA Plate Coating Buffer	0.1 M sodium bicarbonate, pH 9.5
ELISA Substrate Solution	0.1 M sodium citrate, pH 4.2, 2 mM ABTS, 0.03% (v/v) hydrogen peroxide
ELISA Wash Buffer	0.5 M sodium chloride, 10 mM sodium phosphate, pH 7.4, 0.05% (v/v) Tween 20
FCS	fetal calf serum; Sigma #F4010, lot# 11H-0749
$\Gamma$ antiIgG	goat anti-mouse IgG, $\gamma$ and L chain specific CalTag #M30000, lot #1401
$\Gamma$ antiIgM	goat anti-mouse IgM, $\mu$ chain specific; CalTag #M31500, lots #3201 and #3101
$\Gamma$ antiIgG•HRP	goat anti-mouse IgG conjugated to HRP, $\gamma$ chain specific, CalTag #M30107, lot #1403
$\Gamma$ antiIgM•HRP	goat anti-mouse IgM conjugated to HRP, $\mu$ chain specific; CalTag #M31507, lot #1801

Gel Destain	10% (v/v) trichloroacetic acid
Gel Fix	10% (v/v) acetic acid
Gel Running Buffer	0.192 M glycine, 0.025 M Tris-base, 0.1% (v/v) SDS
Gel Stain	0.25% (w/v) Coomassie Brilliant Blue G250, 50% (v/v) methanol, 12.5% (w/v) trichloroacetic acid
Glutamine	L-glutamine; Sigma #G7513, lot #83H4685
Glycerol	anhydrous glycerol; Baker Analyzed #2136-01
High Molecular Weight Standards	Sigma #SDS-6H, lot 53H9450 (rabbit myosin, $\beta$ -galactosidase, phosphorylase b, BSA, ovalbumin, and carbonic anhydrase)
Hyclone™	Hyclone Laboratories #A6165L, fetal clone I, bovine serum product, optimized for hybridomas, lot #61652012
Hydrogen Peroxide	30% hydrogen peroxide; Chempure #831-116, lot #M156 KHML
IgG Standard	Mouse IgG; Sigma #I-8765, lot #052H8895 (IgG standard for homo-isotypic sandwich ELISAs)
IgM Standard	Mouse IgM; see <i>MOPC</i>
Iron sulfate	Mallinckrodt #5056 (to neutralize CNBr waste)
Leupeptin	leupeptin, hemisulfate salt; Sigma #L2884 (protease inhibitor)
MOPC	Mouse IgM, MOPC (mineral oil-induced plasmocytoma originated IgM) 104E, Lambda; Sigma #M3273, lot #074H-8846 (IgM standard for homo-isotypic sandwich ELISAs)
Myosin Dialysis Buffer	0.6 M sodium chloride, 10 mM sodium phosphate, pH 7.0, 10 mM EDTA
NCS	neonatal calf serum; Sigma #N0515, lot #11H-0275
Phosphate Buffered Saline (PBS)	150 mM sodium chloride, 20 mM sodium phosphate, pH 7.4
PBS-Azide	150 mM sodium chloride, 20 mM sodium phosphate, pH 7.4, 0.02% (w/v) sodium azide
PBS-Blotto	150 mM sodium chloride, 20 mM sodium phosphate, pH 7.4, 5% (v/v) powdered milk solution



Pellet Dispersion Buffer #1	1.0 M potassium chloride, 50 mM potassium phosphate, pH 6.7, 20 mM EDTA
Pellet Dispersion Buffer #2	3.0 M potassium chloride, 50 mM potassium phosphate, pH 6.7
PMSF	phenylmethylsulfonyl fluoride; Sigma #P7626 (protease inhibitor)
Pristane	2,6,10,14-tetramethylpentadecane; Sigma #T7620 (to prime recipient animals for ascites production)
Pyronin Y	Sigma #P7017 (SDS-PAGE gel marker)
Reagent A, BioRad D/C Protein Assay Kit	1-5% sodium hydroxide, <1% sodium tartrate, <0.1% copper sulfate
Reagent B, BioRad D/C Protein Assay Kit	<1% of each of the following: lithium sulfate, sodium salt of tungstic acid, sodium salt of molybdic acid, hydrochloric acid, phosphoric acid
Saturated Ammonium Sulfate (SAS)	528 g/L ammonium sulfate, 0.25 mM EDTA, pH 7.2
SDS	sodium dodecyl sulfate; Sigma #L4509
Sodium Azide	MCB #SX00P2781 (bacteriostatic agent)
SDS Sample Buffer, 2X	10% (v/v) SDS, 125 mM Tris hydrochloride, pH 6.8, 0.02% (w/v) bromphenol blue, 0.05% (w/v) pyronin Y, 20% (v/v) glycerol, 4 mM DTT
Sepharose Column Buffer	0.5 M potassium chloride, 50 mM potassium phosphate, pH 7.2, 0.25 mM EGTA
Sepharose Column Buffer-Tween	0.5 M potassium chloride, 50 mM potassium phosphate, pH 7.2, 0.25 mM EGTA, 0.02% (v/v) Tween-20
Trypan Blue	Sigma #T8154 (dye for hybridoma cell counting)
Tween-20	Sigma #P9416

## Materials

Cryovials	Nalge Cryovial #5000-0012, 1.2 mL
Dialysis Tubing	Spectra/Por molecular porous membrane tubing, 12,000-14,000 mwco, #132-676, 6.4 mm diameter and #25225-228, 15.9 mm diameter
Econo Columns	BioRad #737-0706, 0.7 (i.d.) x 5 cm, with polyethylene bed support
Mice	Balb/c mice, Sierra BioSource (Gilroy, California)
Protein A Affinity Matrix	Pierce ImmunoPure IgG purification kit #44667
Rats	Sprague-Dawley, Sierra BioSource (Gilroy, California)
SDS-PAGE Gels	Jule Biotechnology, #12.5 D.75BMC-10G (12.5% custom pre-cast denaturing non-gradient Jule Gel; resolving: 12.5%T 2%C; stacking: 6%T, 3%C) and #7.5 D.75BMC-10P (7.5% standard pre-cast denaturing non-gradient Jule Gel)
Sephacryl S-300-HR	Sigma #S-300-HR, Sephacryl S-300-HR, 25-75 micron beads (wet) fractionation range = 10-1500 kDa
Sephadex G-200	Pharmacia #G-200, 40-120 microns (dry),
Sepharose 2B	Sigma #2B-300, Sepharose 2B, 60-200 micron beads (wet), fractionation range = 70-40,000 kDa
Sepharose CL 4B	Sigma #CL-4B-200, Sepharose CL 4B 60-140 micron beads (dry)
Low-pressure Tubing	BioRad #731-8209 Silicone tubing, 3.2 mm (i.d.)
Snap-cap Tubes	Fisher Scientific #14-956-1J, disposable polypropylene, 15 mL
Three-way Valves	Baxter Pharmaseal #K75

## **Equipment**

American Optical Light Microscope

American Optical Bright Line Hemocytometer

Beckman Model L8-M Ultracentrifuge

Beckman Ultracentrifuge Rotor, Type 70T1/70.1T1, 70,000 RPM

Beckman Ultracentrifuge Rotor, Type SW 41T1-41,000 RPM, Class C, D, F, G, H

BioRad MiniProtean II Dual Slab Electrophoresis Cell

BioRad Model 1125B Dual Temperature Slab Gel Dryer

BioRad Model 500/200 Electrophoresis Power Supply

Corning #25801 Disposable, Sterile 96-well ELISA Plates

Corning #26305-12 ELISA Plate Washer, 12 Channel

Costar Octapette 8-Channel Fixed Volume Pipettors 100  $\mu$ L and 50  $\mu$ L

Eppendorf Model 5415 Microfuge

Eppendorf Model 4810 Autoclavable, Adjustable Pipettes

Forma Scientific HEPA filtered IR Incubator

Hewlett-Packard 8452A Diode Array Spectrophotometer

Hewlett-Packard ScanJet 4c Color Scanner (with Adobe Photoshop v. 3.0)

Hewlett-Packard Vectra ES/12 Computer equipped with  
89531A MS-DOS UV-VIS Operating Software, Revision A.03.00

Hoefer Model PR70 Red Rotor Lab Shaker

IEC Model HN-SNII, Benchtop Clinical Centrifuge

IEC 958 Clinical Centrifuge Rotor with 305 sleeve

IEC Model B20 Refrigerated Centrifuge

IEC 870 Centrifuge Rotor

IEC 872 Centrifuge Rotor

ISCO UA-5 Absorbance/Fluorescence Detector and Chart Recorder

ISCO Retriever II Fraction Collector

ISCO Type 6 Optical Unit with 0.5-cm Flow Cell

Labquake Shaker Model T400-110

Linbrow #IS-FB-96-TC 6-mm Tissue Culture Plates

Millipore MilliQ® Water Purification System

Molecular Devices V<sub>max</sub> Kinetic Microplate Reader

Olympus CK2 Inverted Light Microscope

Softmax Microplate Reader Software Package, v. 2.02 for Macintosh

Taylor Wharton 8K Auto-filling Liquid Nitrogen Cell Bank

Tris Series 1610-008 Peristaltic Pump

## REFERENCES

- Andrew, S.M. and J.A. Titus, "Purification and Fragmentation of Antibodies," In: *Current Protocols in Immunology*, J.E. Coligan, A.M. Krubieek, D.M.H. Margulies, E.M. Shevach, and W. Strober, Eds., J. Wiley & Sons, New York (1994).
- Axén, R., J. Porath, and S. Ernback, "Chemical Coupling of Peptides and Proteins to Polysaccharides by Means of Cyanogen Halides," *Nature* **214**:1302-1304 (1967).
- Barany, M., "ATPase Activity of Myosin Correlated with Speed of Muscle Shortening," *Journal of General Physiology* **50**:197-218 (1967).
- Bouvet, J.-P. and R. Pires, "One-Step Purification of Murine Monoclonal Antibodies of the IgM Class," *Journal of Immunological Methods* **145**:263-266 (1991).
- Bouvet, J.-P., R. Pires, and J. Pillot, "A Modified Gel Filtration Technique Producing an Unusual Exclusion Volume of IgM: a Simple Way of Preparing Monoclonal IgM," *Journal of Immunological Methods* **66**:299-305 (1984).
- Carlson, F.D. and D.R. Wilke, *Muscle Physiology*, Prentice Hall Inc., Englewood Cliffs, New Jersey (1994).
- Catty, D., Ed., *Antibodies: A Practical Approach, Vol. 1*, IRL Press, Oxford, England (1988).
- Chizzonite, R.A., A.W. Everett, W.A. Clark, S. Jakovic, M. Rabinowitz, and R. Zak. "Isolation and Characterization of Two Molecular Variants of Myosin Heavy Chain from Rabbit Ventricle," *Journal of Biological Chemistry* **257**(4): 2056-2065 (1982).
- Cho, M., *Fiber-Type Diversity in Human Muscle Development*, Ph.D. Thesis presented to Stanford University, Stanford, California (1992).
- Cho, M., Hughes, S.M., I. Karsch-Mizrachi, M. Travis, L.A. Leinwand, and H. Blau, "Fast Myosin Heavy Chains Expressed in Secondary Mammalian Muscle Fibers at the Time of their Inception," *Journal Cell Science* **107**:2361-2371 (1994).
- Clezardin, P., G. Buogro, and J.L. McGregor, "Tandem Purification of IgM Monoclonal Antibodies from Mouse Ascites Fluids by Anion-Exchange and Gel Fast Protein Liquid Chromatography," *Journal of Chromatography* **354**:425-433 (1986).
- Coppola, G., J. Underwood, G. Cartwright, and M.T.W. Hearn, "High-Performance Liquid Chromatography of Amino Acids, Peptides, and Proteins: XCIII. Comparison of Methods for the Purification of Mouse Monoclonal Immunoglobulin M Autoantibodies," *Journal of Chromatography* **476**:269-290 (1987).
- Cuatrecasas, P. and C.B. Afinsen, "Affinity Chromatography," *Methods in Enzymology* **22**:345-378 (1971).
- Dan-Goor, M., L. Silberstein, M. Kessel, and A. Muhlrud, "Localization of Epitopes and Functional Effects of Two Novel Monoclonal Antibodies Against Skeletal Muscle Myosin," *Journal of Muscle Research and Cell Motility* **11**:216-226 (1990).

- Deutscher, M.P., Ed., *Guide to Protein Purification*, Vol. 182 of *Methods in Enzymology*, Academic Press, New York (1990).
- Dreisen, P., L. Herman, and J.E. Berger, "Structural Studies of Glycerinated Skeletal Muscle. I. A-Band Length and Cross-Bridge Period in ATP-Contracted Fibers," p. 135-149, In: *Contractile Mechanisms in Muscle*, G.H. Pollack and H. Sugi, Eds., Plenum Press, New York (1984).
- Ebashi, S. and Y. Nonomura, "Proteins of the Myofibril," p 285-340, In: *The Structure and Function of Muscle, Vol. III Physiology and Biochemistry*, G.H. Bourne, Eds., Academic Press, New York (1973).
- Eisen, H.N., *General Immunology*, J.B. Lippincott Co., Philadelphia (1990).
- Englehardt, W.A. and M.N. Ljubimowa, "Myosin and Adenosine Triphosphate," *Nature* **144**:668-669 (1939).
- Fischer, L., *An Introduction to Gel Chromatography*, American Elsevier, New York (1969).
- Fuller, S.A., M. Takahashi, and J.G.R. Hurrell, "Purification of Monoclonal Antibodies," Unit 11.11, In: *Current Protocols in Immunology*, F.M. Ausubel, Ed., J. Wiley & Sons, New York (1988).
- Garrett, R.H. and C.M. Grisham, Eds., "Muscle Contraction," p. 1156-1189, In: *Molecular Aspects of Cell Biology*, Harcourt Brace College Publishing, New York (1995).
- Goding, J.W., *Monoclonal Antibodies: Principals and Practice*, Second Edition, Academic Press, London, U.K. (1986).
- Goldspink, D.F., Ed., *Development and Specialization of Skeletal Muscle*, Volume 7 in the series *Society for Experimental Biology*, Cambridge University Press, Cambridge, England (1980).
- Grant, S., *Epitope Mapping of Anti-Myosin Monoclonal Antibodies*, M.S. Thesis presented to San Jose State University, San Jose, California (1995).
- Hämäläinen, N. and D. Pette, "Patterns of Myosin Isoforms in Mammalian Skeletal Muscle Fibers," *Microscopy Research and Technique* **30**:381-389 (1995).
- Hanson, J. and H.E. Huxley, "Structural Basis of the Cross-Striations in Muscle," *Nature, London* **172**: 530-532 (1953).
- Hardy, R.R., "Purification and Characterization of Monoclonal Antibodies," In: *Handbook of Experimental Immunology, 4th Edition*, Vol. 1 of the series: *Immunochemistry*, D.M. Weir, C. Blackwell, and L.A. Herzenberg, Eds., Blackwell Scientific Publications, Oxford, England (1986).
- Harris, E.L.V. and S. Angal, Eds., *Protein Purification Methods*, IRL Press, New York (1994).
- Hockfield, S., S. Carlson, C. Evans, P. Levitt, J. Pintar, and L. Silberstein, *Selected Methods for Antibody and Nucleic Acid Probes*, Vol. 1 of the series: *Molecular Probes of the Nervous System*, Cold Spring Harbor Laboratory Press, New York (1993).

- Holtzer, A. and S. Lowey, "The Molecular Weight, Size, and Shape of the Myosin Molecule," *Journal of the American Chemical Society* **81**:1370-1377 (1959).
- Hughes, S.M., M. Cho, I. Karsch-Mizarachi, M. Travis, L. Silberstein, L.A. Leinwand, and H.M. Blau, "Three Slow Myosin Heavy Chains Sequentially Expressed in Developing Mammalian Skeletal Muscles," *Developmental Biology* **158**:183-199 (1993).
- Huxley, A., *Reflections on Muscle*, Princeton University Press, Princeton, New Jersey (1980).
- Huxley, H.E., "Electron Microscopic Studies of the Organisation of the Filaments in Striated Muscle," *Biochimica Biophysica Acta* **12**:387-394 (1953).
- Huxley, A. and R. Niedergerke, "Interference Microscopy of Living Muscle Fibers," *Nature* **173**:971-973 (1954).
- Huxley, H.E. and J. Hanson, "Changes in the Cross-striations of Muscle During Contraction and Stretch and their Structural Interpretation," *Nature* **173**:973-976 (1954).
- Kamihira, M., S. Iijima, and T. Kobayashi, "Stabilities of Antigen and Antibody Under Elution Conditions in Immunoaffinity Chromatography Using Monoclonal Antibody," *Bioseparations* **3**:185-188 (1992).
- Köhler, G. and C. Milstein, "Continuous Cultures of Fused Cells Secreting Antibody of a Predefined Specificity," *Nature* **256**:495-497 (1975).
- Komuro, I., H. Tsuchimochi, S. Ueda, M. Kurabayashi, Y. Seko, F. Takaku, and Y. Yazaki, "Isolation and Characterization of Two Isozymes of Myosin Heavy Chain from Canine Atrium," *Journal of Biological Chemistry* **261**(10):4504-4509 (1986).
- Leinwand, L.A., L. Saez, E. McNally, and B. Nadal-Ginard, "Isolation and Characterization of Human Myosin Heavy Chain Genes," *Proceedings of the National Academy of Sciences (USA)* **80**:3716-3720 (1983).
- Ley, P.L., S.J. Prowse, and C.R. Jenkin, "Isolation of Pure IgG<sub>1</sub>, IgG<sub>2a</sub>, and IgG<sub>2b</sub> Immunoglobulins from Mouse Serum Using Protein A-Sepharose," *Immunochemistry* **15**:429-436 (1978).
- Lowe, C.R., "Affinity Chromatography," In: *Lab Techniques in Biochemistry and Molecular Biology, Vol. 7, part II, X*, Eds. (1979).
- Lowey, S., "Myosin Structure," p 563-587, In: *Myology*, A.G. Elgel and B.Q. Banker, Eds., McGraw Hill Publishers, New York (1986).
- Lowey, S. and A. Holtzer, "The Aggregation of Myosin," *Journal of the American Chemical Society* **81**:1378-1384 (1959).
- Margossian, S.S. and S. Lowey, "Interaction of Myosin Subfragments with F-Actin," *Biochemistry* **17**:5431-5439 (1978).
- Margossian, S.S. and S. Lowey, "Preparation of Myosin and its Subfragments from Rabbit Skeletal Muscle," p. 55-71, In: *Structural and Contractile Proteins, Part B, The Contractile Apparatus and the Cytoskeleton, Methods in Enzymology, Vol. 85*, D.W. Frederiksen and L.W. Cunningham, Eds., Academic Press, New York (1982).

- McKinney, M.M. and A. Parkinson, "A Simple, Non-chromatographic Procedure to Purify Immunoglobulins from Serum and Ascites Fluid," *Journal of Immunological Methods* **96**:271 (1987).
- Offer, G., C. Moos, and R. Starr, "A New Protein of the Thick Filaments of Vertebrate Skeletal Myofibrils: Extraction, Purification, and Characterization," *Journal of Molecular Biology* **74**:653-676 (1973).
- Pette, D., Ed. *Plasticity of Muscle*, Walter de Gruyter Publisher, Berlin, Germany (1980).
- Pharmacia LKB Biotechnology, *Affinity Chromatography: Principals and Methods*, Report #18-1022-29, 143 pp (1986).
- Pollack, G.H., *Muscles and Molecules: Uncovering the Principals of Biological Motion*, Ebner & Sons Publishers, Seattle, Washington (1990).
- Poole, C.F. and S.K. Poole, *Chromatography Today*, Elsevier Science Publishers, New York (1991).
- Porath, J., "Molecular Sieving and Adsorption," *Nature* **218**:834-838 (1968).
- Press, E.M. and P.J. Piggot, "The Chemical Structure of the Heavy Chains of Human Immunoglobulin G," p. 45-51, In: *Cold Spring Harbor Symposia on Quantitative Biology, Vol. 32*, Cold Spring Harbor Laboratory Press, New York (1986).
- Rayment, I., W.R. Rypniewski, K. Schmidt-Bäse, R. Smith, D.R. Tomchick, M.M. Benning, D.A. Winkelmann, G. Wesenberg, and H.M. Holden, "Three-Dimensional Structure of Myosin Subfragment-1: A Molecular Motor," *Science* **261**:50-65 (1993).
- Roby, J.F. and B.J. White, *Biochemical Techniques: Theory and Practice*, Brooks/Cole Publishing, Monterey, California (1987).
- Silberstein, L.H., *An Immunological Approach to the Characterization of Myosin Isozymes*, Ph.D. Thesis presented to Brandeis University, University Microfilms International, Ann Arbor, Michigan (1979).
- Silberstein, L. and H. Blau, "Two Fetal-Specific Fast Myosin Isozymes in Human Muscle," p. 253, In: *Molecular Biology of Muscle Development, UCLA Symposium on Molecular and Cellular Biology*, Vol. 29, C. Emerson, D.A. Fishman, B. Nadal-Ginard, and M.A.Q. Siddiqui, Eds., A.R. Liss, Inc. New York (1986).
- Silberstein, L. and S. Lowey, "Isolation and Distribution of Myosin Isoenzymes in Chicken Pectoralis Muscle," *Journal of Molecular Biology* **148**:153-189 (1981).
- Silberstein, L., S.G. Webster, M. Travis, and H.M. Blau, "Developmental Progression of Myosin Gene Expression in Cultured Muscle Cells," *Cell* **46**:1075-1081 (1986).
- Skoog, D.A. and D.M. West, *Fundamentals of Analytical Chemistry*, Third Edition, Holt, Reinhart, and Winston, New York (1976).
- Slater, E., Ed., *Optical Methods in Biology*, J. Wiley & Sons, New York (1970).



- Smith, J.A., "Purification of Proteins by Conventional Chromatography," Unit 10.9, In: *Current Protocols in Molecular Biology*, J.E. Coligan, Ed., J. Wiley & Sons, New York (1988).
- Snyder, L.R. and J.J. Kirkland, *Introduction to Modern Chromatography*, Second Edition, John Wiley & Sons, New York (1986).
- Stellwagen, E., "Gel Filtration," *Methods in Enzymology* **182**:317-328 (1990).
- Stevens, P.W., M.R. Hansberry, and D.M. Kelso, "Assessment of Adsorption and Adhesion of Proteins to Polystyrene Microwells by Sequential Enzyme-Linked Immunosorbent Assay Analysis," *Analytical Biochemistry* **225**:197-205 (1995).
- Stryer, L., *Biochemistry*, First Edition, W.H. Freeman and Co., New York (1975).
- Szent-Györgyi, A.G., E.M. Szentkiralyi, and J. Kendrick-Jones, "The Light Chains of Scallop Myosin as Regulatory Subunits," *Journal of Molecular Biology* **74**:179-185 (1973).
- Szent-Györgyi, A.G., "Proteins of the Myofibril," p 1-54, In: *The Structure and Function of Muscle, Vol. II Physiology and Biochemistry*, G.H. Bourne, Eds., Academic Press, New York (1960).
- Ternynck, T. and S. Avrameas, "Avidin-Biotin System in Enzyme Immunoassays," *Methods in Enzymology* **184**:469-481 (1990).
- von Hippel, P.H., M.F. Gellert, and M.F. Morales, "Studies on the contractile Proteins of Muscle. II. Polymerization Reactions in the Myosin B System," *Journal of the American Chemical Society* **81**:1393-1396 (1958).
- Webster, C., L. Silberstein, A.P. Hays, and H.M. Blau, "Fast Muscle Fibers are Preferentially Affected in Duchenne Muscular Dystrophy," *Cell* **52**:503-513 (1988).
- Whalen, R.G., S.M. Sell, G.S. Butler-Browne, K. Schwartz, P. Bouveret, and I. Pinset-Härström, "Three Myosin Heavy-Chain Isozymes Appear Sequentially in Rat Muscle Development," *Nature* **292**:805-809 (1981).
- Wilcheck, M. T. Miron, and J. Kohn, "Affinity Chromatography," *Methods in Enzymology* **104**:3-55 (1984).
- Yokoyama, W., "Production of Ascites Fluid Containing Monoclonal Antibody," Unit 11.10, In: *Current Protocols in Immunology*, F.M. Ausubel, Ed., J. Wiley & Sons, New York (1988).
- Zubay, G., Ed., *Biochemistry*, Second Edition, MacMillan Publishing Co., New York (1988).

July 7, 1997

total # pages: 1

<b>TO:</b> Dr. Gerald H. Pollack University of Washington Division of Bioengineering, WD-12 Seattle WA 98195 USA  TEL: 206-685-1880 FAX: 206-685-3300	<b>FROM:</b> Ms. Sara E. Acevedo MS 248-1 Space Science Division NASA Ames Research Center Moffett Field CA 94035-1000 USA  TEL: 415-604-4223 FAX: 415-604-8779
---	--

Dear Dr. Pollack,

I am a graduate student in the Department of Chemistry at San Jose State University. I wish to request permission to reprint a figure from one of your publications.

The publication is *Muscles and Molecules: Uncovering the Principles of Biological Motion* by G.H. Pollack (1990). The figure I wish to use is panel C of figure 2.15 on page 28 ("Freeze-fracture imagery of honey-bee flight muscle in rigor").

The figure will be used one time only for educational purposes; it will appear as a figure in my thesis entitled "Development of Monoclonal Antibodies for the Separation of Myosin Isozymes" which will be archived by University Microfilms. I will have less than a dozen copies of the thesis printed for the use of my Department, my thesis advisor, and myself. Credit will be given in my figure legend as "Copied from Pollack, 1990, with permission." (unless you instruct otherwise), and my reference list will include the complete citation for the book. Also, a copy of the letter of permission will appear in my thesis.

I must have the requested permission in writing no later than July 10, 1997.

Thank you for your assistance,



Sara E. Acevedo

I hereby grant permission to S. Acevedo for publication of the above described figure in her thesis.



Dr. Gerald H. Pollack  
 University of Washington

7 July 97

Date

July 7, 1997

total # pages: 1

<b>TO:</b> Copyrights and Permissions J.B. Lippincott Co. 227 E. Washington Square Philadelphia PA 19106-3780  ATTN: Marie  TEL: 215-238-4200 FAX: 215-238-4419	<b>FROM:</b> Ms. Sara E. Acevedo MS 245-1 Space Science Division NASA Ames Research Center Moffett Field CA 94035-1000 USA  TEL: 415-604-4223 FAX: 415-604-6779
--	--

RECEIVED  
JUL 8 - 1997  
LIPPINCOTT RAVEN  
PERMISSIONS

Dear Marie,

I am a graduate student in the Department of Chemistry at San Jose State University. I wish to request permission to reprint two figures from one of your publications.

The publication is *General Immunology* by H.N. Eisen (1990). The figures I wish to use are:

- 14-10 (Linear periodicity in amino acid sequences of an IgG) on page 48, and
- 14-12, parts A, B, and C (Structure of human IgM) on page 49.

The figures will be used one time only for educational purposes; they will appear as figures in my thesis entitled "Development of Monoclonal Antibodies for the Separation of Myosin Isozymes" which will be archived by University Microfilms. I will have less than a dozen copies of the thesis printed for the use of my Department, my thesis advisor, and myself. Credit will be given in my figure legend as "Copied from Eisen, 1990, with permission." (unless you instruct otherwise), and my reference list will include the complete citation for the book. Also, a copy of the letter of permission will appear in my thesis.

I must have the requested permission in writing no later than July 10, 1997.

Thank you for your assistance,

*Sara E. Acevedo*  
Sara E. Acevedo

**Lippincott - Raven**

P U B L I S H E R S



A Wolters Kluwer Company

**Permissions**

Tel: 215-238-4361 Books  
Tel: 215-413-4063 Journals  
Fax: 215-238-4419

July 17, 1997

Sara E. Acevedo  
MS 245-1  
Space Science Division  
NASA Ames Research Center  
Moffett Field, CA 94035-1000

Dear Ms. Acevedo:

Thank you for your recent request to use material from one of our publications in your thesis.

The quoted material may be included in your manuscript, using the standard format and footnotes suggested in the UNIVERSITY OF CHICAGO STYLE MANUAL or those required by your university

However, if your thesis is selected for publication and a contractual agreement has been signed, then you should submit your formal permission request to this office. Please advise the name of your publisher, tentative publication date, number of pages in your forthcoming book and the estimated retail price. Upon receipt of this information this office shall then research your request and respond with the conditions of the permission.

This course of action must be taken since many times representation of the copyrighted material may change between the time a thesis is submitted and the date that a contractual arrangement for publication has been secured.

Congratulations as you complete your advanced studies, and with very best wishes for your future work!

Sincerely,

Marie P. Wayne  
Permissions Editor

July 8, 1997

total # pages: 1

<b>TO:</b>  Permissions Department Harcourt Brace College Publishers 6277 Sea Harbor Drive Orlando FL 32887-6777  ATTN: Academic Press, Inc. (Anna)  TEL: 407-345-2000 FAX: 407-345-4058	<b>FROM:</b>  Ms. Sara E. Acevedo MS 245-1 Space Science Division NASA Ames Research Center Moffett Field CA 94035-1000 USA  TEL: 415-604-4223 FAX: 415-604-6779
--	--

Dear Madame,

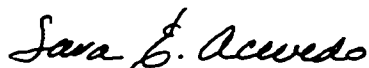
I am a graduate student in the Department of Chemistry at San Jose State University. I wish to request permission to reprint a figure from one of your publications.

The paper is "Three Slow Myosin Heavy Chains Sequentially Expressed in Developing Mammalian Skeletal Muscle," *Developmental Biology* 158:183-199 (1993). The figure I wish to use 9 on page 196 ("A4.951+ fibers are a subset of A4.840+ fibers.").

The figure will be used one time only for educational purposes; it will appear as a figure in my thesis entitled "Development of Monoclonal Antibodies for the Separation of Myosin Isozymes" which will be archived by University Microfilms. I will have less than a dozen copies of the thesis printed for the use of my Department, my thesis advisor, and myself. Credit will be given in my figure legend as "Copied from Hughes *et al.*, 1993, with permission." (unless you instruct otherwise), and my reference list will include the complete citation for the paper. Also, a copy of the letter of permission will appear in my thesis.

I must have the requested permission in writing no later than COB July 10, 1997.

Thank you for your assistance,



Sara E. Acevedo



Academic Press, Inc.  
6277 Sea Harbor Drive  
Orlando, FL 32887  
Tel 407-345-2000  
Fax 407-345-4058

August 4, 1997

Ms. Sara E. Acevedo  
MS 245-1  
Space Science Division  
NASA Ames Research Center  
Moffett Field, CA 94035-1000

Re: Developmental Biology, 158:183-199 (1993)

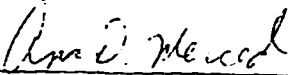
Dear Ms. Acevedo:

**PERMISSION GRANTED** to include Figure 9 page 196 from our above-referenced material in your thesis, provided that 1) complete credit is given to the source, including the Academic Press copyright notice; 2) the material to be used has appeared in our publication without credit or acknowledgment to another source and 3) if commercial publication should result, you must contact Academic Press again.

Optional: You may wish to indicate our web site address: <http://www.apnet.com>.

We realize that University of Microfilms must have permission to sell copies of your thesis, and we agree to this. However, we must point out that we are not giving permission for separate sale of your article.

Date: 8/4/97

  
\_\_\_\_\_  
Ana D. Merced  
Paralegal Department  
Academic Press - Permissions  
407 345 3994 (tel)  
407 345 4058 (fax)  
amerced@harcourtbrace.com

July 7, 1997

total # pages: 1

<b>TO:</b> Permissions Department Harcourt Brace College Publishers 6277 Sea Harbor Drive Orlando FL 32887-6777  ATTN: Saunders College Publishing  TEL: 407-345-2000 FAX: 407-345-4058	<b>FROM:</b> Ms. Sara E. Acevedo MS 245-1 Space Science Division NASA Ames Research Center Moffett Field CA 94035-1000 USA  TEL: 415-604-4223 FAX: 415-604-6779
--	--

Dear Sir or Madame,

I am a graduate student in the Department of Chemistry at San Jose State University. I wish to request permission to reprint four figures from one of your publications.

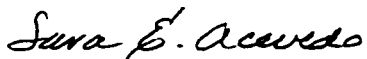
The publication is *Molecular Aspects of Cell Biology* by R.H. Garrett and C.M. Grisham (1995). The figures I wish to use are:

- 36.2 (The structure of a skeletal muscle cell) on page 1158.
- 36.4 (An electron micrograph of a skeletal muscle myofibril) on page 1159,
- 36.8 (An electron micrograph of a myosin molecule and corresponding drawing) on page 1161, and
- 36.11 (the packing of myosin molecules in a thick filament) on page 1164.

The figures will be used one time only for educational purposes; they will appear as figures in my thesis entitled "Development of Monoclonal Antibodies for the Separation of Myosin Isozymes" which will be archived by University Microfilms. I will have less than a dozen copies of the thesis printed for the use of my Department, my thesis advisor, and myself. Credit will be given in my figure legend as "Copied from Garrett and C.M. Grisham, 1995, with permission." (unless you instruct otherwise), and my reference list will include the complete citation for the book. Also, a copy of the letter of permission will appear in my thesis.

I must have the requested permission in writing no later than July 10, 1997.

Thank you for your assistance,



Sara E. Acevedo

HARCOURT  
 BRACE

Harcourt Brace & Company  
6277 Sea Harbor Drive  
Orlando, FL 32887  
Tel 407-345-2000

FAX # 415-604-6779

July 23, 1997

SCP REF: AVEVEDO/

Sara E. Acevedo  
MS 245-1, Space Science Division  
NASA Ames Research Center  
Moffett Field, CA 94035-1000

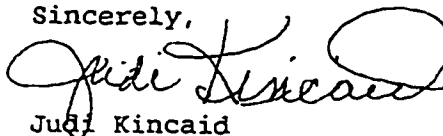
Dear Sara E. Acevedo:

In response to your letter, we are willing to grant permission for the reprinting of Figure 36.11 (page 1164) from MOLECULAR ASPECTS OF CELL BIOLOGY by Reginald H. Garrett, Charles M. Grisham (Request ID Num: 101423) in your forthcoming dissertation, provided it includes the title page and copyright page of our work (or equivalent information which includes: title, author(s) and/or editor(s), copyright (C) year and claimant(s), reprinted by permission of the publisher).

We are also willing to grant permission for your thesis to be reproduced and distributed in 50 copies only, by University Microfilms, provided you give complete credit to the source. If your dissertation is committed for publication, we ask that you reapply.

Our permission DOES NOT cover Figures 36.2, 36.4, or 36.8. Please apply directly to the sources acknowledged in our book. Unfortunately, we have no addresses to provide you.

Sincerely,



Judi Kincaid  
Paralegal Specialist

Saunders College Publishing  
Permissions Dept., 6th Floor  
Orlando, FL 32887-6777  
(407) 345-3979



July 7, 1997

total # pages: 1

<b>TO:</b> Copyrights and Permissions Wiley-Liss Publishers NY NY  ATTN: Mr. Chris Sheridan  TEL: 212-850-8607 FAX: 212-850-6008	<b>FROM:</b> Ms. Sara E. Acevedo MS 245-1 Space Science Division NASA Ames Research Center Moffett Field CA 94035-1000 USA  TEL: 415-604-4223 FAX: 415-604-6779
--	--

Dear Mr. Sheridan,

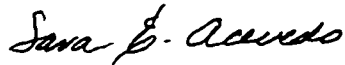
I am a graduate student in the Department of Chemistry at San Jose State University. I wish to request permission to reprint a figure from one of your papers in my Master's thesis.

The paper is *Patterns of Myosin Isoforms in Mammalian Skeletal Muscle Fibers* by N. Hámáláinen and D. Pette in **Microscopy Research and Technique** 30:381-389 (1995). The figure I wish to use is figure 8 on page 386 ("Serial cross sections of mouse soleus muscle atined for mATPase after preincubations at varying pH values.").

The figure will be used one time only for educational purposes; it will appear as a figure in my thesis entitled "Development of Monoclonal Antibodies for the Separation of Myosin Isozymes" which will be archived by University Microfilms. I will have less than a dozen copies of the thesis printed for the use of my Department, my thesis advisor, and myself. Credit will be given in my figure legend as "Copied from Hámáláinen and Pette, 1995, with permission." (unless you instruct otherwise), and my reference list will include the complete citation for the paper. Also, a copy of the letter of permission will appear in my thesis.

I must have the requested permission in writing no later than July 10, 1997.

Thank you for your assistance.



Sara E. Acevedo



605 Third Avenue  
New York, NY 10158-0012  
212.850.6000  
FAX 212. 850.6088

**John Wiley & Sons, Inc.**  
*Publishers Since 1807*

July 28, 1997

Ms. Sara E. Acevedo  
MS 245-1  
Space Science Division  
NASA Ames Research Center  
Moffett Field, CA 94035-1000

Dear Ms. Acevedo:

RE: Your letter dated July 7, 1997 requesting permission to reuse up to a maximum of 5 figures and/or 300 words in print media only from MICROSCOPY RESEARCH AND TECHNIQUE, a work published by John Wiley & Sons, Inc.

1. Permission is granted for this use, except that you must obtain authorization from the original source to use any material that appears in our work with credit to another source.
2. Permitted use is limited to the original edition of your forthcoming work described in your letter and does not extend to future editions of your work. In addition, permission does not include the right to grant others permission to photocopy or otherwise reproduce this material except for versions made by non-profit organizations for use by blind or physically handicapped persons.
3. Appropriate credit to our publication must appear on every copy of your work, either on the first page of the quoted text or in the figure legend. The following components must be included: Title, author(s) and /or editor(s), journal title (if applicable), Copyright © (year and owner). Reprinted by permission of John Wiley & Sons, Inc.
4. This permission is for non-exclusive world rights in the English language only. (For translation, please contact our Subsidiary Rights Department.)
5. This permission is for print rights only. If you wish permission for non-print media rights, please contact Judith Spreitzer, for requests for material from our books, and Neil Adams, for requests for material from our journals, when you have firm plans for publishing your book in a specific non-print medium.
6. If your published work contains more than 5 figures and/or 300 words from our title, this permission shall be void.

Sincerely,

Irina Lumelsky  
John Wiley & Sons, Inc.  
Permissions Department

If you have any questions regarding permissions, please call (212) 850-6011.

VISIT OUR WEBSITE @ "[HTTP://WWW.WILEY.COM](http://www.wiley.com)" FOR PERMISSIONS INFORMATION AND REQUEST FORMS

To Ms Sarah Acevedo

August 18, 1997

total # pages: 3

<p><b>TO:</b></p> <p>Dr. Hugh Huxley          Brandeis University          415 South Street          Waltham MA 02254-9110</p> <p>TEL: 617-736-2000          FAX: 617-736-2405</p>	<p><b>FROM:</b></p> <p>Ms. Sara E. Acevedo          MS 245-1          Space Science Division          NASA Ames Research Center          Moffett Field CA 94035-1000</p> <p>TEL: 415-804-4223          FAX: 415-804-6779</p>
--	--

Dear Dr Huxley,

I am a graduate student in the Department of Chemistry at San Jose State University. I wish to request permission to reprint figure 36.4 from *Molecular Aspects of Cell Biology* by R.H. Garrett and C.M. Graham, Saunders College Publishing (1995). A photocopy of the figure is attached for your reference. Since the figure includes a photo credited to you the Publisher referred me to you for permission.

The figure will be used one time only for educational purposes; it will appear as a figure in my thesis entitled "Development of Monoclonal Antibodies for the Separation of Myosin Isozymes" which will be archived by University Microfilms. I will have less than a dozen copies of the thesis printed for the use of my Department, my thesis advisor, and myself. Credit will be given in my figure legend as "Reproduced with permission from Dr. Hugh Huxley (figure 36.4, Garrett and C.M. Graham, 1995)." (unless you instruct otherwise), and my reference list will include the complete citation for the book. Also, a copy of the letter of permission will appear in my thesis.

Thank you for your assistance,

8/18/97.

Sara E. Acevedo

Sara E. Acevedo

You are very welcome to use the figure mentioned above in your thesis. Just return

Hugh Huxley

August 13, 1997

total # pages: 1

<p><b>TO:</b></p> <p>Dr. I. Rayment Department of Biochemistry and the Institute for Enzyme Research University of Wisconsin, Madison Madison WI</p> <p>ATTN: Sheryl Busatel</p> <p>TEL: 608-262-3028 FAX: 608-262-2904</p>	<p><b>FROM:</b></p> <p>Ms. Sara E. Acevedo MS 245-1 Space Science Division NASA Ames Research Center Moffett Field CA 94035-1000</p> <p>TEL: 650-604-4223 FAX: 650-604-6779</p>
---	---

Post-It™ brand fax transmittal memo 7571 # of pages 1

TO <i>SARA ACEVEDO</i>	From <i>JUAN RAYMENT</i>
Co.	Co.
Dept.	Phone #
Fax #	Fax #

Dear Dr. Rayment,

I am a graduate student in the Department and request permission to reprint a figure from

The paper is *Three-Dimensional Structure of Myosin Subfragment-1: A Molecular Motor* by I. Rayment, W.R. Ryanlewald, K. Schmidt-Bäse, R. Smith, D.R. Tomchlok, M.M. Benning, D.A. Winklemann, G. Wesenberg, and H.M. Holden in *Science* 261:50-57 (1993). The figure I wish to use is figure 4 on page 53 ("A ribbon representation of the entire model for myosin S1.").

The figure will be used one time only for educational purposes; it will appear as a figure in my thesis entitled "Development of Monoclonal Antibodies for the Separation of Myosin Isozymes" which will be archived by University Microfilms. I will have less than a dozen copies of the thesis printed for the use of my Department, my thesis advisor, and myself. Credit will be given in my figure legend as "Copied from Rayment et al., 1993, with permission" (unless you instruct otherwise), and my reference list will include the complete citation for the paper. Also, a copy of the letter of permission will appear in my thesis.

I must have the requested permission in writing no later than August 22.

Thank you for your assistance.

*Sara E. Acevedo*

Sara E. Acevedo

*Permission granted*  
*Juan Rayment*